CHALMERS

Vehicle Control in Cooperative Driving

Master's Thesis in Systems, Control and Mechatronics

ALIREZA EBADIGHAJARI

Department of Signals and Systems
Division of Automatic Control, Automation and Mechatronics
CHALMERS UNIVERSITY OF TECHNOLOGY
Göteborg, Sweden, 2011
Report No. EX045/2012

Vehicle Control in Cooperative Driving
Alireza Ebadighajari

© Alireza Ebadighajari, 2011/12

Report No. EX045/2012
Department of Signals and Systems
Division of Automatic Control, Automation and Mechatronics
Chalmers University of Technology
Göteborg, 2011

SE-412 96 Göteborg
Sweden
Telephone: +46 (0)31-7721000

Abstract

Cooperative driving aims to reduce traffic congestion, air pollution, and it increases safety. One of the applications of cooperative driving is platooning**,** where string of vehicles drives automatically in the same lane. The cooperative driving system consists of such components as communication box, sensor fusion, radar, and controller.

In this work, the design and development of the controller is discussed. The developed controller uses different information from the vehicles in the platoon, e.g. from the preceding vehicle or the vehicle in front of the preceding vehicle, by using a radar or wireless communication, and it only controls the vehicle in the longitudinal direction. Besides tracking the desired speed or distance and handling the constraints, the controller should guarantee that the string of vehicles is stable, i.e. when a disturbance such as acceleration shockwave is applied to the system, it won't amplify when propagating down the string.

The controller developed was implemented in a Volvo S60 and was used in the Grand Cooperative Driving Challenge in the Netherlands, which was organized to stimulate the development of the cooperative driving systems [1], [2].

Key words: Platooning, String stability, Cooperative Driving, Adaptive Cruise Control.

ACKNOWLEDGEMENTS

I would like to thank all the people who helped me to carry out this work. I want to express my gratitude to my supervisor Dr. Paolo Falcone from Chalmers University of Technology for his support, comments and interesting discussions all the way in the project. I want to greatly extend my thanks to Volvo Technology Corporation (VTEC) and my co-supervisor Mr. Erik Nordin for his excellent guidance, providing the opportunity to join Volvo Group and support in supplying me with the required resources. Also, I would like to thank Victoria Institute for their cooperation in this work.

Finally, I would like to thank my friends and family for their support during this time.

Acronyms

GCDC	Grand Cooperative Driving Challenge
ACC	Adaptive Cruise Control
CACC	Cooperative Adaptive Cruise Control
V2V	Vehicle to Vehicle
V2I	Vehicle to Infrastructure
R-D	Relative Distance
R-ASD	Relative Acceleration, Relative Speed, Relative Distance
MPC	Model Predictive Control
TF	Transfer Function
Ax	longitudinal acceleration
F_{aero}	equivalent longitudinal aerodynamic drag forces
F_{xf}	longitudinal tire force at the front tires
F_{xr}	longitudinal tire force at the rear tires
R_{xf}	force due to rolling resistance at the front tires
R_{xr}	force due to rolling resistance at the rear tires
m	mass of the vehicle
g	acceleration due to gravity
θ	angle of the inclination of the road in which the vehicle is traveling
τ	time constant of the vehicle model
T	actuation delay (input delay)
T_a	measurement time delay on relative acceleration
T_v	measurement time delay on relative speed
T_d	measurement time delay on relative distance
BW	bandwidth of the system

CONTENTS

Chapter 1: Introduction

1.1 Background

Recent advances in sensing and vehicle technologies have enabled a significant progress in the area of the active safety of passenger cars. Safety systems, assisting the driver in complex accident avoidance maneuvers, are already available in passenger cars. Even more complex vehicle systems, with autonomous driving capabilities, are expected to be available soon.

Such smart vehicles are envisioned to not only improve drivers' and passengers' safety, but also the overall vehicle efficiency and fuel consumption. These results will be achieved by exploiting newly available information, about the surrounding environment, provided either by the other vehicles on the road or the infrastructure.

1.2 Problem Description

The cooperative driving system composed of different components, such as positioning, radar and communication (hardware part), and also sensor fusion and controller (software part). The focus of this thesis work is on the controller development for a cooperative driving system. There are a number of cooperative tasks that have to be accomplished by the controller, such as

- Vehicle platooning, i.e., a set of vehicles, in a platoon configuration, performing different maneuvers, e.g., accelerating or decelerating to different speeds
- Guaranteeing stability of the platoon, bounding the inter-vehicle spacing and more importantly guaranteeing safety in all cases

1.3 Thesis Objectives

The aims of this thesis are:

- To design a control algorithm to perform a set of maneuvers in the platoon while satisfying a set of given requirements
- Implementing different type of controllers to evaluate and compare the performance of each of them
- Experimental validation of the proposed controllers

1.4 Autonomous Driving

In automated driving, when the vehicle uses only the information from sensors, such as the radar and the camera in order to regulate the speed or the distance to the preceding vehicle, the term 'Autonomous Drive' is used. The two most popular autonomous driving systems that are currently in production are the Cruise Control and the Adaptive Cruise Control systems.

1.4.1 Cruise Control (CC)

By using Cruise Control system, the vehicle is able to travel at a set speed. This system is composed of two level controllers where the high level controller translates the reference speed to acceleration command and the low level controller translates the latter into throttle or brake commands.

Figure 1-1 shows a simplified structure of the cruise control system. In this figure, speed error is the difference between the reference speed and the actual speed of the vehicle.

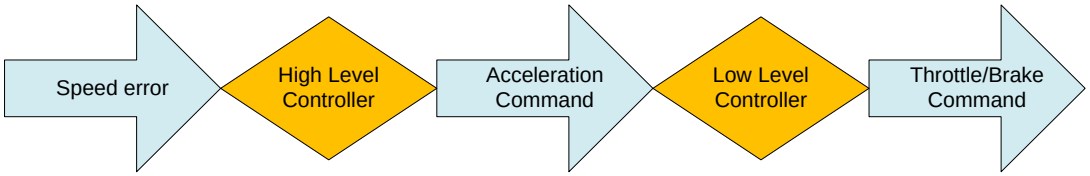

Figure 1-1. Cruise Control scheme

1.4.2 Adaptive Cruise Control (ACC)

Adaptive Cruise Control (ACC) is an extension of the Cruise Control (CC) system. The vehicle is equipped with radar and it can travel at a speed set-point (Speed Control) until the radar detects a vehicle in front of it. That is when the ACC system switches to spacing control operating mode if travelling at the set speed would result in a collision. In the spacing control mode, the vehicle keeps a certain distance to the preceding vehicle. Hence, in this mode, the ACC system controls the distance to the preceding vehicle.

Similar to the CC system, the ACC system is composed of two level controllers namely the high level and the low level controllers.

The inputs to the high level controller depend on the operating mode of the ACC system if it is in the speed control or in the spacing control operating modes. When the speed control mode is active the reference input is the 'desired speed' (reference speed) as it is shown in Figure 1-2, and the other input to the high level controller in this mode is the vehicle speed which is a feedback from speed sensors. When the spacing control mode is active the reference input is the desired inter-vehicle distance. Other inputs to the high

level controller in this mode are all the relative information such as relative distance and relative speed with respect to the preceding vehicle.

The following scheme shows the ACC system architecture:

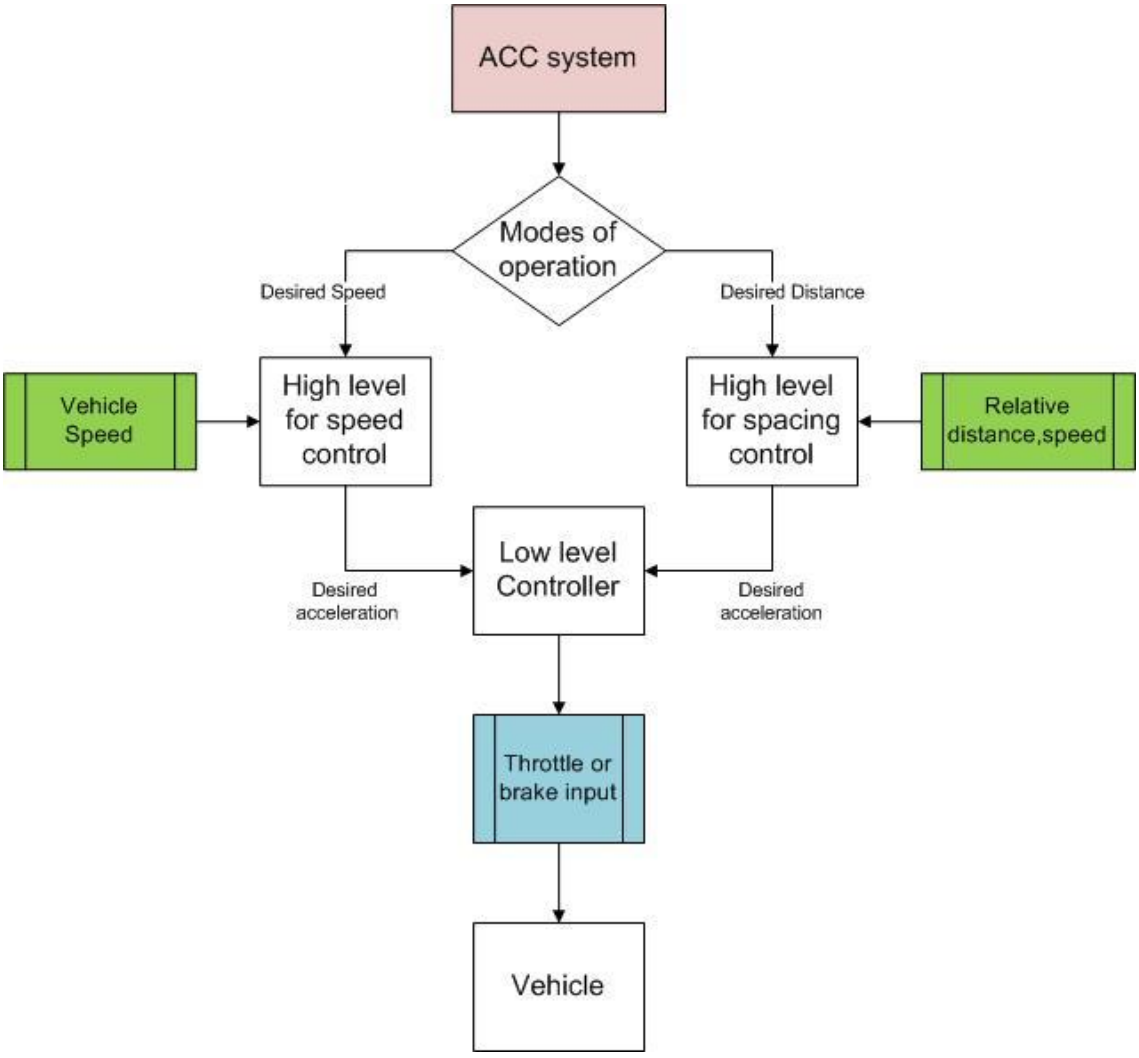

Figure 1-2. ACC system architecture

1.5 Cooperative Driving

In automated driving, where different automatic systems have been developed and even produced for commercial use, cooperative driving technologies are recognized to level up the current automated systems, efficiently use the current roads and increase driving safety as well as to reduce fuel consumption.

Cooperative driving is based on communication between vehicles (V2V) or communication between vehicles and infrastructures (V2I) or both. Cooperative Adaptive Cruise Control (CACC) is an example of a cooperative driving system which is the ACC system with wireless communication, aimed to increase traffic throughout by enabling the vehicles to travel in a shorter inter-vehicle distance and to reduce the fuel consumption.

Having the possibility to obtain information about the position, the speed or the acceleration of other vehicles as well as knowing the future status of the infrastructures, such as traffic light, can potentially increase safety, decrease traffic congestions, and reduce fuel consumption by, for example, avoiding unnecessary braking.

1.6 Platooning

A vehicle platoon is a string of vehicles that are driving automatically in the same lane. The first vehicle in the string is called the leader and the rest of them are called the followers. The follower vehicles should adapt their speed based on the leader vehicle behavior while the motion of the vehicles is subjected to stability requirements.

Vehicles in the platoon can share information using different communication topologies. This information in general is about the dynamics of the vehicles such as position, speed or acceleration.

Figure 1-3. Platoon of vehicles in NAHSC demonstration 1997

1.6.1 Grand Cooperative Driving Challenge (GCDC)

In May 2011, the Grand Cooperative Driving Challenge (GCDC) took place in the Netherlands. The GCDC was a competition where several teams consisting of car companies and suppliers, universities and research centers competed to accomplish a number of cooperative driving tasks.

Two main scenarios, namely urban and highway scenarios were used in the competition. They included a number of platooning tasks such as joining a platoon or stopping and going at a traffic light in the urban scenario and acceleration or deceleration to different speeds in the highway scenario. Figures 1-4 and 1-5 show an overview of different parts of the competition.

In the urban scenario, a platoon of vehicles (platoon 2 in figure 1-4) waiting at the traffic light should accelerate smoothly when the lights turns green and a platoon of vehicles further upstream from the traffic light (platoon 2 in figure 1-4) should smoothly join the platoon in front them. This part of the competition test the participants' ability to perform set of cooperative tasks.

In the highway scenario, the GCDC vehicle is driving in front of both platoons, and introduces disturbances by accelerating or decelerating to different speeds and all the participants' vehicles should smoothly accelerate or decelerate accordingly while they satisfy the stability requirement for the platoon.

The rules of the competition together with all information about this event are included in GCDC Rules and Technology document [2].

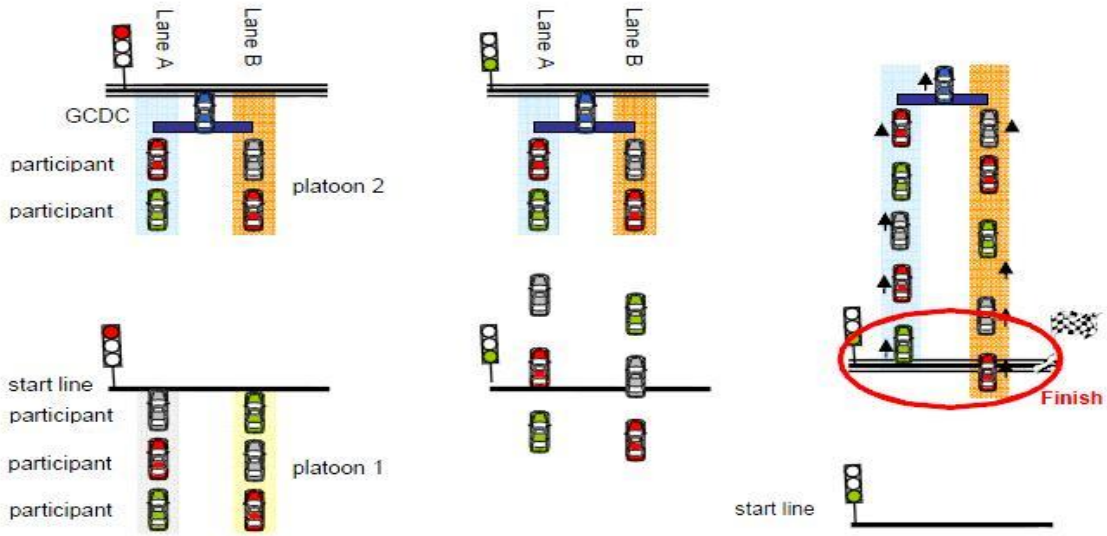

Figure 1-4. Overview of the urban scenario

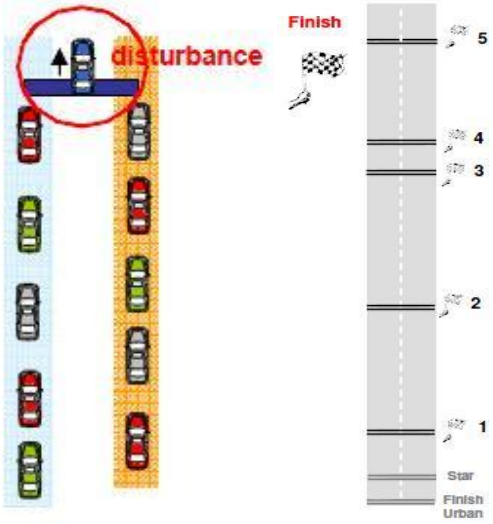

Figure 1-5. Overview of the highway scenario

Chapter 2: Vehicle Modeling

In this chapter, modeling of the vehicle used for controller design is discussed. To do this, first an overview of longitudinal vehicle dynamics is shown and then the vehicle model is presented. The proposed model shows the relation between the desired longitudinal acceleration (control input) and the actual acceleration of the vehicle.

2.1 Overview of Longitudinal Vehicle Dynamics

As the focus of the thesis is the control of the longitudinal dynamics, it is necessary to obtain a model for longitudinal motion of the vehicle. According to Rajamani [3], "longitudinal vehicle model is composed of vehicle dynamics and driveline dynamics". Vehicle dynamics is introduced in the following subsection. Detailed information about the driveline dynamics is presented in [3].

2.1.1 Vehicle Dynamics

The longitudinal forces acting on the vehicle in the longitudinal direction are

- Drag forces (F_{aero})
- Longitudinal tire forces in the front and the rear tires(F_{xf} , F_{xr})
- Rolling resistance forces in the front and the rear tires(R_{xf}, R_{xr})
- Gravitational force ($mgSin(\theta)$ in the inclined road where m is the vehicle mass, g is the gravity acceleration and θ is the inclination angle of the road on which the vehicle is traveling. According to the definition, θ is positive when the longitudinal motion of the vehicle is towards the left.)

Figure 2-1 in the next page shows all these forces.

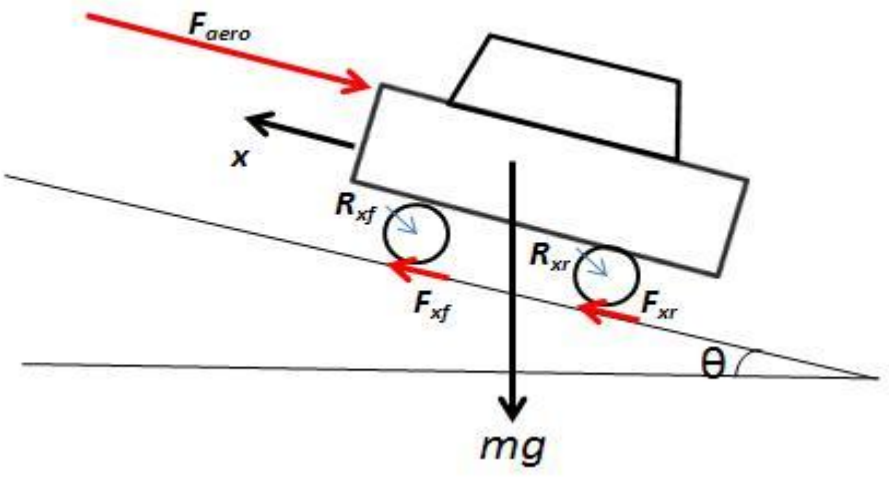

Figure 2-1. Longitudinal forces on the vehicle

Applying Newton's second law results in the following balance equation

$$m\ddot{x} = F_{xf} + F_{xr} - F_{aero} - R_{xf} - R_{xr} - mgsin(\theta) \quad (2.1)$$

$\ddot{x}$ is the longitudinal vehicle acceleration.

Rajamani [3] has provided a detailed description of the above mentioned forces.

2.2 Vehicle Modeling for Control Design

As mentioned in the beginning of this chapter, in this thesis the control input is the desired longitudinal acceleration. Hence, the vehicle model that is suitable for control design describes the response of the vehicle to the desired acceleration.

The model that is used for control design from the desired acceleration to the actual acceleration is

$$P(s) = \frac{k}{\tau s+1} e^{-Ts} \qquad (2.2)$$

Where τ is the time constant of the system (actuator dynamics), k is the system gain and T is the actuation delay.

The state space representation of the vehicle model considering acceleration, speed and position of the vehicle as states and the desired acceleration as the control input is

$$\dot{x}_1 = x_2(t)$$

$$\dot{x}_2 = x_3(t) \qquad (2.3)$$

$$\dot{x}_3 = \frac{1}{\tau} u(t-T) - \frac{1}{\tau} x_3(t)$$

x_1, x_2 and x_3 are position, speed and acceleration of the vehicle respectively (all in longitudinal direction) and u is the control input.

The test data in figures 2-4 and 2-5 show that the model (2.2) well describes the system's response from the desired acceleration (green line) to the actual acceleration of the vehicle. The identified model in figures 2-4 and 2-5 was chosen according to the model (2.2) and worked in both acceleration and braking maneuvers and for different speeds.

In these test data, an acceleration command was applied to the vehicle travelling at a constant speed, and the response of the actual acceleration of the vehicle was measured.

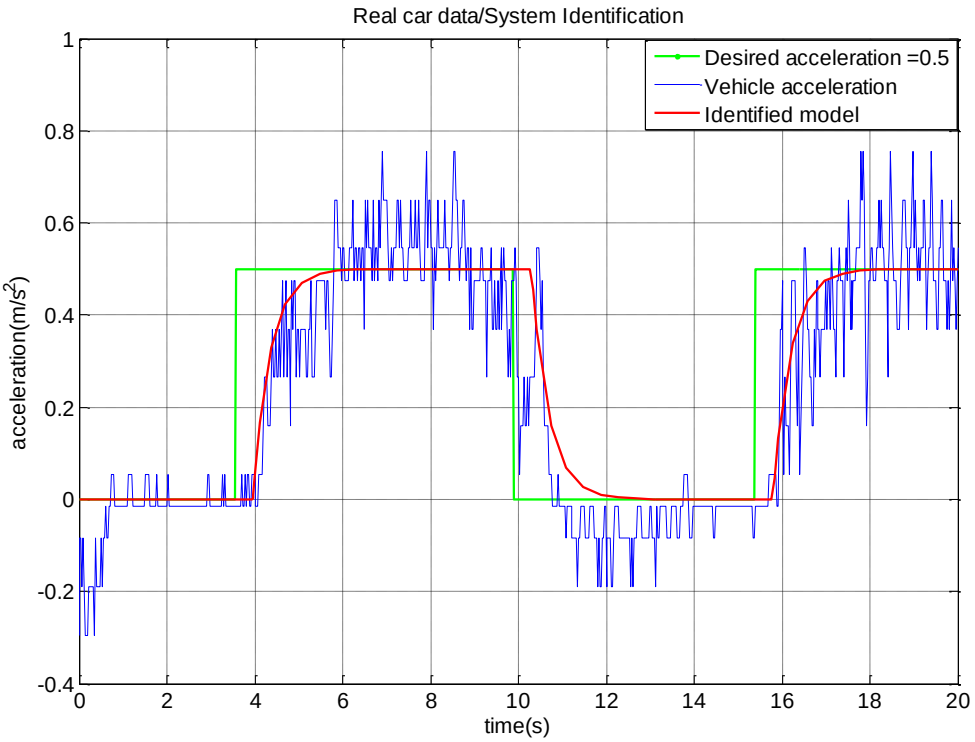

Figure 2-4. Identification of the plant model P(s), modeling from the desired acceleration to the actual acceleration (Vstart = 15 Km/h)

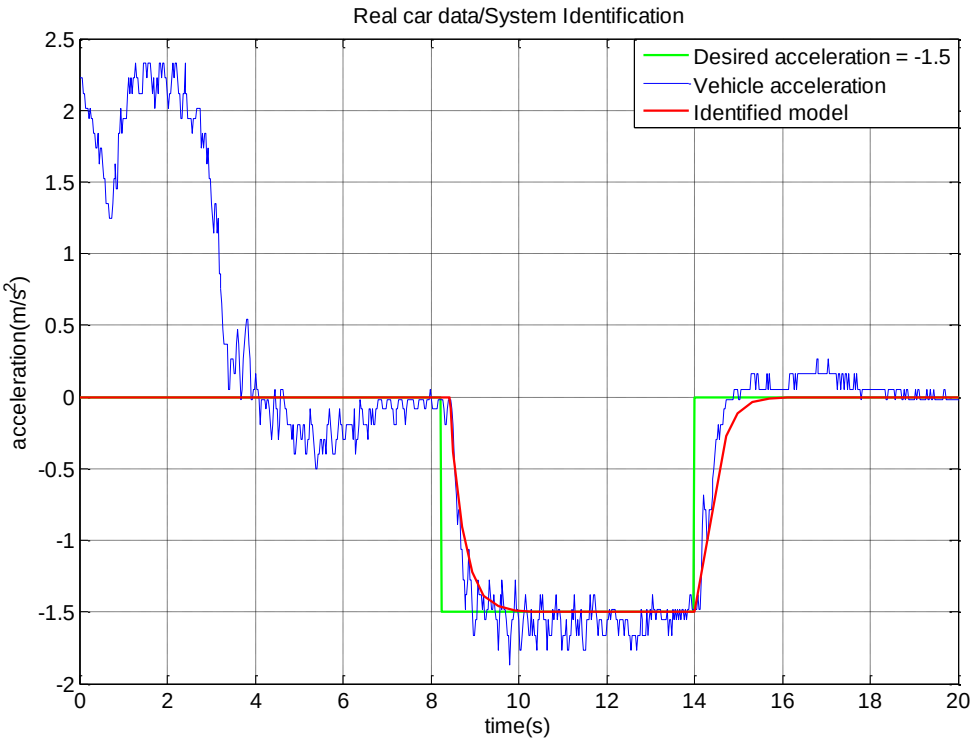

Figure 2-5. Identification of the plant model P(s), modeling from the desired acceleration to the actual acceleration (Vstart = 40 Km/h)

Chapter 3: Controller Design

Platooning, as it was mentioned earlier in the first chapter, is one of the approaches towards cooperative driving. “Cooperative information” in general is the information about the dynamics of the vehicles in the platoon such as acceleration, speed and position which are communicated between the vehicles.

When a vehicle is the leader of a platoon, it only needs to follow a specific speed, and a speed controller is required. If the vehicle is a follower in a platoon, the spacing controller is needed, as the vehicle requires keeping a certain distance from the preceding vehicle.

Hence, in section 3.1 the design of a speed controller is presented. In section 3.2 an introduction to spacing controller is introduced. Different approaches used for the spacing control in platooning are introduced and motivated in section 3.2.1. It is important to define what is meant by platooning. In this work, platooning means: ‘controlling the longitudinal motion of the vehicle in the string of vehicles in order to achieve the desired distance between the vehicles such that all the vehicles are individually stable, and the platoon is string stable’. String stability is discussed in section 3.2.2 which is an important criterion in spacing control. Later, in section 3.3 the design of different types of spacing controllers is discussed. **The main purpose of introducing different types of controllers is to investigate different communication topologies on the control design**.

In section 3.3.1 the design of the R-D (Relative Distance) controller using only the relative distance from the preceding vehicle is presented. In section 3.3.2 the design of the R-ASD (Relative Acceleration, Speed and Distance) controller that uses more information about the preceding vehicle compared to the R-D controller. In section 3.3.3 these two controllers are compared in order to find out the advantage of using more information from the preceding vehicle. Finally, in section 3.3.4 information about other vehicles (only the acceleration of the vehicle in front of the preceding vehicle is used in this work) is added to the R-ASD controller for designing the spacing controller and the advantage of using this extra information is discussed.

3.1 Speed Controller Design

The objective of the speed controller design is to bring the vehicle to the reference speed. The following figure shows a general scheme of the speed controller.

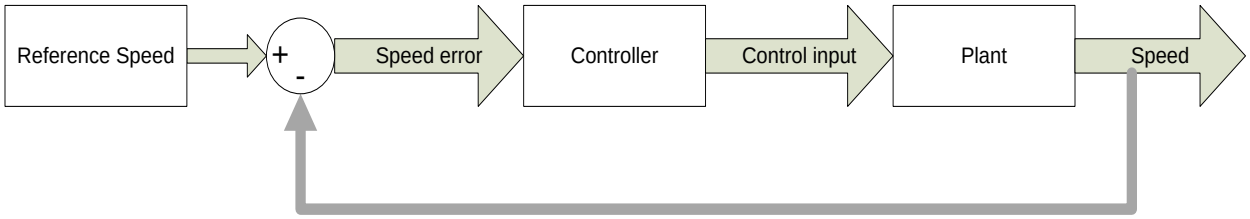

Figure 3-1. General scheme of the speed controller

The design procedure includes the following steps

- Design the controller considering that there is no input delay (actuation delay)
- Meeting the constraint on the control input
- Redesign the controller considering input delay

Assuming that there is no actuation delay in the system, the plant model is

$$G(s) = \frac{1}{s(\tau s + 1)} \qquad (3.1)$$

The input to the plant is the acceleration command, and the output of the plant is the vehicle speed. The closed loop system has the following transfer function where V(s) is the vehicle speed, V_{ref} is the reference speed and K(s) is the controller

$$T(s) = \frac{V(s)}{V_{ref}(s)} = \frac{K(s)}{\tau s^2 + s + K(s)} \qquad (3.2)$$

Considering the closed loop transfer function, the simplest choice for K(s) is a proportional controller (k_p) because

$$K(s) = k_p \xrightarrow{\text{Final value theorem}} \lim_{s\to 0} sT(s) = \lim_{s\to 0} s\frac{k_p}{\tau s^2 + s + k_p} = 1$$

Therefore the vehicle speed can track the reference speed with zero steady state error. For controller design, the time constant is approximated from the real car data ($0.4 \leq \tau \leq 0.6$), and the value of τ = 0.6 (s) is chosen. To select suitable values for the controller both Root-Locus analysis and frequency response analysis were used. Notice that no input delay and no constraint on the control input is considered here.

Root-Locus (RL) analysis (figure 3-2) shows how the closed loop poles change when the k_p varies. Values of the gain which result in poles on the negative real axis are of interest as the system's response (vehicles' speed) doesn't have any overshoot in the response of the system. Also in the bode plot (figure 3-3) a change in the gain parameter will result in a change of system's bandwidth. Here the criteria to choose the gain parameter are to have Minimum or no overshoot in the response and also to have a fast response meaning to have a large bandwidth.

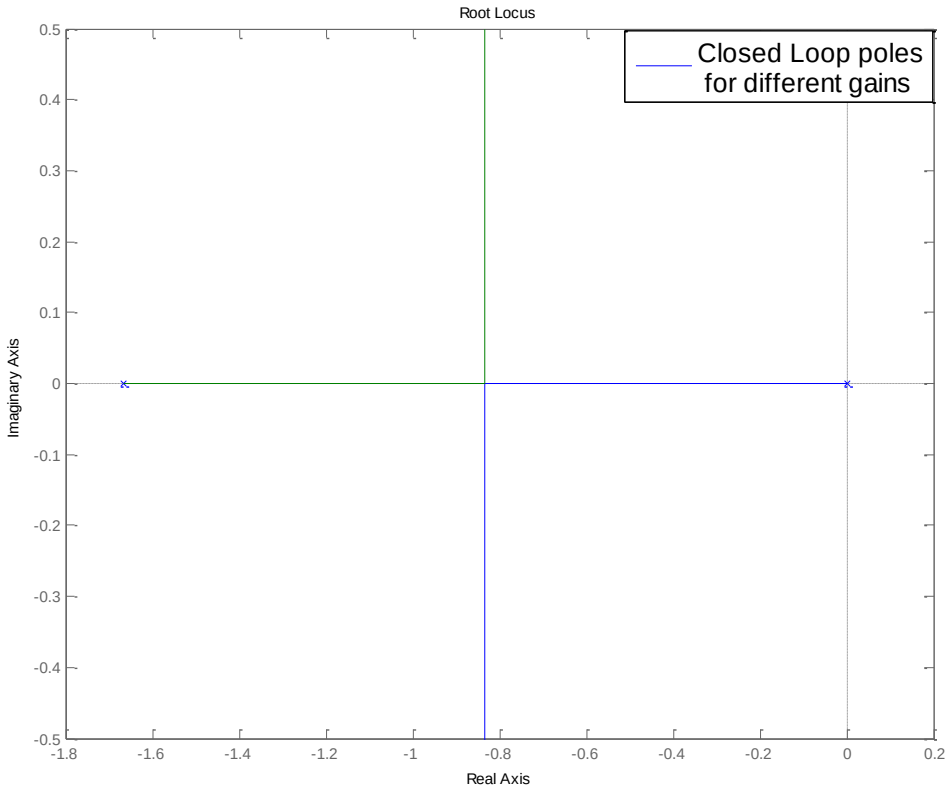

Figure 3-2. Root-Locus analysis showing the location of poles of the closed loop system in (3.2)

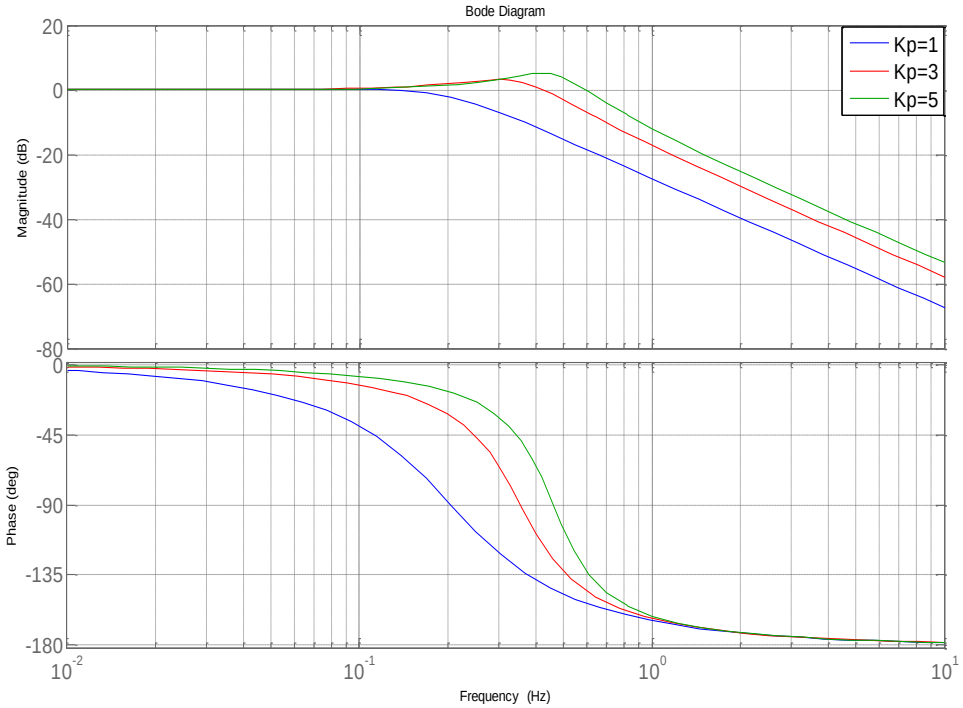

Figure 3-3. Bode plot for different gain parameters for the closed loop system in (3.2)

As it can be seen from RL plot, for all values of the proportional gain the system is always stable.

The same result is obtained by calculating the phase margin and the gain margin of the system for different values of the proportional gain (k_p). Figure 3.3 shows that for higher values of the proportional gain, the bandwidth of the system is increased while the overshoot in the response of the closed loop system is also increased.

For the next step, we consider a constraint on the control input which is the acceleration command (desired acceleration). This constraint is in line with the requirement of the GCDC competition. Also in practice there is always a constraint on how much it is possible to accelerate or decelerate according to the actuator capabilities. Based on the GCDC requirements, the maximum allowed acceleration is 2 (m/s^2) and the maximum allowed deceleration is - 4.5 (m/s^2).

In figure 3-4, the performance of the proposed controller to track the reference speed is shown in the upper plot, and in the lower plot the acceleration command is shown in order to show how the controller responds while having this constraint. Based on figure 3-2, values of the controller parameter are chosen such that the response of the system can track the reference speed without having an overshoot and by having a fast rise time (for the small values of the gain (<0.4) there is no overshoot, however, the response of the system is very slow).

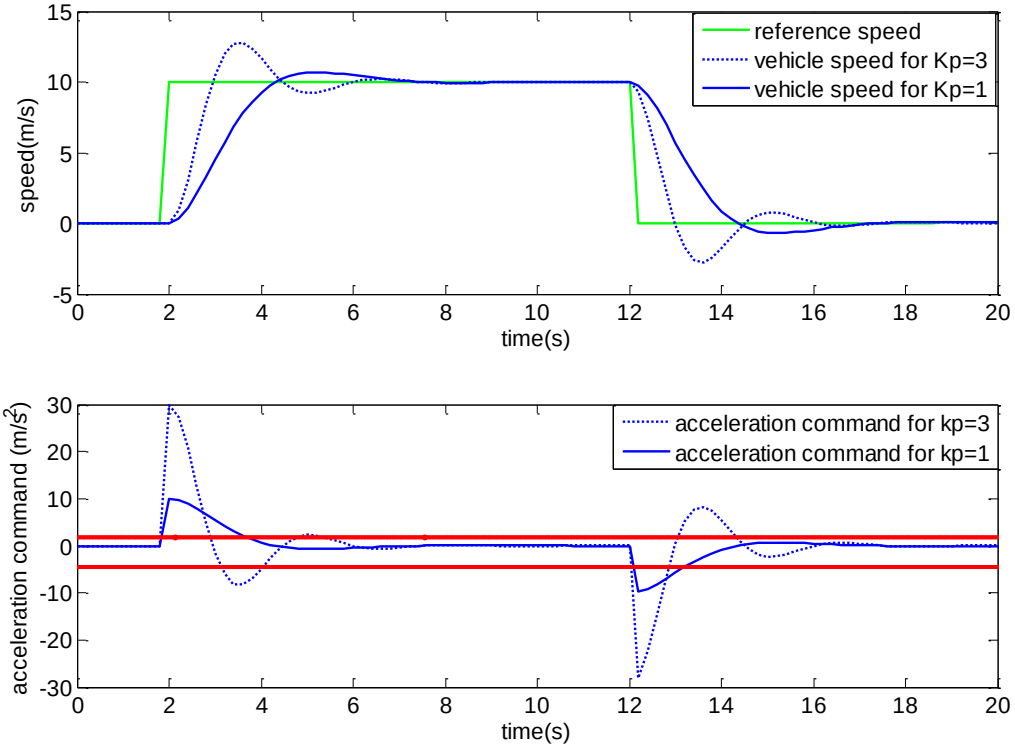

Figure 3-4. Tracking performance and the control input (red lines are the constraints on the control input)

A typical trade-off in the controller design can be seen by comparing the tracking performance in the upper plot and the control input in the lower plot of figure 3-4. Increasing the control input by choosing a higher controller gain will result in a faster tracking compared to the lower controller gains, but at the same time the control input is exceeding the constraint limit. Faster tracking means to have a shorter rise time which will result in a larger overshoot. The control input sensitivity function is

$$S(s) = \frac{U(s)}{R(s)} = \frac{A_{x_{com}}(s)}{V_{ref}(s)} = \frac{k_p s(\tau s + 1)}{\tau s^2 + s + k_p} \qquad (3.3)$$

By increasing the controller gain, poles of the closed loop system will possess an imaginary part (figure 3-2) and therefore an oscillatory behavior can be seen in the control input.

In order to avoid violating the constraint on the control input, the controller gain should be chosen such that the magnitude of the control input doesn't exceed the limits of the constraint. However, according to the analysis that follows, this will result in a poor tracking performance, i.e., a large rising time

$$S(s) = \frac{U(s)}{R(s)} = \frac{A_{x_{com}}(s)}{V_{ref}(s)} = \frac{k_p s(\tau s + 1)}{\tau s^2 + s + k_p} \;\; \& \;\; R(s) = \frac{A}{s} \quad A \in [0, A_{max}]$$

$$=> U(s) = R(s)S(s) = \frac{Ak_p(\tau s + 1)}{\tau s^2 + s + k_p} \qquad (3.4)$$

To comply with the constraint $=> \left|\frac{Ak_p(\tau j\omega + 1)}{-\tau\omega^2 + j\omega + k_p}\right| \leq \left|\frac{\min(u_1, u_2)}{j\omega}\right|$ (3.5)

Where u_1 and u_2 are the lower and the upper bound on control input.

replacing $A = A_{max} = 10, u_2 = u_{max} = 2$ in (3.5) and calculating the magnitudes yields

$$0.36\left(0.04 - {k_p}^2\right)\omega^4 + \left(0.04 - 0.048k_p - {k_p}^2\right)\omega + 0.04\,{k_p}^2 \geq 0 \qquad (3.6)$$

To satisfy the last inequality, it is necessary to recall the following background

$$\alpha\omega^4 + \beta\omega^2 + \gamma > 0 \quad , \quad \forall\omega \in (-\infty, \infty) \qquad (3.7)$$

The above inequality is always true if either of the followings holds

- $\alpha > 0, \beta > 0, \gamma > 0$ (3.8)

  or
- $\alpha > 0, \beta < 0, \gamma > 0\,, \beta^2 - 4\alpha\gamma < 0$ (3.9)

Hence, according to condition (3.8)

$$k_p{}^2 \leq 0.04 => \; k_p \leq 0.2$$

$$0.04 - 0.048k_p - k_p{}^2 > 0$$

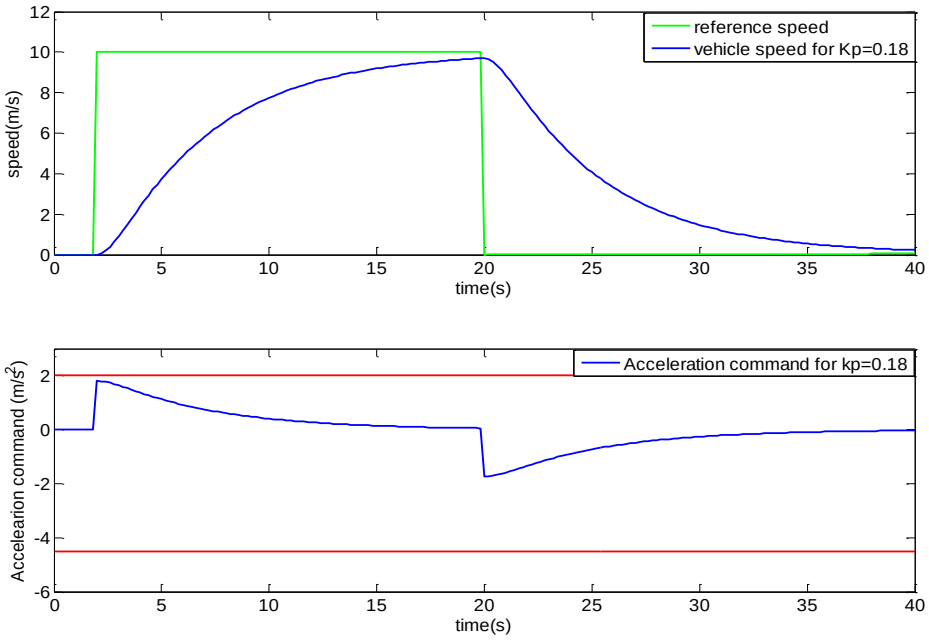

Figure 3-5. Tracking performance and control input for the controller that satisfies the condition 3.8 (red lines are the constraints)

In figure 3-5, the performance of the controller that satisfies the control input conditions is shown. To solve this problem (slow tracking of the reference speed), a saturation function is used. Using saturation on the control input will result in a faster rise time and settling time compared to the previous case, as it is shown in figure 3-6.

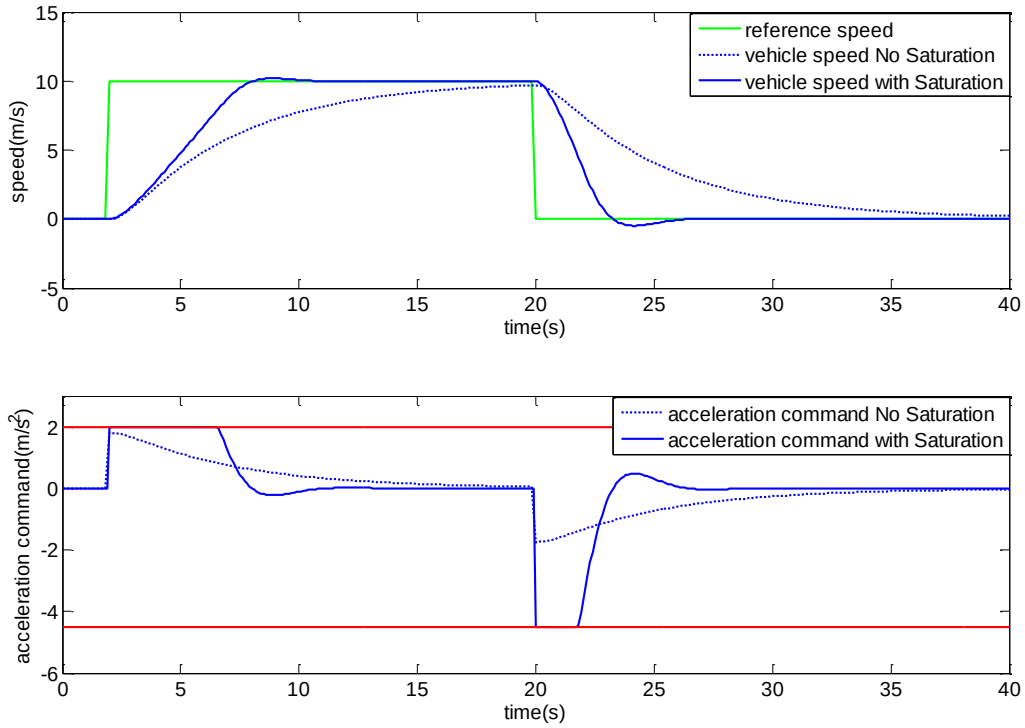

Figure 3-6. Tracking performance and control input comparison with and without saturation (red lines are the constraints)

However, this saturation is a nonlinear function and can introduce an oscillation in the system and affect the stability of the system. The saturation function has the following describing function which is denoted by *N(A)* (*A* is the amplitude).

$$f(u) = \begin{cases} H & u > D \\ (H/D)u & |u| < D \\ -H & u < -D \end{cases} \qquad (3.9)$$

$$if\ (A > D)\ => N(A) = \frac{2(H/D)}{\pi}\left(\sin^{-1}(\frac{D}{A}) + \frac{D}{A}\sqrt{1-\frac{D^2}{A^2}}\right) \qquad (3.10)$$

$$if\ (A < D) => N(A) = 1$$

The describing function of a static nonlinearity basically describes an amplitude dependent gain. If this nonlinearity is connected to a linear system ($G_L(i\omega)$) in a negative feedback loop, the oscillation condition is

$$N(A)G_L(i\omega) = -1 \qquad (3.11)$$

The saturation function in (3.9) is odd symmetric and therefore (3.10) holds for an odd symmetric saturation function. Deriving describing function of a non-odd symmetric saturation is more complex. Thus, to simplify the analysis, the oscillation condition (3.11) is solved once for the values of *D=H=2* for the acceleration maneuver and once for the values of *D=H=-4.5* for the deceleration maneuver. Notice that the describing function of saturation mentioned in (3.10) is positive real valued.

D=H=2

$$G_L(s) = \frac{k_p}{s(\tau s + 1)} => G_L(j\omega) = \frac{k_p}{j\omega - \tau\omega^2} = \frac{-\tau k_p \omega^2}{\tau^2\omega^4 - \omega^2} + j\frac{-\omega k_p}{\tau^2\omega^4 - \omega^2} \qquad (3.12)$$

$$Im\{G_L(j\omega)\} = 0 => \frac{-\omega k_p}{\tau^2\omega^4 - \omega^2} = \frac{k_p}{\omega - \tau^2\omega^3} = 0 \qquad (3.13)$$

Thus, there is no $k_p > 0$, such that the Nyquist plot intersects with the negative real axes. Thus, the oscillation condition (3.11) can't be satisfied. The same result is obtained for *D=H=-4.5*. Hence, using the saturation function doesn't cause an oscillation in the response of the system.

So far for the controller design, it was assumed that there was no input delay. According to the real car data, the maximum input delay is approximately 0.5 seconds. Considering input delay, the plant model is

$$G(s) = \frac{1}{s(0.6s + 1)} e^{-0.5s} \qquad (3.14)$$

Now the aim is to redesign the controller such that the effect of the input delay is compensated. Time delays can affect the stability as they reduce the phase margin of the stable system by introducing a negative phase in the system. So the controller should compensate for this phase shift which could result even in unstable closed loop behavior. Figure 3-7 shows the effect of the actuation delay on the tracking performance and the control input.

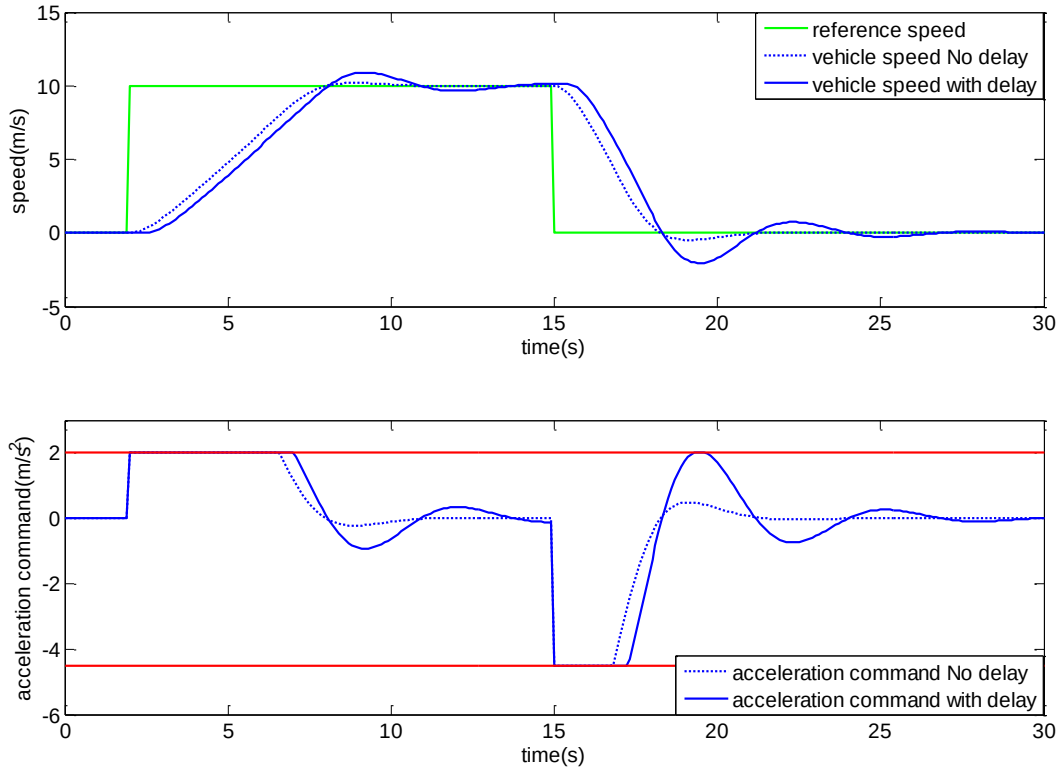

Figure 3-7. Effect of actuation delay on tracking performance and control input (red lines are the constraints)

The bold blue line shows more oscillation for both the control input and the tracking performance of the controller which is because of the reduction of phase margin caused by actuation delay.

The class of Lead-Lag compensators can solve this problem. Lead compensators feed a positive phase to the system and at the same time they can affect the amplitude of the output response. In figure 3-9 the performance of the revised controller is shown together with the previous controller. The choice of the lead controller is based on the following analysis

$$C_{lead}(s) = \frac{k_l(s+\alpha)}{(s+\beta)} \text{ Lead controller} \qquad (3.15)$$

The magnitude of the open loop transfer function is not affected by the input delay as $\left|e^{-j\omega T}\right| = 1$. Consequently the phase margin of the system with input delay is $\varphi - \omega T$ where φ is the phase margin of the system without the input delay.

Therefore the following relation should hold in order for the system to remain stable

$$\varphi - \omega T + \tan^{-1}\frac{\omega}{\alpha} - \tan^{-1}\frac{\omega}{\beta} \geq 0 \quad ,\forall\omega \in (-\infty,\infty) \qquad (3.16)$$

Since $\varphi > 0$, therefore

$$\tan^{-1}\frac{\omega}{\alpha} - \tan^{-1}\frac{\omega}{\beta} \geq \omega T \Rightarrow (T = 0.5s)$$

$$\Rightarrow \tan^{-1}\frac{\omega}{\alpha} - \tan^{-1}\frac{\omega}{\beta} \geq \frac{\omega}{2}, \forall \omega \in (-\infty, \infty) \qquad (3.17)$$

Solving this inequality requires numeric algorithms; instead a MATLAB toolbox named 'sisotool' was used to determine the Lead controller parameters. For values of $T = 0.5(s)$ and $\tau = 0.6(s)$, the phase margin of the system without the input delay was 62º while it decreased down to 36º in the presence of the input delay. So the Lead controller parameters (zero, pole and the constant gain) were chosen such that this decrease in the phase margin of the system was compensated. It is required to also check the effect of saturation function by using the describing function method.

$$G_L(s) = \frac{k_p k_l (s + \alpha)}{s(\tau s + 1)(s + \beta)} \qquad (3.18)$$

The Nyquist plot of (3.18) in figure 3-10, shows that $G_L(j\omega)$ doesn't intersect the negative real axes. Considering the describing function of saturation which is a positive real valued (3.10), the oscillation condition (3.11) is not satisfied. For the figure 3-10, values of $(\alpha = 1, \beta = 3, k_p k_l = 2)$ are used in $G_L(j\omega)$ mentioned in (3.18).

The final speed controller scheme considering the constraint on the control input, the actuation delay and also the design objectives is shown below

Figure 3-8. Speed controller scheme

In all these steps, the plant model (1) was used without considering any model mismatch. An integrator in the controller is needed in order to compensate for the model mismatch but according to the plant model there already exists an integrator in the model

$$G(s) = \frac{V(s)}{U(s)} = \left(\frac{V(s)}{A(s)}\right)\left(\frac{A(s)}{U(s)}\right)$$

$$\Rightarrow G(s) = \frac{1}{s(\tau s + 1)} = \left(\frac{1}{s}\right)\left(\frac{1}{\tau s + 1}\right) = \left(\frac{1}{s}\right)P(s) \qquad (3.19)$$

Hence, the mismatch in modeling is affected by $P(s)$ as the first part of $G(s)$ is only an integrator.

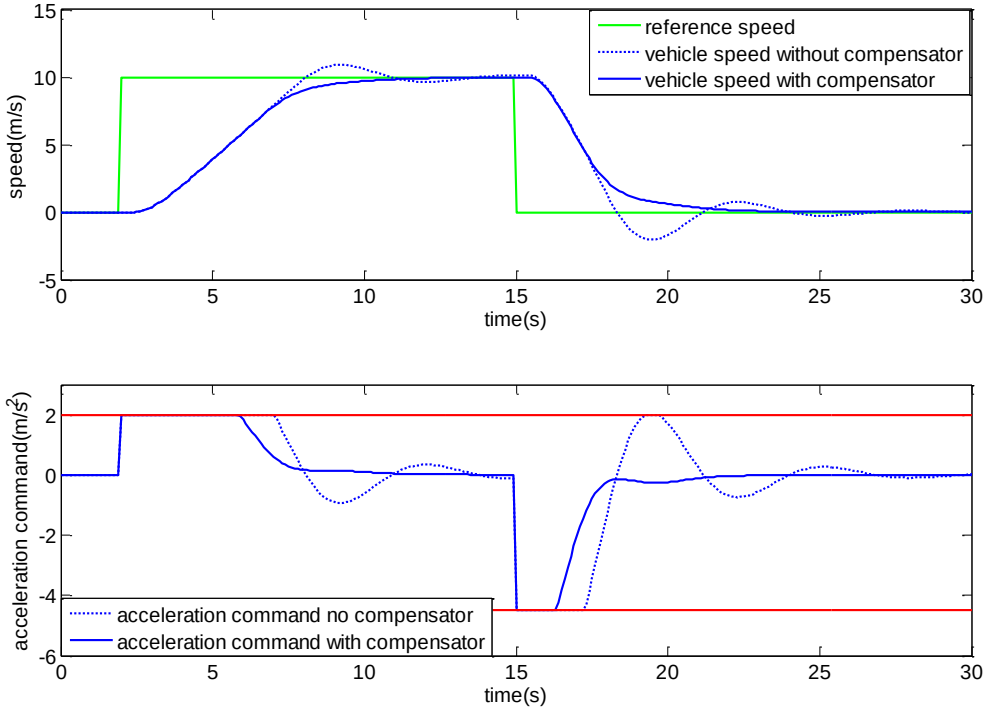

Figure 3-9. Tracking performance and the control input with and without the lead compensator

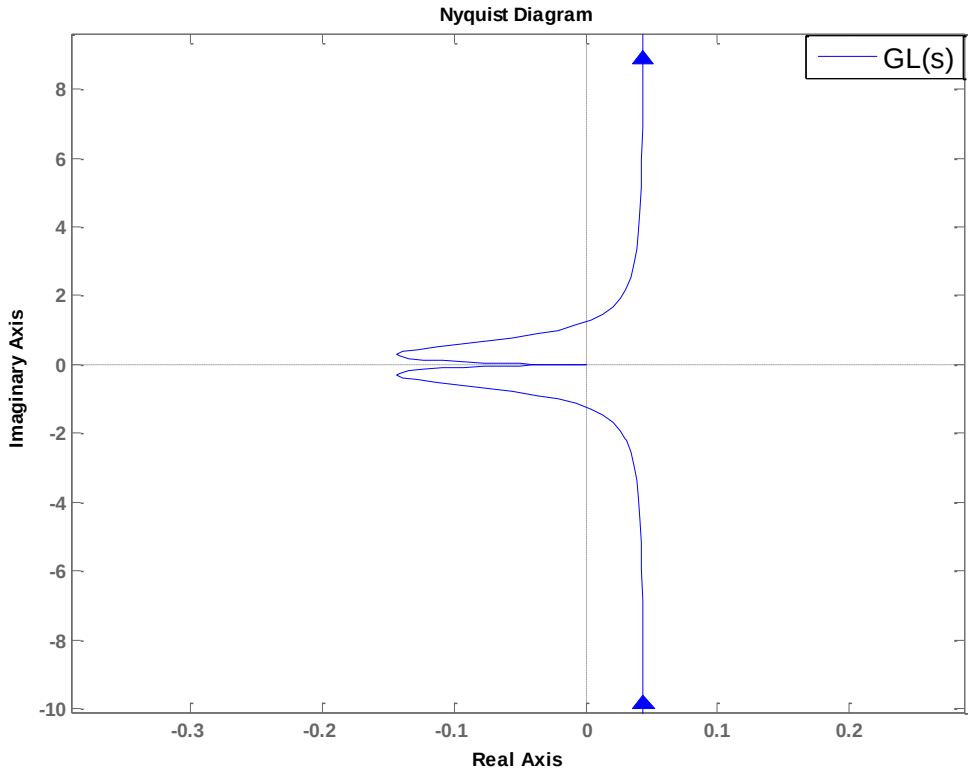

Figure 3-10. Nyquist plot of transfer function $G_L(j\omega)$ in equation 3.18

3.2 Introduction to Spacing Control

3.2.1 Different Approaches for Spacing Controller Design

There are two major approaches for the spacing control in platooning:

1) Constant spacing policy
2) Constant headway time or Constant time gap policy

The first approach is based on keeping a fixed distance between the vehicles in the platoon at different speeds.

The second approach is based on keeping constant the headway time defined as the distance difference between the ego vehicle[1] and the vehicle in front of it divided by the speed of the host vehicle. In other words, the headway time is the time required by the host vehicle to travel the distance to the preceding vehicle travelling at the current speed.

Constant spacing policy has the advantage that by defining a short distance between the vehicles, congestion problems can be reduced and at the same time the road capacity will increase. In the constant headway time policy, the distance between the vehicles is dependent on the speed. Hence, at higher speeds the distance is larger.

3.2.2 String Stability

In platooning, string stability plays an important role in the controller design procedure. By ensuring string stability it is possible to form a train of vehicles that can travel together while keeping a short distance between each other. According to literatures (e.g., see [4], [5]), the standard definition of string stability is "to attenuate the spacing errors as they propagate to the tail of the platoon".

According to Rajamani [3] and considering figure 3-11, the spacing error is defined as

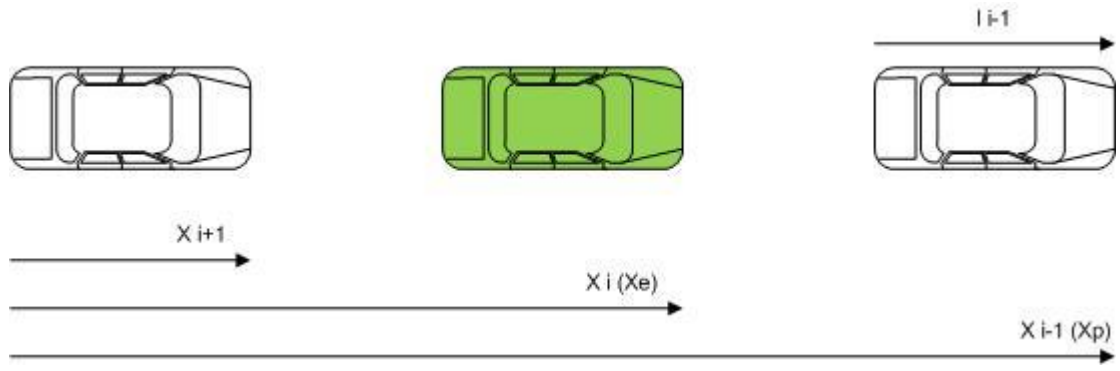

Figure 3-11. Platoon of vehicles (ego vehicle is colored in green)

1- Ego vehicle is our own vehicle that the controller is designed for.

$$\varepsilon_i = x_{i-1} - x_i - l_{i-1} \qquad (3.20)$$

$$\delta_i = \varepsilon_i - hv_i \qquad (3.21)$$

Where δ_i is the spacing error, ε_i is the distance difference between two consecutive vehicles, l_{i-1} is the length of the preceding vehicle, hv_i is the desired inter-vehicle spacing taking into account that the constant headway time policy is used (in the constant spacing policy, the desired inter-vehicles spacing is L_{des}) and h is the headway time.

$$H(s) = \frac{\delta_i(s)}{\delta_{i-1}(s)} \qquad (3.22)$$

$$1) \left\| \frac{\delta_i(j\omega)}{\delta_{i-1}(j\omega)} \right\|_\infty \leq 1 \qquad (3.23)$$

$$2)\ h(t) > 0\ ,\quad \forall t \geq 0 \qquad (3.24)$$

Where δ_i and δ_{i-1} are the consecutive spacing errors.

Seiler et al. [5] showed that for any linear controller if the vehicles in the homogeneous platoon[1] only use relative distance information with respect to the preceding vehicle to maintain a constant spacing, the string instability is unavoidable. Seiler et al. [5] proved that this limitation is due to a complementary sensitivity integral constraint. By including information about relative distance to the leader vehicle, the string stability can be achieved.

Hence, when the constant spacing policy is used by utilizing only the on-board sensors to obtain information about the relative distance to the preceding vehicle, the string of vehicles will be unstable. However, by using communication devices to obtain information about other vehicles, such as the relative distance to the leader vehicle of the platoon, the string stability for constant spacing policy is ensured.

In [6], Swaroop used a rigorous definition for the string stability of interconnected systems. According to this, string stability will be ensured if all the states of the interconnected systems are bounded providing that the initial states of them are uniformly bounded.

There are only a few works that have been done for heterogeneous platoon. Among them are works done by Sheikholeslam and Desoer [7], [8] and also by Yang [9].

Hedrick and Shaw [10]-[11], investigated the string stability for the heterogeneous platoon[2] based on the spacing error propagation. According to this, in the heterogeneous platoon the difference between the vehicles' dynamics causes that the spacing errors do not attenuate or amplify uniformly when they propagate down the string. The constant spacing policy was considered and Hedrick and Shaw provided a definition for the string

1- Homogeneous platoon refer to a vehicle platoon where vehicles have the same characteristics.
2- Heterogeneous platoon refer to a vehicle platoon where vehicles have different characteristics.

stability of the heterogeneous platoon as follows:

"A heterogeneous vehicle string is string stable if the propagating errors stay uniformly bounded for all string lengths and vehicle type ordering."

Naus et al [1] revised the definition of string stability using the frequency domain approach. The focus of Naus et al. [1] was the feasibility of implementation meaning that a heterogeneous traffic with a limited communication structure and decentralized control architecture was considered, and the string stability condition below is the necessary and sufficient frequency domain condition for a platoon of vehicles

$$\left\| \frac{X_i(j\omega)}{X_{i-1}(j\omega)} \right\|_\infty \leq 1 \quad , \quad i > 1 \qquad (3.25)$$

Where X is the system state and is directly related to absolute vehicle position or velocity. For a velocity-dependent inter-vehicle spacing, Naus et al. [1] showed that by keeping stability of the string, traveling in a short inter-vehicle distance is possible while for the velocity-independent inter-vehicle spacing string stability is not ensured (it could only be marginally stable).

3.3 Spacing Controller Design

In this and the following sections, design of different types of spacing controllers is discussed. In each of these controllers, a different set of information is used by the controller. For example, in section 3.3.1 where R-D (Relative Distance) controller is introduced, the controller uses only information about the relative distance from the preceding vehicle while in section 3.3.2, the controller uses also the relative speed and acceleration of the preceding vehicle. This way it is clear how using more information about other vehicles in the platoon, can improve the controller performance.

3.3.1 Relative Distance (R-D) Controller Based on Only Preceding Vehicle's Information Using Constant Headway Time Approach

In this thesis, the controller is designed according to the constant headway time policy. According to this policy, the distance between two vehicles depends on their speed. In particular, distance between the vehicles increases with the speed.

According to the definition, the headway time is defined as the time required by the ego vehicle to travel the distance to the preceding vehicle

$$h(t) = \frac{x_p(t) - x_e(t) - l_p}{v_e(t)} \qquad (3.26)$$

Where

$x_p(t) =$ Preceding vehicle position

$x_e(t) =$ Ego vehicle position

$l_p =$ length of the preceding vehicle

$v_e(t) =$ Ego vehicle speed

Note that the position of the vehicle is the position of its front bumper with respect to a fixed point. In figure 3-11, indices i and i-1 should be replaced here with e and p, denoting the ego and the preceding vehicles respectively.

Considering the definition of the constant headway time, the main objective for the controller design is to regulate the speed of the ego vehicle considering the distance to the preceding vehicle such that the headway time remains constant

$$x_p(t) - x_e(t) - l_p = hv_e(t) \qquad (3.27)$$

The position error is defined as

$$e(t) = x_p(t) - l_p - hv_e(t) - x_e(t) \quad (3.28)$$

The R-D controller scheme is shown in figure 3-12.

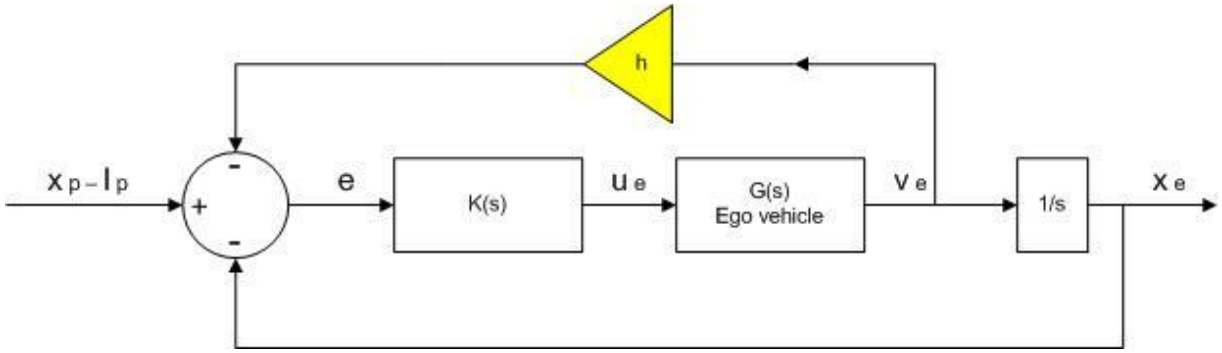

Figure 3-12. R-D controller scheme

Here the scenario for the vehicles is that both the ego and the preceding vehicles are traveling in a longitudinal direction and the preceding vehicle accelerates or decelerates to different speeds.

Objectives for the controller (K(s)) design for platooning include the followings:

1) Zero steady state position and speed error, closed loop stable system and satisfactory performance (No overshoot, fast rise time)
2) Meeting the constraint on the control input (u) and the relative distance
3) Ensuring string stability condition, i.e., attenuating the preceding vehicle's acceleration

Definition1. In this thesis, the string stability condition refers to the following condition

$$\left\| \frac{A_e(s)}{A_p(s)} \right\|_\infty \leq 1 \qquad (3.29)$$

Where A_e and A_p are the acceleration of ego and preceding vehicles respectively. This criterion was used in the GCDC competition for evaluation of string stability [2]. Hence, control objective (3.29) is added for determination of string stability.

Assumption1. In this thesis, when the string stability condition (3.29) is applied to a platoon of vehicles, it is assumed that all the follower vehicles use the same controller architecture while they can have different dynamics. This was not the case in the GCDC competition as each of the participants had only one vehicle in the platoon. Hence, this assumption is only used in this thesis in order to study the specific type of vehicles platoon where all of the followers have the same controller architecture. In the platoon configuration, indices 'e' and 'p' are replaced with 'i' and 'i-1'.

Assumption2. In this thesis, the acceleration of the preceding vehicle is in the interval of [4.5, 2] (m/s^2).

Starting with the first objective, the error function and also the closed loop transfer function are required

$$\Delta X(s) = X_p(s) - X_e(s) - \frac{l_p}{s} \qquad (3.30)$$

$$E(s) = \Delta X(s) - hV_e(s) \qquad (3.31)$$

Using figure 3-12 and the model showed in the previous chapter for the controller design, the followings can be obtained

$$X_e(s) = \frac{K(s)}{\tau s^3 + s^2 + shK(s) + K(s)}(X_p(s) - \frac{l_p}{s}) \qquad (3.32)$$

By replacing (18) into (16)

$$\Delta X(s) = \frac{\tau s^3 + s^2 + shK(s)}{\tau s^3 + s^2 + shK(s) + K(s)}(X_p(s) - \frac{l_p}{s}) \qquad (3.33)$$

The transfer function from the input signal $(X_p(s) - \frac{l_p}{s})$ to the speed of the ego vehicle is

$$V_e(s) = \frac{sK(s)}{\tau s^3 + s^2 + shK(s) + K(s)}(X_p(s) - \frac{l_p}{s}) \qquad (3.34)$$

To have zero positioning and speed error based on the constant headway time policy, the following equations must be satisfied

1) $\lim_{s\to 0} sV_e(s) = \lim_{s\to 0} sV_p(s) = \lim_{s\to 0} s^2 X_p(s)$

2) $\lim_{s\to 0} sE(s) = 0 \xrightarrow{\text{yields}} \lim_{s\to 0} s\Delta X(s) = \lim_{s\to 0} sh\, V_e(s)$
$\xRightarrow[\text{(from condition 1)}]{} \lim_{s\to 0} s\Delta X(s) = \lim_{s\to 0} hs^2 X_p(s)$

The first condition is zooming at the speed error while the second condition focuses on the position error.

According to the calculation below, choosing any linear controller K(s), provided that the system is stable, satisfies both of the above mentioned conditions.

$$\lim_{s\to 0} sV_e(s) = (from\ 3.34) = \lim_{s\to 0} \frac{s^2 K(s)}{shK(s) + K(s)}(X_p(s) - \frac{l_p}{s}) =>$$

$$\lim_{s\to 0} sV_e(s) = \lim_{s\to 0} \frac{s^2}{sh + 1}(X_p(s) - \frac{l_p}{s}) = \lim_{s\to 0} s^2 X_p(s) =>$$ condition 1 is satisfied

$$\lim_{s\to 0} s\Delta X(s) = (from\ 3.33) = \lim_{s\to 0} \frac{s^2 hK(s)}{shK(s) + K(s)}(X_p(s) - \frac{l_p}{s}) =>$$

$$\lim_{s\to 0} s\Delta X(s) = \lim_{s\to 0} \frac{s^2 h}{sh+1}(X_p(s) - \frac{l_p}{s}) = \lim_{s\to 0} hs^2 X_{i-1}(s) \Rightarrow \text{condition 2 is satisfied}$$

Among the linear controller, we start with the well known P, PD and PI controllers. There is already an integrator in the vehicle model (3.1) from the control input (u) to the vehicle speed (v). Therefore, only P and PD controllers are considered.

Stability conditions are found through the Routh criterion [12].

$\Delta(s) = \tau s^3 + s^2 + hk_p s + k_p$ Characteristic polynomial[1] using P controller

s^3	τ	hk_p
s^2	1	k_p
s^1	$hk_p - \tau k_p$	
s^0	k_p	

for stability $\Rightarrow$ $k_p > 0$ & $(h-\tau)k_p > 0 \Rightarrow h > \tau$ (3.35)

This is an interesting result which means that it is not possible to choose a headway time that is smaller than the time constant of the vehicle model.

Using Routh criterion for the PD controller results in

$\Delta(s) = \tau s^3 + (1+hk_d)s^2 + (hk_p + k_d)s + k_p$ Characteristic polynomial using PD controller

s^3	τ	$hk_p + k_d$	$(hk_p + k_d) > 0$
s^2	$1 + hk_d$	k_p	
s^1	$((hk_p + k_d)(1+hk_d) - \tau k_p)/(1+hk_d)$		
s^0	k_p		

for stability $\Rightarrow k_p > 0$ & $(1+hk_d) > 0$ & $(h-\tau)k_p + (h^2 k_p + 1 + hk_d)k_d > 0$ (3.36)

To comply with the constraint on control input ($u \in [-4.5,2]$ (m/s^2)), the control input sensitivity function plays an important role which is

$$U_e(s) = K(s)E(s) \rightarrow U(s) = K(s)\big(\Delta X(s) - hV_e(s)\big) \quad (3.37)$$

$$(19)\&(20) \Rightarrow U_e(s) = \frac{K(s)(\tau s^3 + s^2)}{\tau s^3 + s^2 + shK(s) + K(s)}(X_p(s) - \frac{l_p}{s}) \quad (3.38)$$

$$\big(A_p(s) = s^2 X_p(s)\big) \Rightarrow U(s) = \frac{K(s)(\tau s + 1)}{\tau s^3 + s^2 + shK(s) + K(s)} A_p(s) \quad (3.39)$$

1- Characteristic polynomial is the denumerator of the input-output transfer function.

Considering the string stability condition (3.29) and the vehicle model, the following relation is derived for the control input u

$\left\|\frac{A_e(s)}{A_p(s)}\right\|_\infty \leq 1$ String stability condition

$\frac{A_e(s)}{U_e(s)} = \frac{1}{\tau s + 1}$ Vehicle model

to have string stability => $\left\|\frac{U_e(s)}{A_p(s)(\tau s + 1)}\right\|_\infty \leq 1$ (3.40)

From the Matrix norm properties

$\|AB\| \leq \|A\|\|B\|$ (holds for all p-norms $1 \leq p \leq \infty$)

=> $\left\|\frac{U_e(s)}{A_p(s)(\tau s + 1)}\right\|_\infty \leq \left\|\frac{U_e(s)}{A_p(s)}\right\|_\infty \left\|\frac{1}{\tau s + 1}\right\|_\infty$ (3.41)

We also have $\left\|\frac{1}{\tau s+1}\right\|_\infty \leq 1$

Therefore by having $\left\|\frac{U_e(s)}{A_p(s)}\right\|_\infty \leq 1$ (3.42)

And considering assumption (2), the string stability condition is satisfied and also the control input doesn't violate the constraint

Assumption (2) => *- 4.5 (m/s²) ≤ $a_p(t)$ ≤ 2 (m/s²)*

$\left\|\frac{U_e(s)}{A_p(s)}\right\|_\infty \leq 1$ => $\|U_e(s)\|_\infty \leq \|A_p(s)\|_\infty$ => *- 4.5 (m/s²) ≤ u_e ≤ 2 (m/s²)*

Also this condition results in having no overshoot in the control input response (smooth control command).

Considering transfer function (3.39) and using the P controller

$$U_e(s) = \frac{K(s)(\tau s + 1)}{\tau s^3 + s^2 + shK(s) + K(s)} A_p(s)$$

K(s)=k_p => $U_e(s) = \frac{k_p(\tau s + 1)}{\tau s^3 + s^2 + shk_p + k_p} A_p(s) = L(s)A_p(s)$ (3.43)

In order to fulfill (3.42)

=> $\left|k_p(j\tau\omega + 1)\right| \leq \left|-j\tau\omega^3 - \omega^2 + jhk_p\omega + k_p\right|$ (3.44)

=> $\tau^2\omega^4 + (1 - 2\tau hk_p)\omega^2 + {k_p}^2(h^2 - \tau^2) - 2k_p \geq 0 \quad , \quad \forall\omega \in (-\infty, \infty)$ (3.45)

$\alpha = \tau^2$, $\beta = 1 - 2\tau h k_p$, $\gamma = {k_p}^2(h^2 - \tau^2) - 2k_p$

$=>$ $\alpha\omega^4 + \beta w^2 + \gamma \geq 0$, $\forall\omega \in (-\infty, \infty)$

In order to satisfy the above inequality, either of the following should hold according to equations (3.7) to (3.9)

- $\alpha > 0, \beta > 0, \gamma > 0$

- $\alpha > 0, \beta < 0, \gamma > 0$ & $\beta^2 - 4\alpha\gamma < 0$

$\alpha\omega^4 + \beta w^2 + \gamma = 0$ if and only if $\alpha = \beta = \gamma = 0$ (which is not satisfied as $\alpha = \tau^2 > 0$)

Hence, according to (3.8)

$(1 - 2\tau h k_p) > 0$, ${k_p}^2(h^2 - \tau^2) - 2k_p > 0$

$=>$ $k_p < \frac{1}{2h\tau}$ & $k_p > \frac{2}{h^2 - \tau^2}$ $\xRightarrow{\text{in order to exist a value for } k_p}$ $\frac{1}{2h\tau} > \frac{2}{h^2 - \tau^2}$

$=> h^2 - 4h\tau - \tau^2 > 0$ $=> \Delta = 16\tau^2 + 4\tau^2 < 0$ (3.46)

Equation (3.46) can never be satisfied. Also according to condition (3.9)

$\beta^2 - 4\alpha\gamma = (1 + 4\tau^4){k_p}^2 + (8\tau^2 - 4\tau h)k_p + 1 < 0$ (3.47)

To satisfy (3.47), both $(\Delta = 48\tau^4 + 16\tau^2h^2 - 64\tau^3h - 4 < 0)$ and $(1 + 4\tau^4 < 0)$ should hold. As $(1 + 4\tau^4 \geq 1)$ is always true, the equation (3.47) can't be satisfied. Thus, there is no $k_p$that can satisfy condition (3.42).

Using the PD controller and calculating the magnitude of the transfer function (3.39) yields

$\left|(k_p + jk_d\omega)(j\tau\omega + 1)\right| \leq \left|-j\tau\omega^3 - \omega^2 + j\omega h(k_p + jk_d\omega) + k_p + jk_d\omega\right|$ (3.48)

$=>$

$\omega^2(1 - {k_d}^2\tau^2 + h^2{k_d}^2 + 2hk_d + \tau^2\omega^2 - 2h\tau k_p - 2\tau k_d) \geq 2k_p - h^2{k_p}^2 + \tau^2{k_p}^2$ (3.49)

$\alpha = \tau^2,\ \beta = 1 - {k_d}^2\tau^2 + h^2{k_d}^2 + 2hk_d - 2h\tau k_p - 2\tau k_d\ ,\ \gamma = -2k_p + h^2{k_p}^2 - \tau^2{k_p}^2$

$=>$ $\alpha\omega^4 + \beta w^2 + \gamma \geq 0$, $\forall\omega \in (-\infty, \infty)$

The same conditions mentioned on equations (3.8) and (3.9) are required to satisfy the last inequality.

For the values of h=1s, τ =0.5(s), k_p= 4 and k_d =1, the control input sensitivity function is shown in figure 3-13 for both P and PD controllers.

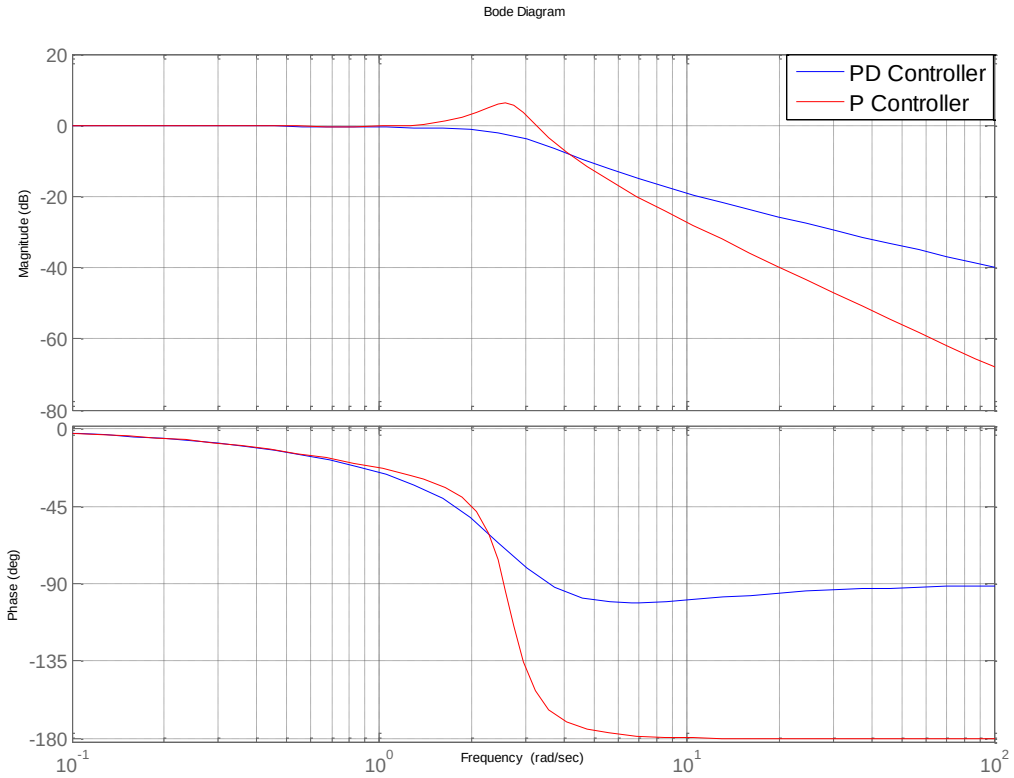

Figure 3-13. Effect of P and PD controllers on control input U in Transfer function (3.39)

The following inequality is obtained for the P controller based on equation (3.45)

$$0.25\omega^4 - 3\omega^2 + 4 \geq 0 \qquad (3.50)$$

Which isn't valid for $1.23 \leq \omega \leq 3.23$

While for the PD controller, the following inequality based on (3.49), is true for all values of $\omega \in (-\infty, \infty)$

$$0.25\omega^4 - 1.25\omega^2 + 4 \geq 0 \qquad (3.51)$$

In order to meet the constraint on minimum distance to the preceding vehicle, the following condition should be satisfied

$$\Delta x(t) \geq (\text{safety distance}) + 0.6v_e(t) \qquad (3.52)$$

The safety distance is 10(m) and the minimum allowed headway time is (0.6) seconds according to the GCDC requirements

$$\Delta X(s) \geq \left(\frac{10}{s}\right) + 0.6V_e(s) \qquad (3.53)$$

$$=> |\Delta X(s) - 0.6V_e(s)| \geq \left|\left(\frac{10}{s}\right)\right| => \frac{\left|\left(\frac{10}{s}\right)\right|}{|\Delta X(s) - 0.6V_e(s)|} \leq 1 \qquad (3.54)$$

Using (19) and (20) to replace $\Delta X(s)$ and $V(s)$

$$=> \frac{\left|\left(\frac{10}{s}\right)\right|}{\left|\frac{\tau s^3 + s^2 + (h-0.6)sK(s) + K(s)}{\tau s^3 + s^2 + shK(s) + K(s)}\right| \left|X_p(s) - \frac{l_p}{s}\right|} \leq 1 \qquad (3.55)$$

The last inequality depends on the magnitude of the input signal ($X_p(s) - \frac{l_p}{s}$). Hence, guaranteeing the condition above can't be met only by choosing appropriate control parameters. In simulation results, this magnitude was known and therefore it was possible to determine controller parameters to satisfy the above mentioned condition but, as will be shown in the chapter 4, this condition isn't always satisfied in practice, especially when the vehicle is going to a full stop. In order to maintain a certain margin from this minimum distance, the headway time was chosen to be greater than the minimum allowed headway time ($0.8 \leq h \leq 1$).

Before presenting the simulation results, it should be mentioned that for safety issues, besides required spacing for having a constant headway time, a safety distance of L_{safe} was defined (10 meters in this work). According to the constant headway time policy the distance between vehicles is proportional to speed. Thus, for low speeds it requires a very short distance between the vehicles. This safety distance prevents from such cases to happen.

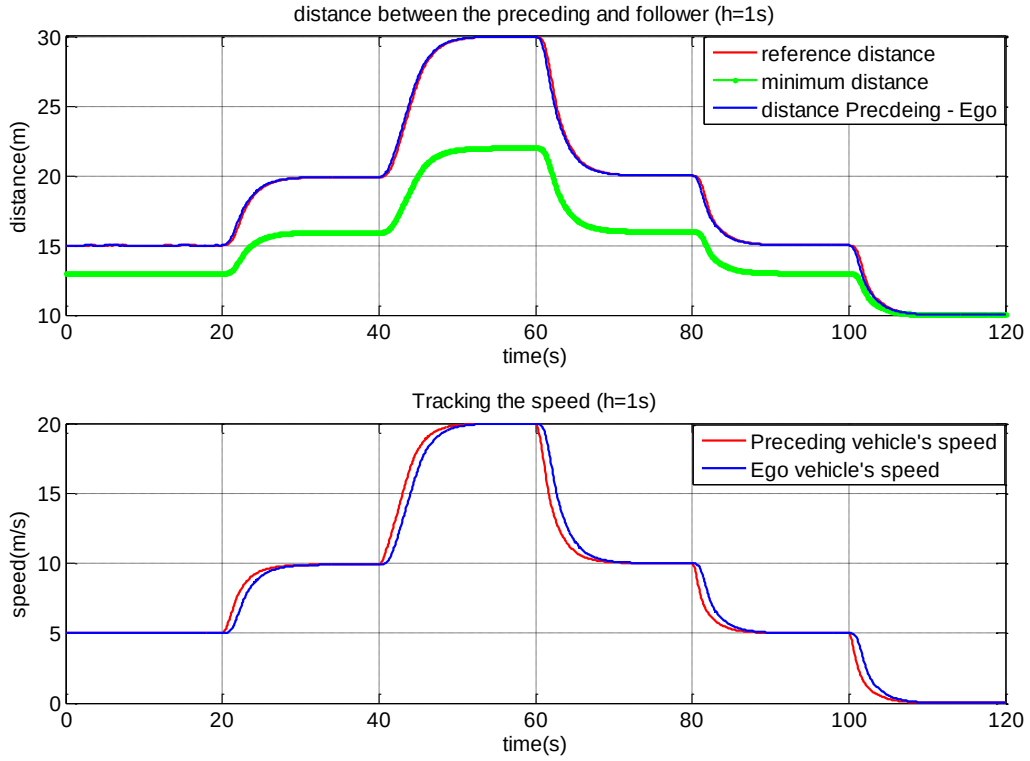

Figure 3-14. Performance of the R-D controller for tracking the reference distance and speed using the PD controller (it is assumed that there is no initial position error and the platoon is traveling at a constant speed in the beginning).

The reference and the minimum distances are:

$$d_{ref} = safety\ distance + h * V_e \ , \ d_{min} = safety\ distance + 0.6 * V_e$$

In figure 3-14, it is assumed that there is no initial position error between the vehicles and the platoon is travelling at a constant speed in the beginning. The headway time that is used for control design can be varied but it can't be set to a value less than the minimum allowed headway time.

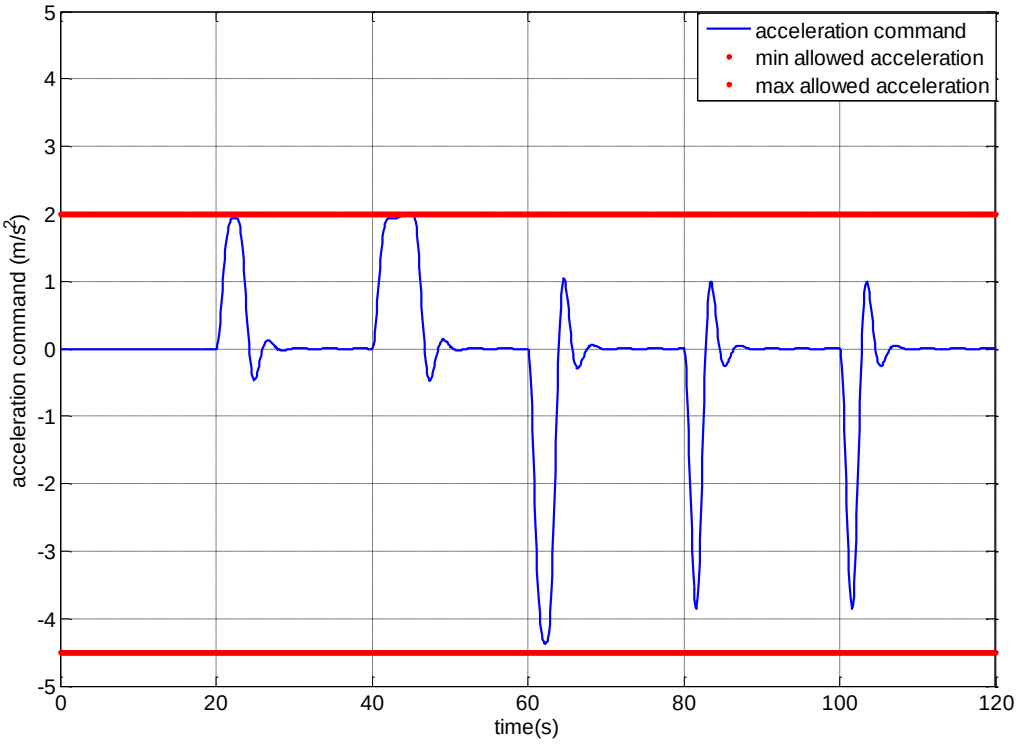

Figure 3-15. Control input signal

Figure 3-14 shows that when the preceding vehicle accelerates or decelerates to different speeds, the follower vehicle is able to track the speed of the preceding vehicle. Moreover, the distance between vehicles matches the spacing defined by the constant headway time which is 1 second.

Figure 3-15 shows that, for the maneuver used in figure 3-14, the control input complies with the constraint provided that assumption (2) holds. A saturation function can be used to make sure that the control input never violates the constraint. The time when this saturation function is necessary is when the vehicles start moving from standstill when the initial position error is unknown. At this time, the controller might send a high acceleration command to compensate for the position error. The saturation function will prevent it from happening. During normal traveling, saturation function is working mostly in its linear part.

By using saturation function, it is required to check the oscillation condition (3.11) for the open loop transfer function in figure 3-12

closed loop TF $T(s) = \dfrac{K(s)G(s)}{s^2 + shK(s)G(s) + K(s)G(s)}$ (3.56)

from (3.1) => $G(s) = \dfrac{1}{s(\tau s + 1)}$

(3.1) and $K(s) = k_d s + k_p$ => $T(s) = \dfrac{k_d s + k_p}{\tau s^3 + (1 + hk_d)s^2 + (hk_p + k_d)s + k_p}$ (3.57)

Open loop TF $F(s) = \dfrac{T(s)}{1 - T(s)} = \dfrac{k_d s + k_p}{\tau s^3 + (1 + hk_d)s^2 + (hk_p)s}$ (3.58)

The Nyquist plot of (3.58) in figure 3-16, shows that $F(j\omega)$ doesn't intersect with the negative real axes. Considering the describing function of saturation which is a positive real valued (3.10), the oscillation condition (3.11) is not satisfied. In figure 3-16, values of ($h = 1, \tau = 0.6, k_d = 1, k_p = 4$) are used in *F(s)* mentioned in (3.58).

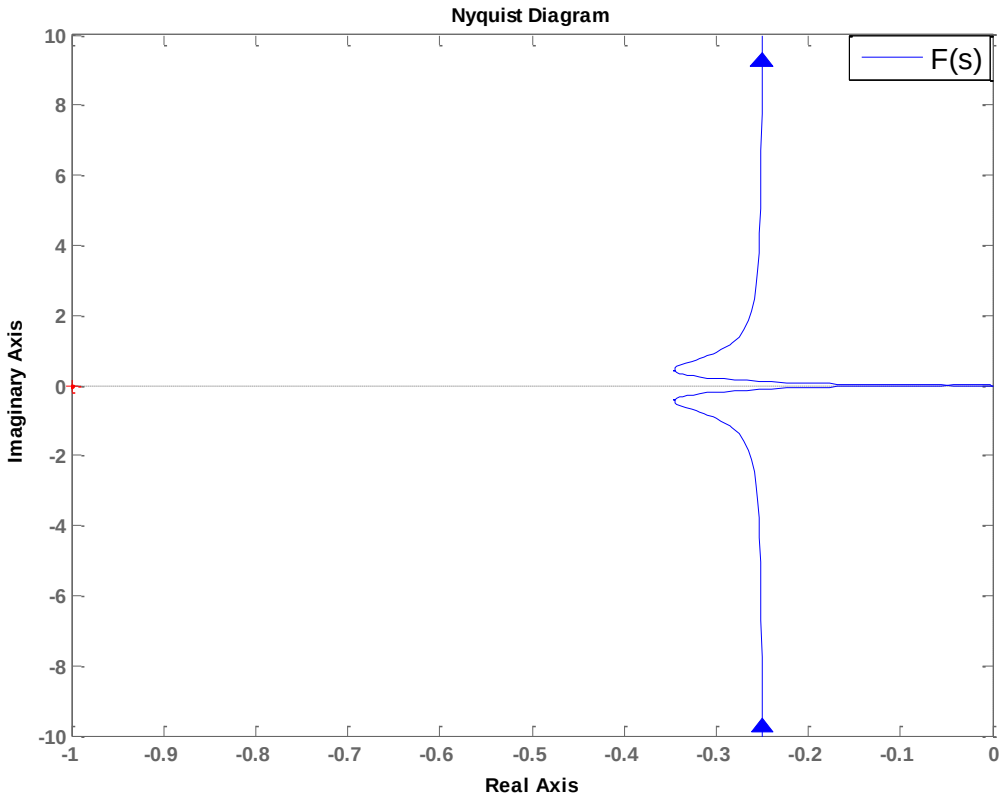

Figure 3-16. Nyquist plot of transfer function F(s) in (3.58)

Figure 3-17 shows the stability margin of the closed loop system in figure 3-12 (transfer function 3.32), for different controller parameters that are satisfying all the objectives. The higher the proportional gain is, the higher stability margin can be achieved. The same relation holds for the bandwidth of the system which also increases as the proportional gain increases.

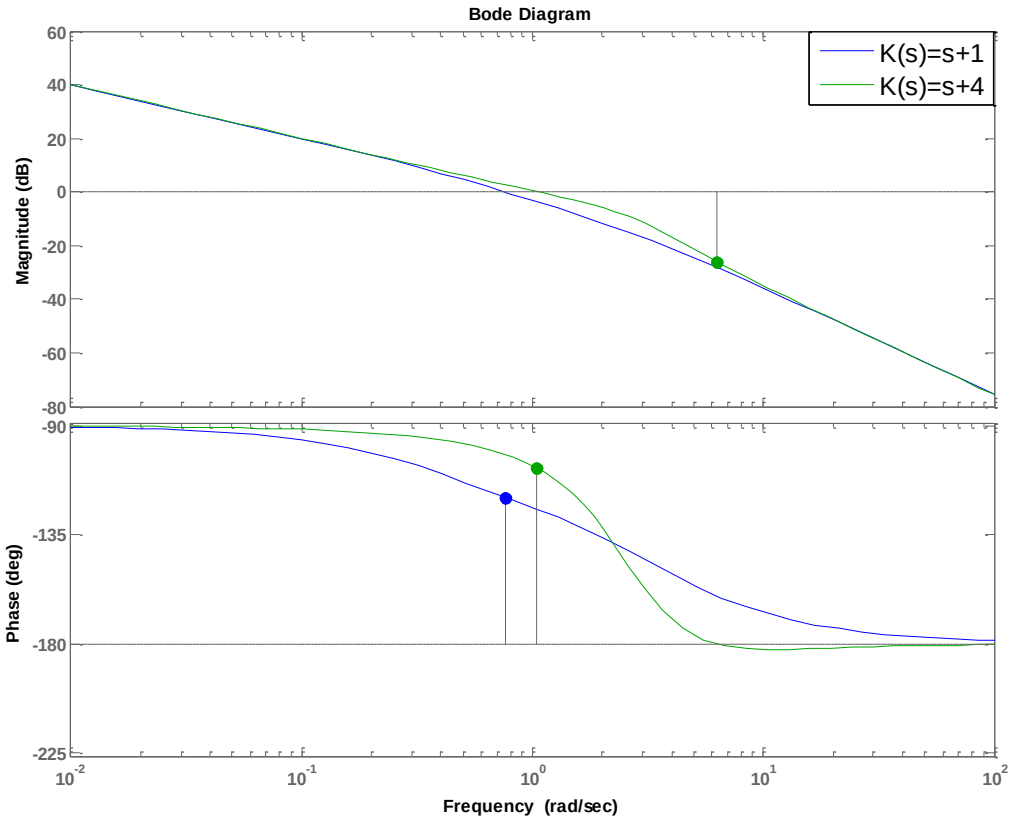

Figure 3-17. Bode plot of the open loop transfer function in figure 3-12 using PD controller

The plot of acceleration profile of the preceding vehicle and the ego vehicle (figure 3-18) shows the attenuation of preceding vehicle's acceleration. The transfer function from the preceding vehicle's acceleration to the ego vehicle's acceleration is

$$A_e(s) = \frac{K(s)}{\tau s^3 + s^2 + shK(s) + K(s)} A_p(s) \quad (3.59)$$

To check the condition of the string stability in the frequency domain, the bode plot for a fixed value of the headway time and different values of the controller based on the analysis on page 36 and 37, are used and the string stability condition is satisfied (figure 3-19).

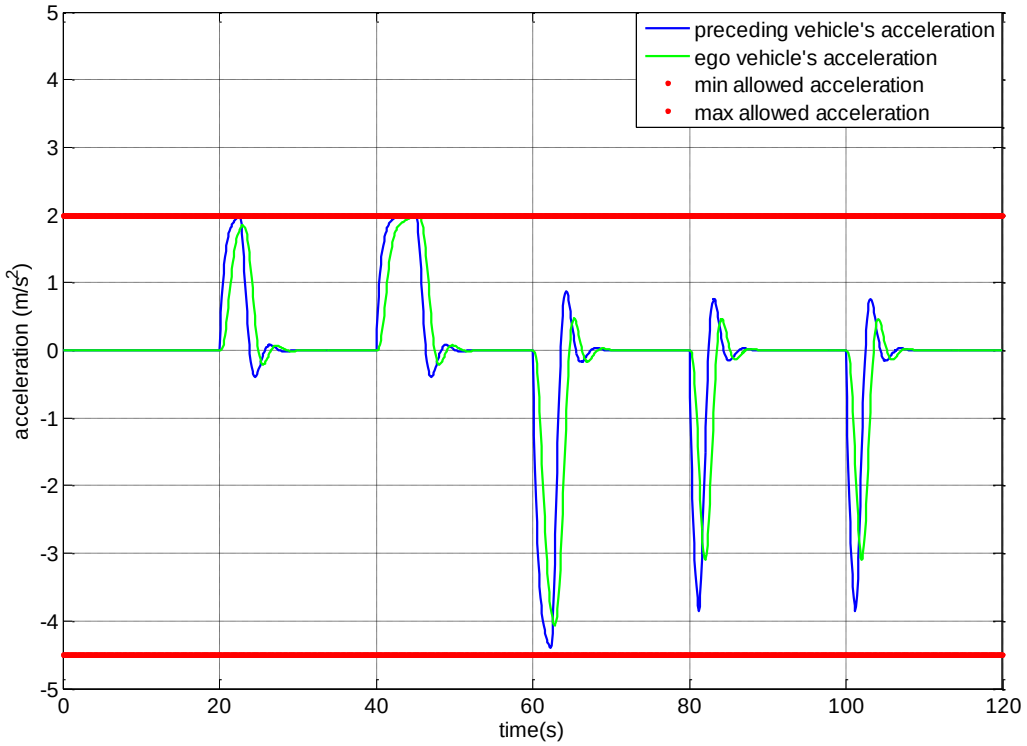

Figure 3-18. Acceleration profiles of the ego and the preceding vehicles

Remark

- The aforementioned controller scheme was based on the relative distance information that is provided by the radar sensor. Thus, there is no cooperative information used. But it is possible to obtain this information from V2V communication because in this thesis work, each vehicle sends its dynamic information including position, speed and acceleration with a fixed frequency to all other vehicles, and all of them are equipped with GPS. Therefore the information can also be cooperative in this case. In general, this information can be fused from both the radar and V2V communication.

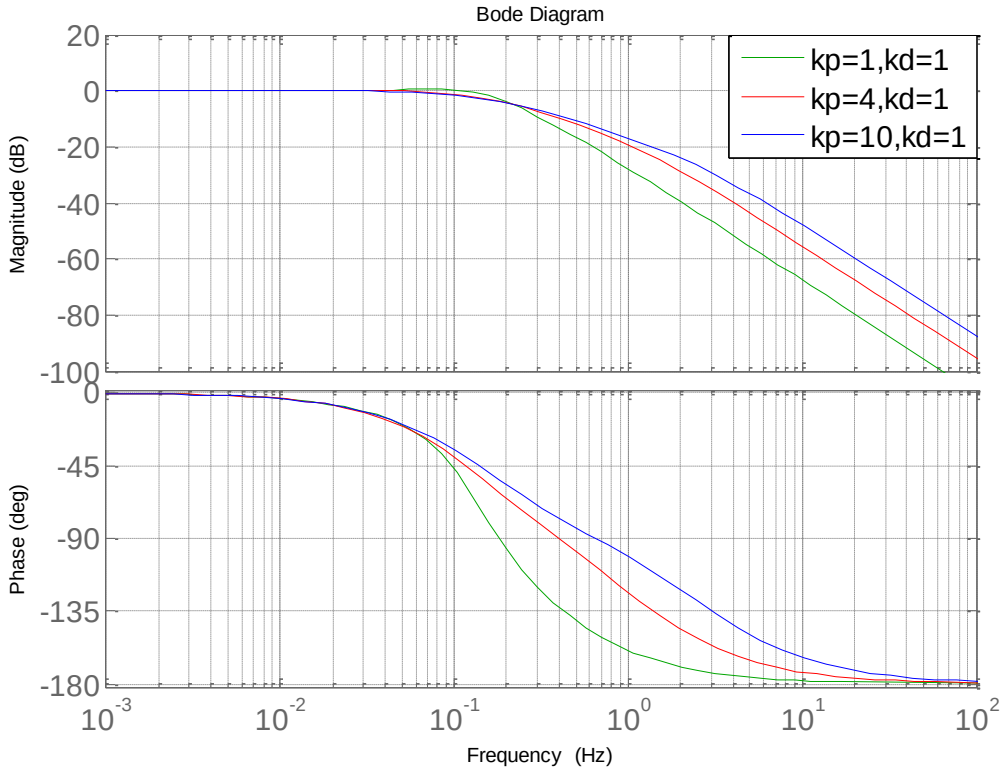

Figure 3-19. String stability condition for the R-D controller scheme using PD controller (transfer function 3.59)

3.3.2 Relative Acceleration, Speed and Distance (R-ASD) Controller Based on Only Preceding Vehicle's Information Using Constant Headway Time Approach

In the R-ASD controller scheme, the idea is to use more information about the preceding vehicle. To do this, besides the relative distance, the relative speed and acceleration are used, all with respect to the preceding vehicle. R denotes relative and A, S and D denote acceleration, speed and distance respectively. The information about the relative distance and the relative speed can be fused from radar and V2V, but the acceleration of preceding vehicle is provided by V2V communication.

Figure 3-20 shows the R-ASD controller scheme

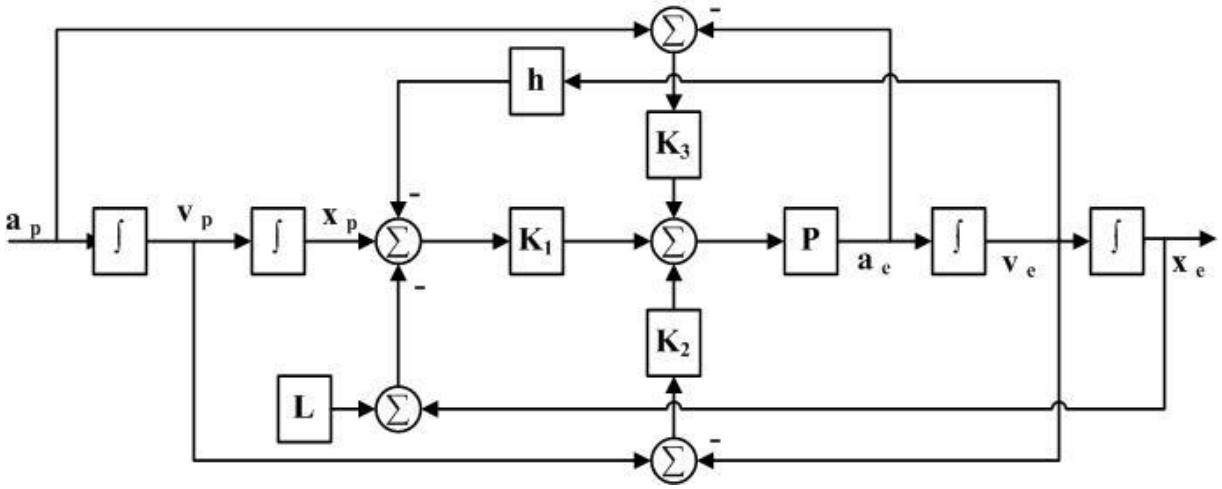

Figure 3-20. The R-ASD controller scheme (K_1, K_2, K_3 are the controllers, P is the plant model, h is the headway time, L is the safety distance and a, v, x are the longitudinal acceleration, speed and position of the ego vehicle (indices 'e') and preceding vehicle (indices 'p')

The control input has the following form

$$u = K_1(s)\left(X_p(s) - X_e(s) - \frac{l_p}{s} - hV_i(s) - \frac{L_{safe}}{s}\right) + K_2(s)\left(V_p(s) - V_e(s)\right) + K_3(s)\left(A_p(s) - A_e(s)\right)$$

$$u = K_1(s)\Delta\mathrm{X}(\mathrm{s}) + \mathrm{K}_2(s)\Delta V(s) + K_3(s)\Delta A(s) \quad (3.60)$$

$K_1(s)$, $K_2(s)$ and $K_3(s)$ are the controllers. Indices 'e' and 'p' are related to the ego and the preceding vehicles respectively. The control command is a summation of the output of three individual controllers that are acting on relative distance, speed and relative acceleration, as stated in equation.

It is important to mention that the relative distance and the relative speed (figure 3-20) are double and first integrations of the relative acceleration respectively. Thus, it is

possible to assume that the input to the system is the acceleration of the preceding vehicle. This assumption is considered in deriving transfer function (3.61) below.

The reference distance is

$$d_{ref} = safety\ distance\ +\ h * V_{ego}$$

The transfer function from the preceding vehicle's acceleration to the ego vehicle's acceleration is required for control design as it includes both the condition for the string stability and the characteristic polynomial of the closed loop system

$$\frac{A_e(s)}{A_p(s)} = \frac{s^2K_3(s)P(s) + sK_2(s)P(s) + K_1(s)P(s)}{s^2(1 + K_3(s)P(s)) + s\big(K_2(s)P(s) + hK_1(s)P(s)\big) + K_1(s)P(s)} \quad (3.61)$$

where $P(s) = \dfrac{1}{\tau s + 1}$

Controller parameters should be chosen in order satisfy all of the objectives mentioned in section 3.3.1. To have zero speed error, the same transfer function as in (3.61) holds from speed of the preceding vehicle to speed of the ego vehicle, meaning that

$$T(s) = \frac{V_e(s)}{V_p(s)}$$

$$=> T(s) = \frac{s^2K_3(s)P(s) + sK_2(s)P(s) + K_1(s)P(s)}{s^2\big(1 + K_3(s)P(s)\big) + s\big(K_2(s)P(s) + hK_1(s)P(s)\big) + K_1(s)P(s)} \quad (3.62)$$

$$\lim_{s\to 0} s\frac{V_e(s)}{V_p(s)} = 1 \quad (3.62)$$

Also for the positioning error

$$\frac{X_e(s)}{X_p(s)} = \frac{(1/s)V_e(s)}{(1/s)V_p(s)} = T(s) \quad , \quad \Delta X(s) = X_p(s) - X_e(s) \quad ,$$

$$V_e(s) = T(s)V_p(s) = sT(s)X_p(s) \quad (3.63)$$

$$=> E(s) = \big(1 - F(s)\big)X_p(s) - hsF(s)X_p(s) \quad (3.64)$$

$$\lim_{s\to 0} sE(s) = 0 => \lim_{s\to 0} s\Delta X(s) - shV_e(s) = 0 \quad (3.65)$$

To satisfy the above mentioned conditions, three proportional controllers (k_1, k_2, k_3) are sufficient.

To check the stability, characteristic polynomial of transfer function (3.61) is considered and the Routh stability criterion is used to determine for which values of the controller parameters (k_1, k_2, k_3), the closed loop system is stable.

$$\Delta(s) = s^2\big(1 + k_3P(s)\big) + s\big(k_2P(s) + hk_1P(s)\big) + k_1P(s) \quad (3.66)$$

$$P(s) = \frac{1}{\tau s + 1} \Rightarrow \Delta(s) = \tau s^3 + (1 + k_3)s^2 + (k_2 + hk_1)s + k_1 \quad (3.67)$$

s^3	τ	$hk_1 + k_2$	$(hk_1 + k_2) > 0$
s^2	$1 + k_3$	k_1	
s^1	$((hk_1 + k_2)(1 + k_3) - \tau k_1)/(1 + k_3)$		
s^0	k_1		

for stability $\Rightarrow k_1 > 0 \ \& \ (1 + k_3) > 0 \ \& \ (hk_1 + k_2)(1 + k_3) - \tau k_1 > 0 \quad (3.68)$

Condition (3.42) guarantees the string stability condition and considering assumption (2), the control input stays within the constraint limits$(-4.5(m/s^2) \leq u \leq 2(m/s^2))$. Hence, in order to satisfy condition (3.42), the control input sensitivity function is required

$$\frac{U(s)}{A_p(s)} = \frac{\left(s^2 K_3(s)P(s) + sK_2(s)P(s) + K_1(s)P(s)\right)}{\left(s^2\left(1 + K_3(s)P(s)\right) + s\left(K_2(s)P(s) + hK_1(s)P(s)\right) + K_1(s)P(s)\right)P(s)} \quad (3.69)$$

according to (3.42) $\Rightarrow \left\| \frac{U_i(j\omega)}{A_{i-1}(j\omega)} \right\|_\infty \leq 1$

Using k_1, k_2, k_3 and $P(s) = \frac{1}{\tau s + 1}$

$$\Rightarrow \frac{U(s)}{A_p(s)} = \frac{(s^2 k_3 + sk_2 + k_1)(\tau s + 1)}{\tau s^3 + (1 + k_3)s^2 + (k_2 + hk_1)s + k_1} \quad (3.70)$$

$$\Rightarrow \left\| \frac{U(j\omega)}{A_p(j\omega)} \right\|_\infty = \left\| \frac{(-k_3\omega^2 - \tau k_1\omega^2 + k_1) + j(k_1 + \tau k_1 - \tau k_3\omega^3)}{(-k_3\omega^2 - \omega^2 + k_1) + j(k_2 + hk_1 - \tau\omega^3)} \right\|_\infty \quad (3.71)$$

$$\Rightarrow \left\| \frac{U(j\omega)}{A_p(j\omega)} \right\|_\infty = \frac{(-k_3\omega^2 - \tau k_1\omega^2 + k_1)^2 + (k_1 + \tau k_1 - \tau k_3\omega^3)^2}{(-k_3\omega^2 - \omega^2 + k_1)^2 + (k_2 + hk_1 - \tau\omega^3)^2} \leq 1 \quad (3.72)$$

Thus, the values of controller parameters should satisfy the condition (3.72). To make sure that the constraint on control input is always met, a saturation function is used. By using saturation function, it is necessary to check the oscillation condition (3.11). Using closed loop transfer function in $(3.61), k_1, k_2, k_3$ and $P(s) = \frac{1}{\tau s + 1}$

$$(\text{open loop } TF)\ F(s) = \frac{T(s)}{1 - T(s)} \quad (3.73)$$

$$\Rightarrow F(s) = \frac{\tau s^3 + s^2 + hk_1 s}{\tau s^3 + (1 + k_3)s^2 + (k_2 + hk_1)s + k_1} \quad (3.74)$$

The Nyquist plot of the open loop transfer function *F(s)* in figure 3-21, doesn't intersect with the negative real axes. Considering the describing function of saturation which is a positive real valued (3.10), the oscillation condition (3.11) is not satisfied.

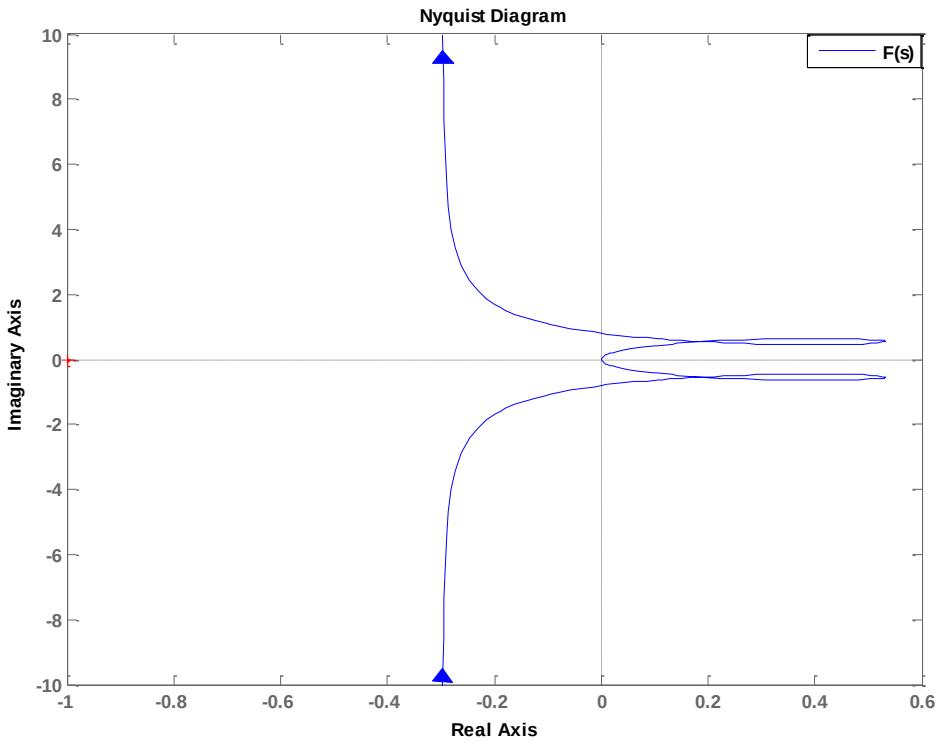

Figure 3-21. Nyquist plot of F(s) in (3.72)

The simulation results show the performance of the R-ASD controller in a platoon of vehicles. Based on the assumption (1), all of the follower vehicles in the platoon use the R-ASD controller architecture, with the same headway time. The vehicles can have different dynamics, which in this thesis means to have different time constants in the vehicle model, or they can have the same dynamics. In both cases, to guarantee string stability, condition (3.29) should be satisfied meaning that each vehicle should attenuate the acceleration of its preceding vehicle (indices 'e' and 'p' are replaced with 'i' and 'i_{-1}' when a platoon is considered).

Figure 3-22 shows the performance of the controller to meet the string stability condition. The string stability condition (3.29) for the R-ASD controller was obtained in (3.61). According to figure 3-22, the acceleration of ego vehicle is attenuating the acceleration of preceding vehicle. Hence, in a platoon where all of the follower vehicles use the R-ASD controller, each vehicle attenuates the acceleration of its preceding vehicle which is shown in figure 2-23 for a platoon of 6 vehicles.

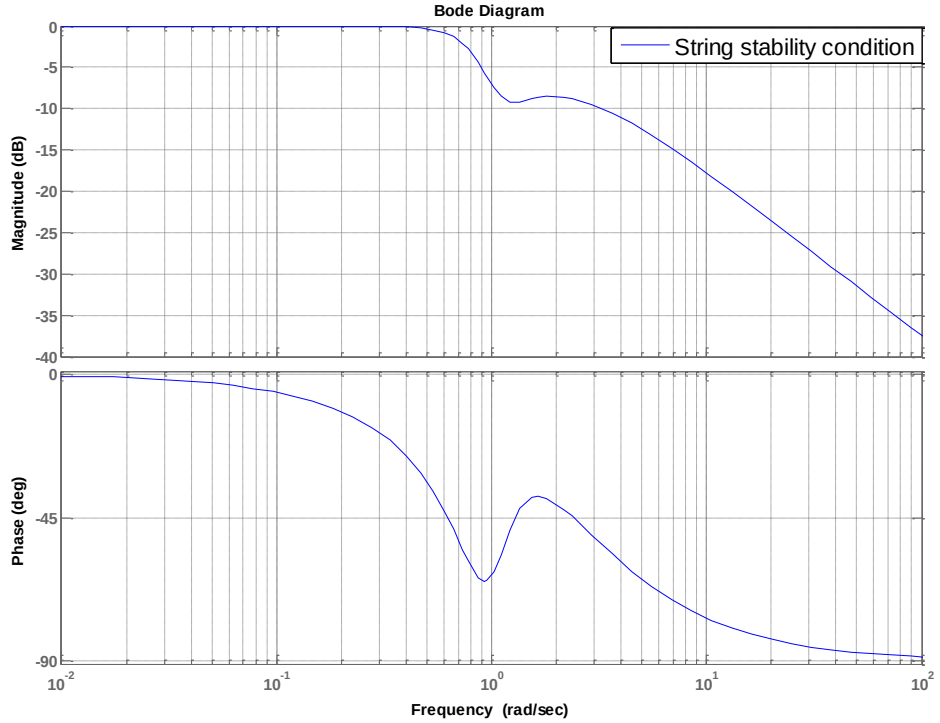

Figure 3-22. Frequency response of transfer function (3.61) (string stability condition)

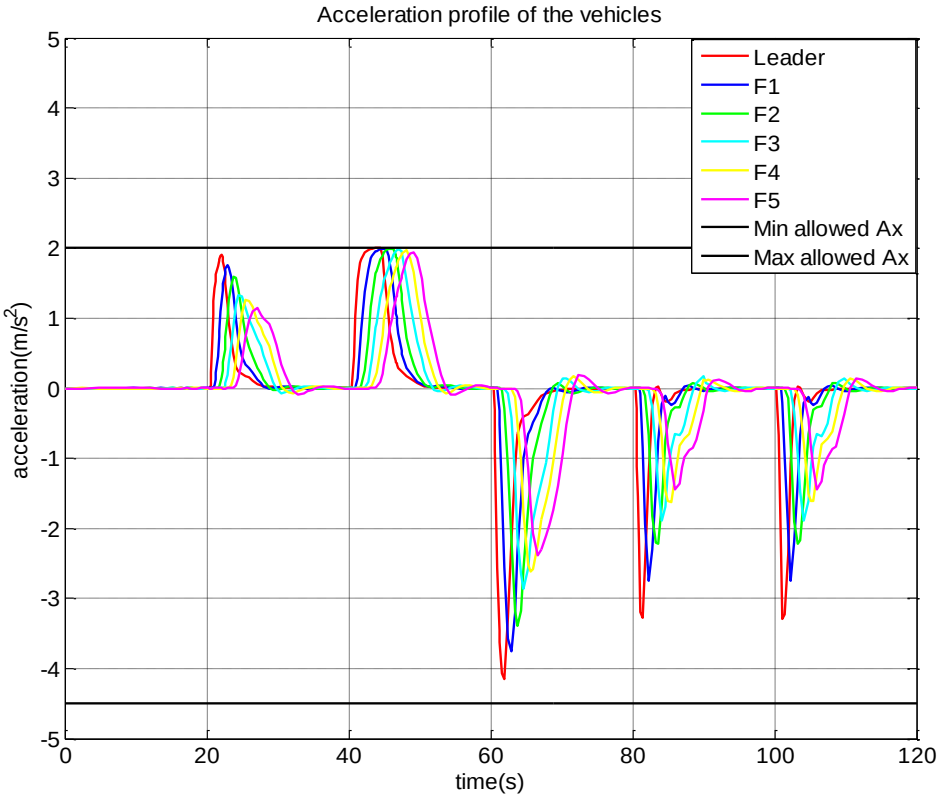

Figure 3-23. Acceleration profiles using the R-ASD controller in a platoon of vehicles ('F' denotes the follower vehicle and Ax is the longitudinal acceleration of the vehicle)

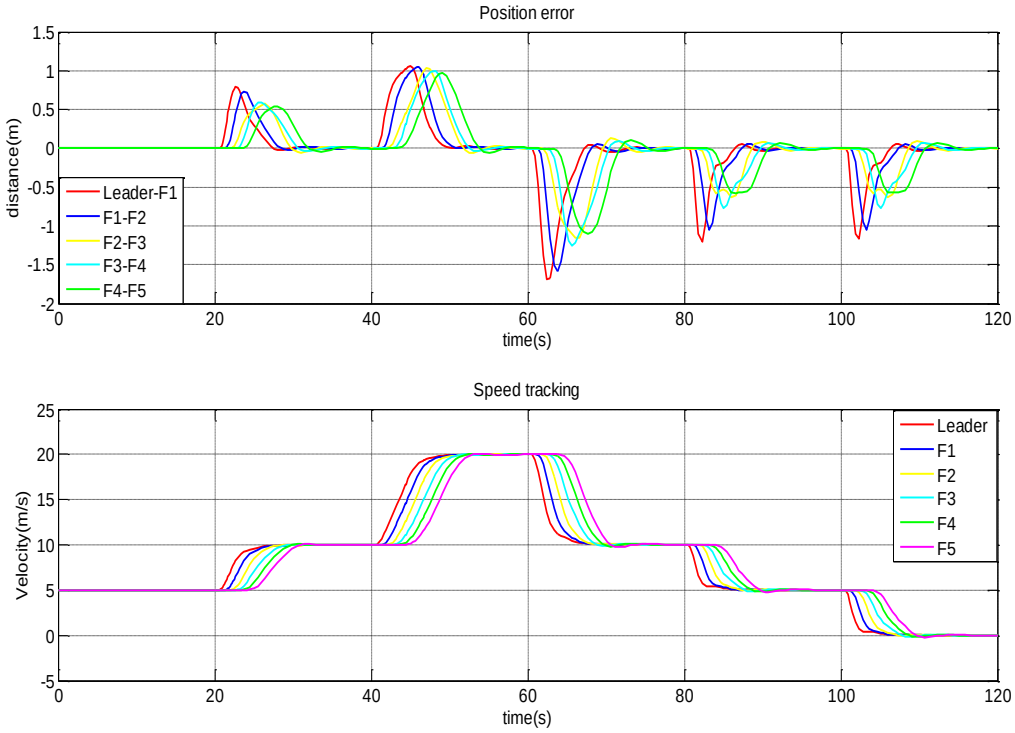

Figure 3-24. Position error and speed tracking using the R-ASD controller in a platoon of vehicles ('F' denotes the follower vehicle and Ax is the longitudinal acceleration of the vehicle)

The vehicle models used for the simulation result of figures 3-23 and 3-24 are as following

$$P_{F2}(s) = \frac{1}{0.5s + 1}$$

$$P_{F1}(s) = P_{F4} = \frac{1}{0.6s + 1}$$

$$P_{F3}(s) = P_{F5} = \frac{1}{0.4s + 1}$$

3.3.3 Comparison between the R-D and R-ASD Controllers[1]

It is interesting to compare the performance of both R-D and R-ASD controllers to see the difference and the advantage of using more information about the preceding vehicle.

According to the discussion that follows, the main advantage of the R-ASD controller compared to the R-D controller is that the R-ASD controller has higher stability margin compared to the R-D controller for the same system's bandwidth**.** Hence, the closed loop system with the R-ASD controller is more robust to actuation delay, compared to the closed loop system with the R-D controller. The design of the R-D and R-ASD controllers, were done without considering the actuation delay in the vehicle model (T=0). Figures 3-31 and 3-32 show the stability margin of the system using the R-D and R-ASD controllers for a zero actuation delay and the same system's bandwidth of 1 (rad/sec) (Time constant of the system is 0.6 seconds and the headway time is 1 second).

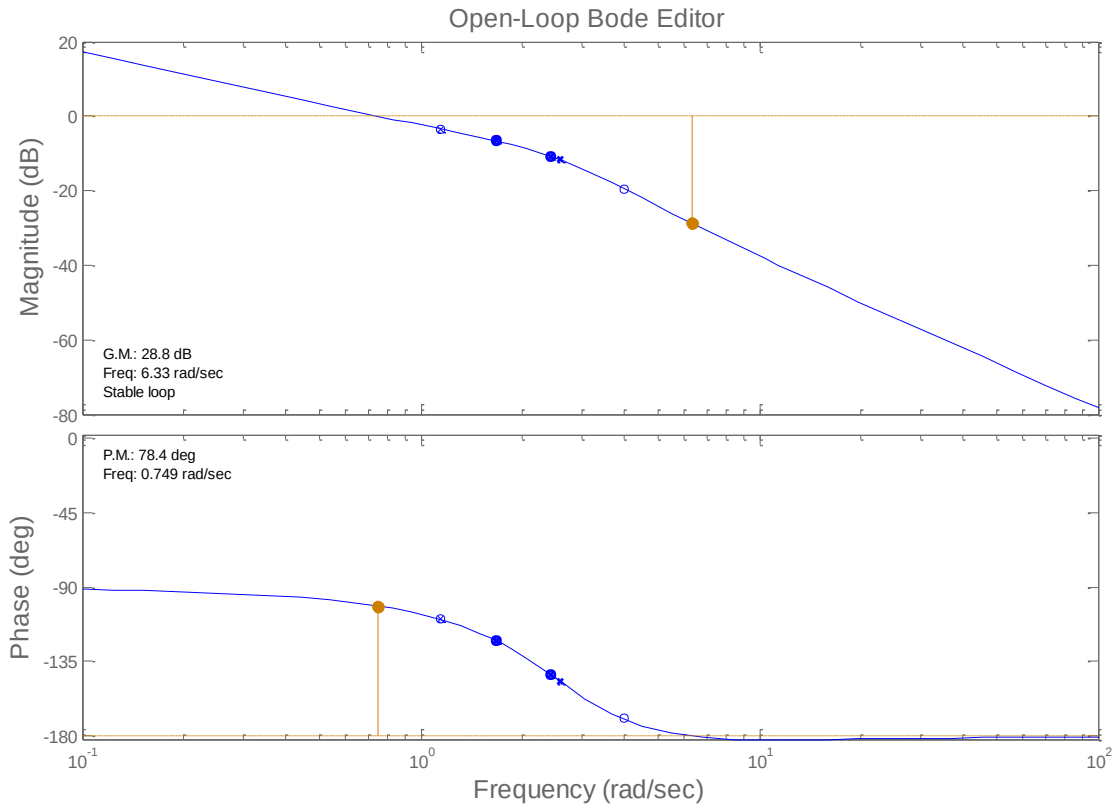

Figure 3-25. Open loop bode for the R-D controller using the PD controller scheme without the actuation delay (transfer function 3.58)

1- In this work, R-D and R-ASD controllers are only based on the preceding vehicle.

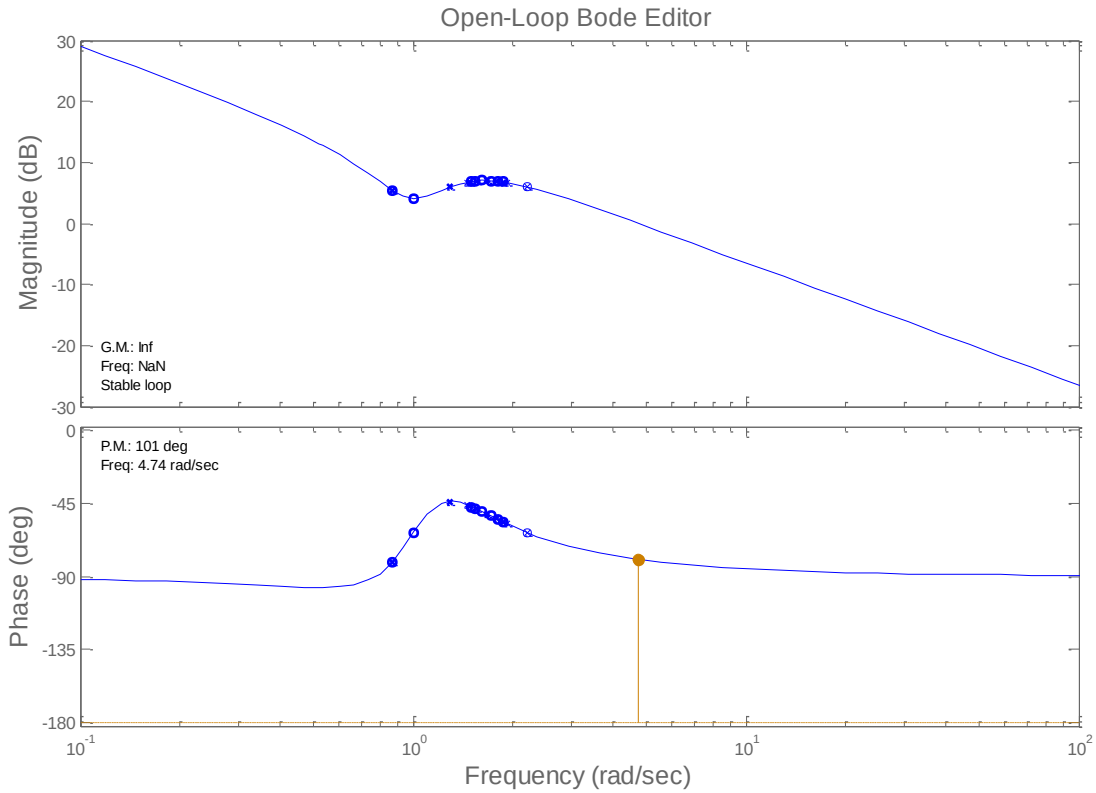

Figure 3-26. Open loop bode for the R-ASD controller scheme without the actuation delay (transfer function 3.73)

Hence, when there is no actuation delay in the vehicle model, for the same system's bandwidth, the stability margin of the system with the R-ASD controller is higher than the stability margin with the R-D controller. Therefore, the system with the R-ASD controller can remain stable for the larger values of the actuation delay. According to figure 3-25, for the system's bandwidth of 1 (rad/sec), the maximum actuation delay that is possible in order to have a stable loop with the R-D controller is

$$PM - \omega T \geq 0 \Rightarrow 1.368 - 0.749T \geq 0 \Rightarrow T \leq 0.18 \text{ s}$$

Based on the real car data, the actuation delay of the vehicle model varies between 0.2 to 0.5 seconds. Figures 3-27 shows the performance the R-ASD controller in presence of an actuation delay of 0.3 seconds and the system's bandwidth of 1(rad/sec). According to this figure the R-ASD controller, maintains a high stability margin which shows the robustness of the R-ASD controller to the actuation delay. The open loop transfer function used in figure 3-27, is the transfer function (3.73)

$$(\text{open loop } TF)\ F(s) = \frac{T(s)}{1 - T(s)}$$

Where T(s) is the closed loop transfer function mentioned in (3.62).

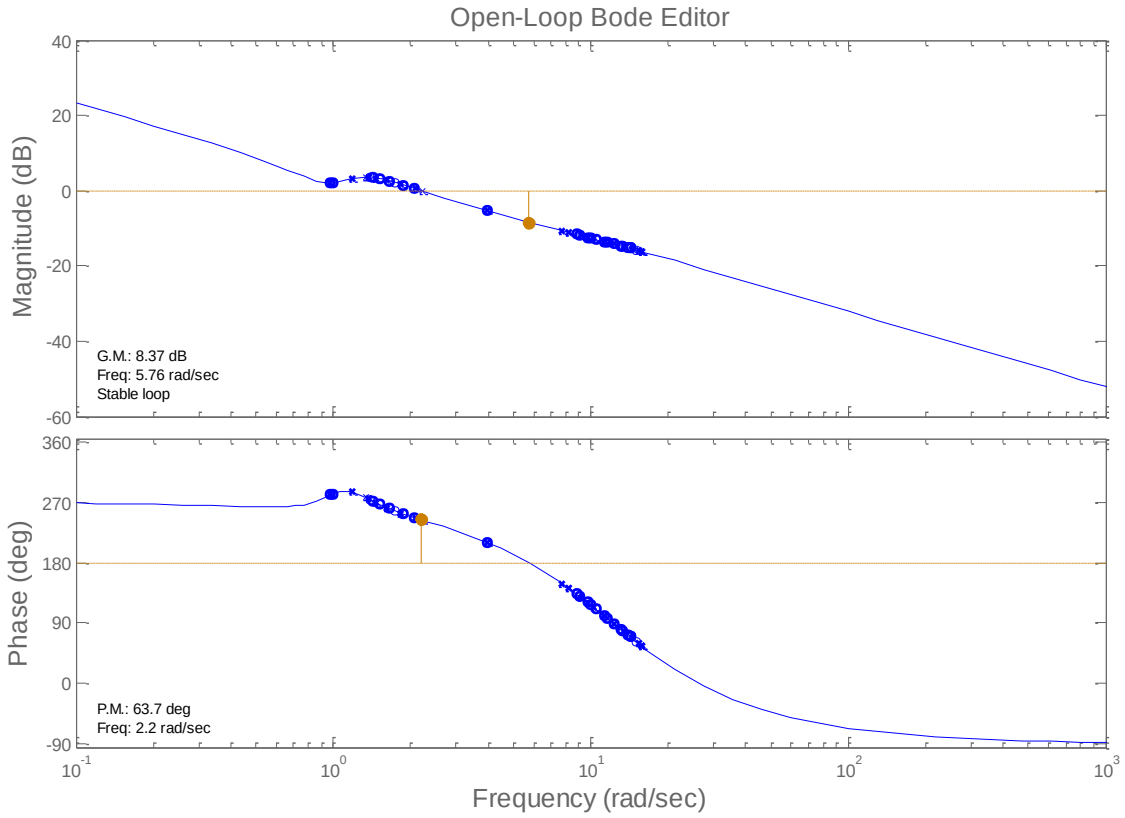

Figure 3-27. Open loop bode for the R-ASD controller scheme with actuation delay= 0.3 (s) (transfer function 3.73)

When there is no actuation delay (which is not the case in practice), both the R-D and the R-ASD controllers have a satisfactory performance meaning that both satisfy the string stability condition (damping the preceding vehicle's acceleration) and both have a good tracking performance. Figure 3-28 shows the comparison between these two controllers in terms of the string stability condition, when there is no actuation delay in the vehicle model.

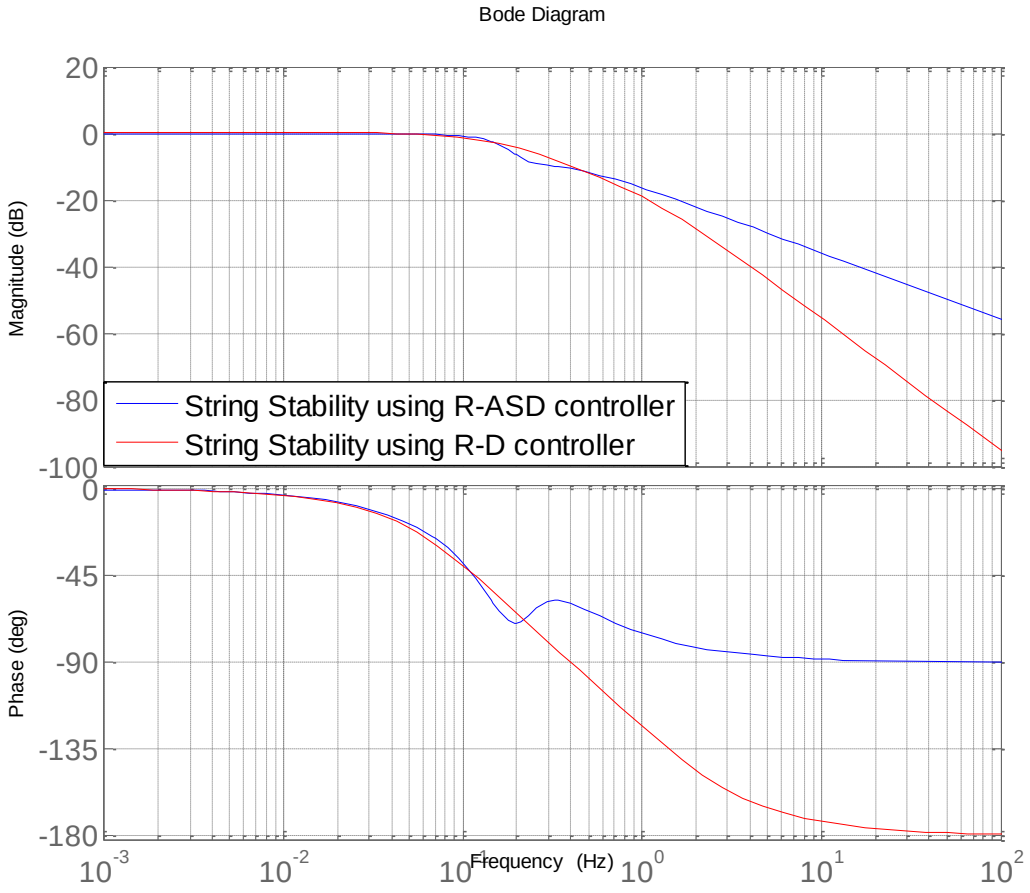

Figure 3-28. Comparison between the R-D and the R-ASD controllers in terms of string stability when the actuation delay is zero (h = 1s and τ = 0.6s)

In the design of the R-D and R-ASD controllers, no measurement noise was considered on the radar and V2V signals. According to the real car data, the relative distance and speed provided by the radar were already filtered and the only signal that was noisy was the vehicle's acceleration.

By using the experimental results, it is possible to roughly calculate the noise specifications including the frequency range of operation and also the mean value and the variance. Figure 3-29 shows the one sided frequency spectrum of the vehicle's acceleration based on the experimental data showed in figure 2-5.

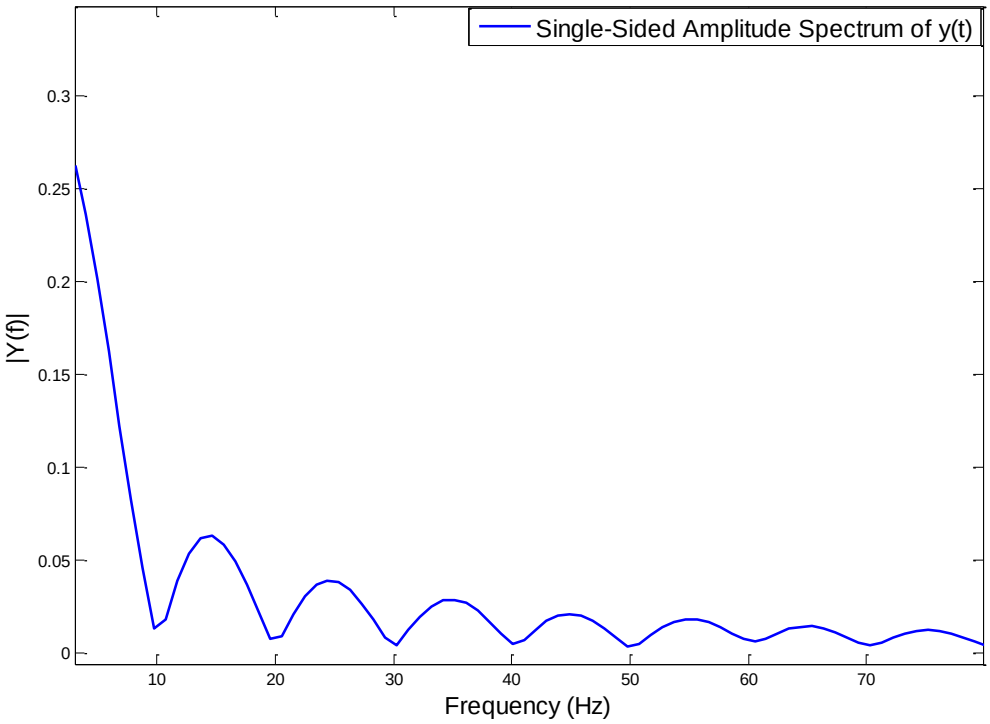

Figure 3-29. One Sided frequency spectrum of the vehicle's acceleration in figure 2-5

The commanded acceleration in figure 2-5 was a constant acceleration. Considering the plant model in (2.2) which has a low pass characteristic, it is expected that the large amplitudes at low frequencies are related to the signal spectrum, and the noise which approximately has a frequency range greater than 10 Hz, is filtered by the plant model. In the next chapter, it will be shown that plant model filters the noise on the acceleration signal.

The R-D controller doesn't use the acceleration signal and therefore it is not affected by the measurement noise. Also the R-ASD controller isn't affected by the noise on the acceleration signal, as the plant model has a low pass character.

Regarding the measurement time delays, it is expected that they decrease the stability margin of the system. The closed loop transfer function using the R-D and R-ASD controllers, considering the measurement time delays are as following

For the R-D controller, from (3-56)

$$T(s) = \frac{K(s)e^{-sT_a}G(s)}{s^2 + shK(s)e^{-sT_a}G(s) + K(s)e^{-sT_a}G(s)} \quad (3.75)$$

And for the R-ASD controller, from (3.62)

$$\frac{A_e(s)}{A_p(s)} = \frac{s^2K_3(s)e^{-sT_a}P(s) + sK_2(s)e^{-sT_v}P(s) + K_1(s)e^{-sT_d}P(s)}{s^2(1 + K_3(s)e^{-sT_a}P(s)) + s\left(K_2(s)e^{-sT_v}P(s) + hK_1(s)e^{-sT_d}P(s)\right) + K_1(s)e^{-sT_d}P(s)} \quad (3.76)$$

Where T_a, T_v and T_d are measurement time delays on the relative acceleration, speed and distance respectively. $K_1(s)$, $K_2(s)$ and $K_3(s)$ are the controllers on the relative distance, speed acceleration respectively and P(s) is the plant model in (2.2).

A system with the R-D controller is affected by one measurement time delay on relative distance while a system with the R-ASD controller encounters three measurement time delays on relative distance, speed and acceleration. Thus, having a high stability margin for the system with the R-ASD controller is more important than the R-D controller. Figure 3-30 shows the stability margin of both controllers for the same system's bandwidth of 0.8 (rad/s) considering their respective measurement time delays. The delay values are adapted according to the specification data from the radar and communication.

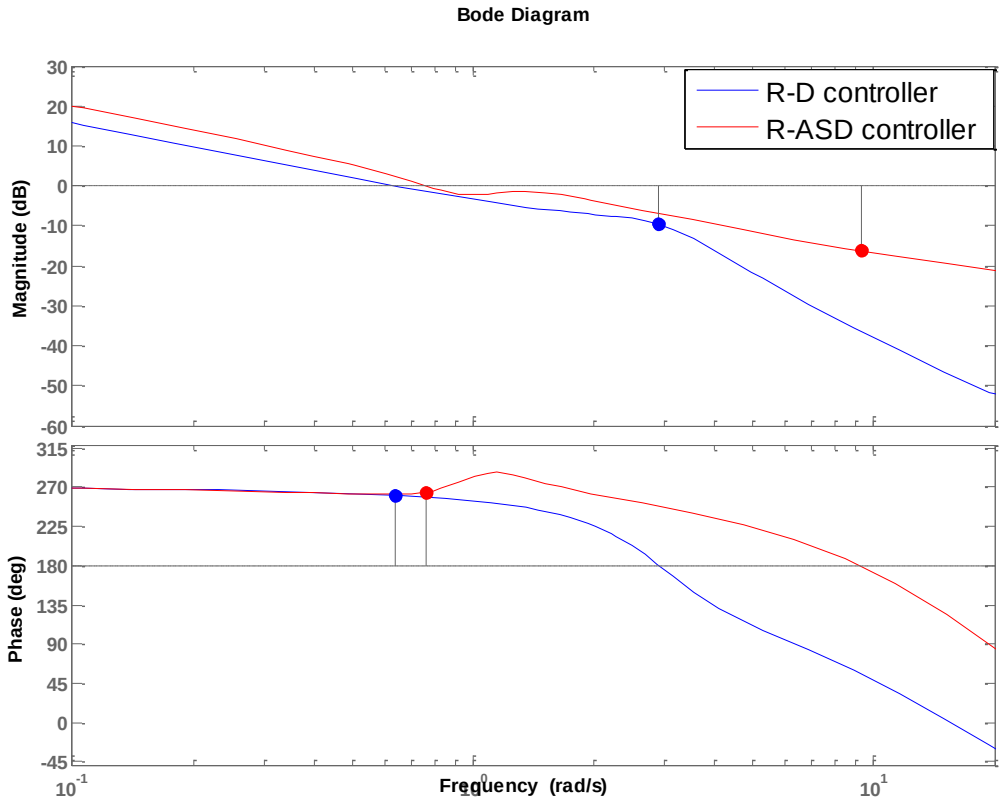

Figure 3-30. Stability margin of the systems with the R-D and R-ASD controllers considering the measurement time delays

$$(\tau = 0.6\ s, h = 1, T_a = 0.025\ s, T_v = 0.1\ s, T_d = 0.2\ s\ , BW = 0.8\ \frac{rad}{s})$$

3.3.4 Using Information of Other Vehicles in Control Design

3.3.4.1 Why using information from other vehicles?

The concept of the cooperative driving is aimed to reduce traffic congestions as well as to increase safety and reduce fuel consumption. When one vehicle has information about other vehicles on the road, it can decide in advance which action to take. So it is possible to drive safer and smoother.

Imagine a string of vehicles is travelling in the same lane on the highway. If these vehicles communicate their dynamic information, such as acceleration, speed and position, it is possible for the vehicles further back in the string to know in advance about braking or accelerating of other vehicles in front of the string. With this information they can avoid unnecessary braking (reducing fuel consumption) or brake smoothly when a sudden brake is happening in front of the string.

Considering these advantages, in this work the idea is to include the information about the acceleration of the vehicle in front of the preceding vehicle (figure 3-32) which from now on is called “preceding + 1 vehicle”.

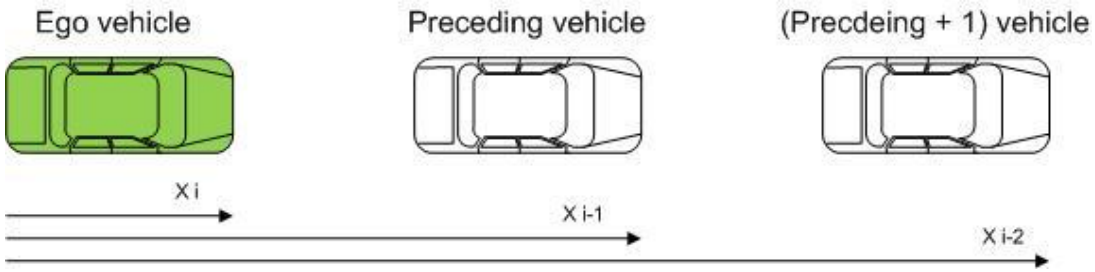

Figure 3-31. Position of (preceding + 1) vehicle in the platoon

3.3.4.2 Control Scheme and Formulation

The scheme of the proposed controller is shown in figure 3-32 below

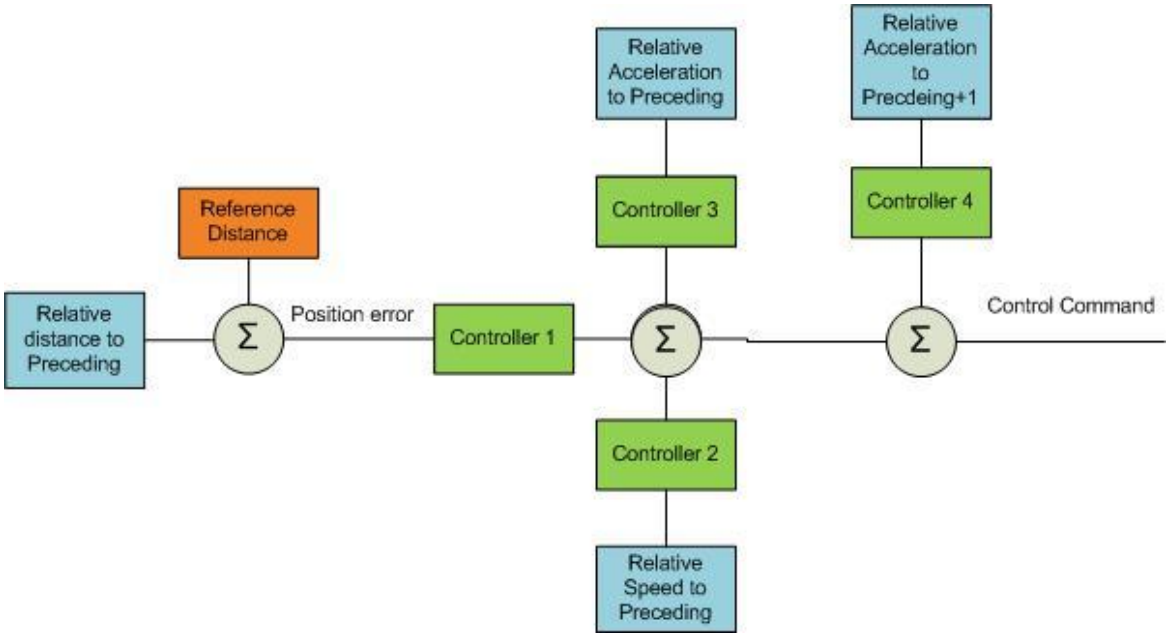

Figure 3-32. Control scheme based on the preceding and the precdeing+1 vehicles

The difference with the scheme of the R-ASD controller is that another controller is included that regulates the relative acceleration to the preceding+1 vehicle.

For the reference distance, we still look at the preceding vehicle. The main reason is safety, as it is always necessary to have control over the relative distance to the preceding vehicle. Another reason is that calculating the relative distance to other vehicles in front of the ego vehicle requires exact positioning equipment which is not the case in this work.

Considering the relative speed to both the preceding+1 and the preceding vehicles can also be challenging because the performance of other vehicles in front can influence the performance of our vehicle. For example, if the preceding+1 vehicle accelerates to 50 (km/h) but the preceding vehicle accelerates to 40 (Km/h), then we must also accelerate to 40(km/h) as we don't want to hit the front vehicle. Therefore, controlling the relative speed to the preceding+1 vehicle is dependent on the preceding vehicle's performance. Therefore, we keep using the dynamic information of the preceding vehicle (as in the R-ASD controller) and try to improve the platooning performance by using extra information from other vehicles.

The control input has the following form

$$u = K_1(s)\left(\Delta X_p\right) + K_2(s)\left(\Delta V_p\right) + K_3(s)\left(\Delta Ax_p\right) + K_4(s)\left(\Delta Ax_{pp}\right) \qquad (3.77)$$

And the plant model is

$$P(s) = \frac{1}{\tau s + 1} e^{-Ts}$$

Where

ΔX_p : Relative distance to the preceding vehicle

ΔV_p : Relative speed to the preceding vehicle

ΔAx_p : Relative acceleration to the preceding vehicle

ΔAx_{pp} : Relative acceleration to the preceding+1 vehicle

Since the acceleration of the preceding+1 vehicle is used in control scheme of figure 3-32, the system has two different accelerations as inputs.

The transfer function from the preceding vehicle's acceleration to the ego vehicle's acceleration is

$$\frac{A_i(s)}{A_{i-1}(s)} = \frac{s^2 K_3(s)P(s) + sK_2(s)P(s) + K_1(s)P(s)}{s^2 + \big(K_3(s) + K_4(s)\big)s^2 P(s) + \big(hK_1(s) + K_2(s)\big)sP(s) + K_1(s)P(s)} \qquad (3.78)$$

P(s) is the plant model and $K_{1,2,3,4}$(s) are the controllers.

For the string stability, the controller design should be such that the infinity norm of (3.78) is less than or equal to one. Controller parameters are chosen such that all of the aforementioned criteria in section 3.3.1 are satisfied (the procedure is the same as for the R-D and the R-ASD controllers).

In figure 3-33, the performance of the controller to track the reference distance and reference speed is shown for the platoon of three vehicles. The ego vehicle is assumed to be at the end of the platoon. Here the preceding+1 vehicle is also the leader vehicle. All of the vehicles in figure 3-33 and 3-34 have the same dynamics. Follower 1 uses the R-ASD controller, while follower 2 uses controller (3.77). Both followers use the same headway time. The scenario used for the simulation results of figures 3-33 and 3-34 is based on the speed profile showed in figure 3-14 for the leader vehicle.

The reference and minimum distances are

d_{ref}=safety distance $+ h * V_{ego}$, d_{min} = safety distance $+ 0.6 * V_{ego}$

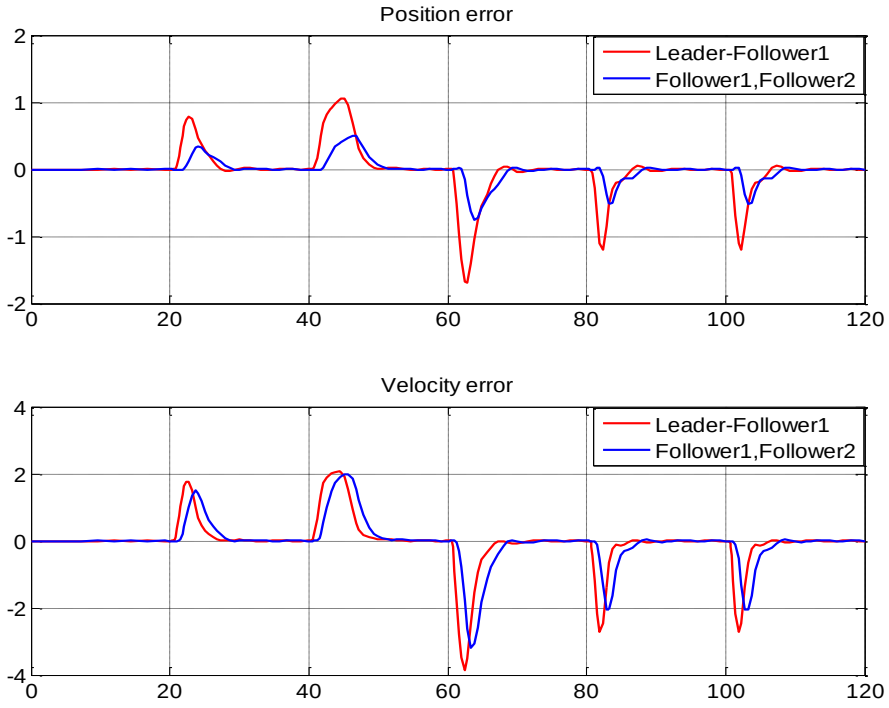

Figure 3-33. The position error and the speed error while using controller (3.77) for follower 2 and R-ASD controller for follower 1

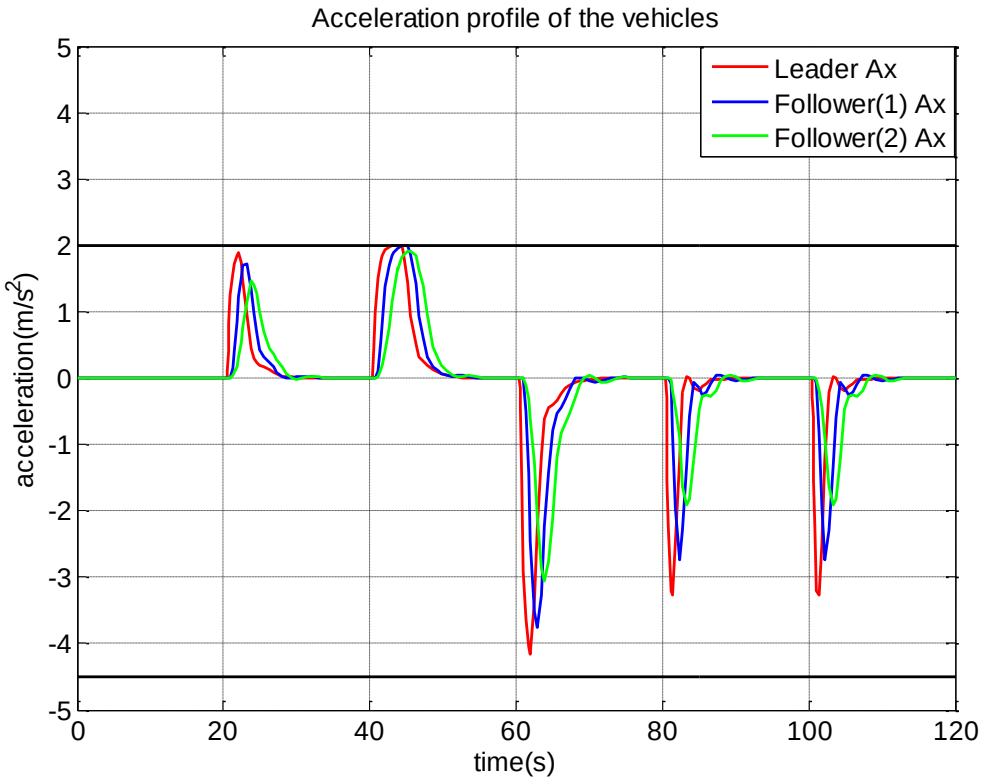

Figure 3-34. Acceleration profiles of the preceding+1, the preceding and the ego vehicles

In figure 3-34 the acceleration profiles of the preceding+1, the preceding and the ego vehicles are shown where the acceleration of ego vehicle is damping the preceding vehicle's acceleration. Using the bode plot in figure 3-35 also confirms this fact.

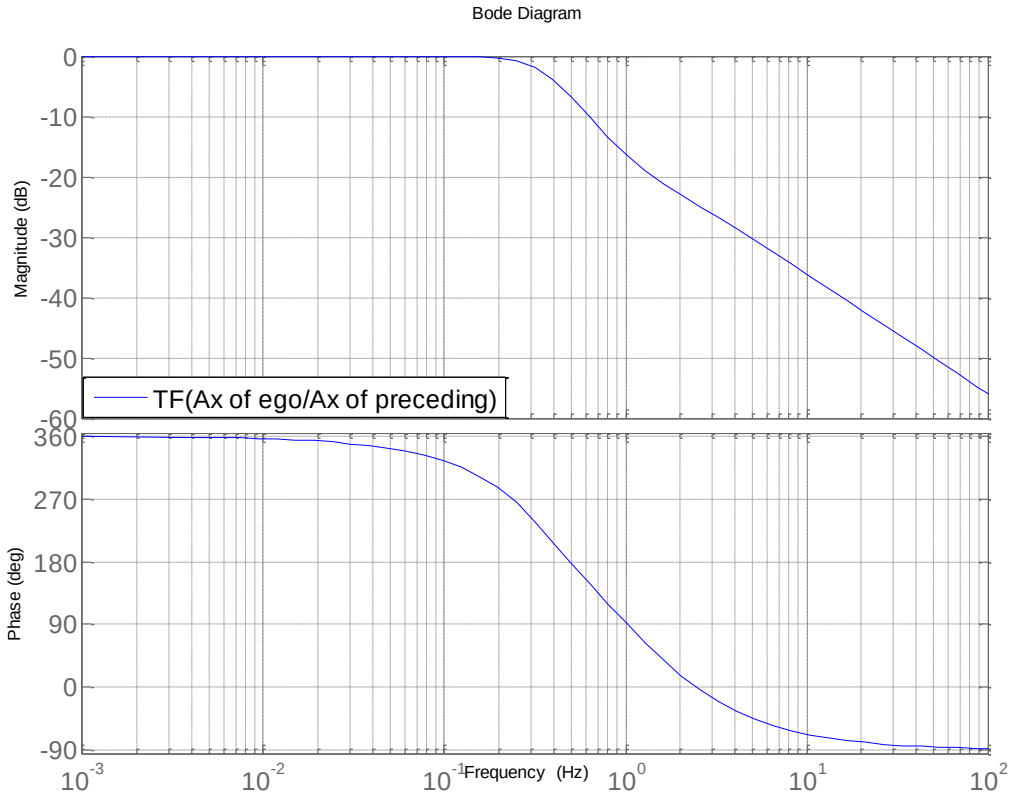

Figure 3-35. Bode plot of transfer functions (3.78) showing the string stability condition

It would be interesting to see the effect of this extra information on string stability. In figure 3-36, a comparison between this controller (controller (3.77)) and the R-ASD controller is shown using the bode plot.

As can be seen in figure 3-36, the attenuation level of the preceding vehicle's acceleration in both controllers is almost the same. But it is important for a string stable platoon to attenuate the preceding vehicle's acceleration. So, in this regard both controllers have almost the same quality. It should be mentioned that both frequency responses (with and without the preceding+1 vehicle) were plotted for the tuned controllers[1].

1- k_1, k_2 and k_3 for the tuned controller in (3.77) are different from k_1, k_2 and k_3 in the tuned R-ASD controller.

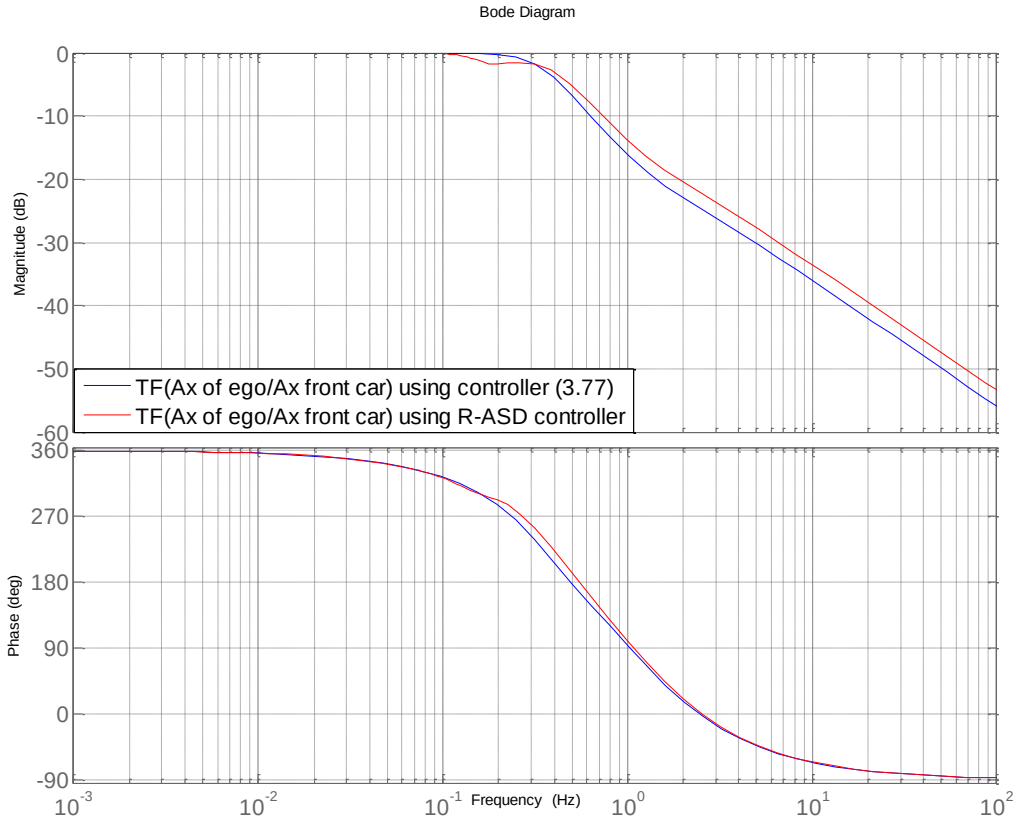

Figure 3-36. Effect of using controller (3.77) on string stability (Ax is the longitudinal acceleration)

In all of the results shown so far, controller (3.77) was used where the only extra information was the acceleration of preceding+1 vehicle compared to the R-ASD controller. Having this information can enable the ego vehicle to become aware of the state in front of the platoon earlier than the time when it only uses information from the preceding vehicle. This could result in a faster reaction to disturbances affecting the platoon, such as changes in the acceleration of vehicles further in front, compared to the case when this information isn't used. This result was observed in the simulation, focusing on the 'position error'. The position error addresses the platoon's length and shows the variation of platoon's length when a disturbance (such as a change in the leader vehicle's acceleration) is affecting the platoon.

Figure 3-37 shows that by using the acceleration of preceding+1 vehicle, the length of the platoon can be reduced when a disturbance is affecting the platoon and the ego vehicle is able to travel in a shorter inter-vehicle distance. Due to limited time and scope of this study, the analysis of this hasn't been included. The scenario used for this simulation result is based on the speed profile showed in figure 3-14 for the leader vehicle. In this figure, the position error between follower 1 and follower 2, when follower 2 uses the R-ASD controller, is compared with the position error when follower 2 uses controller (3.77).

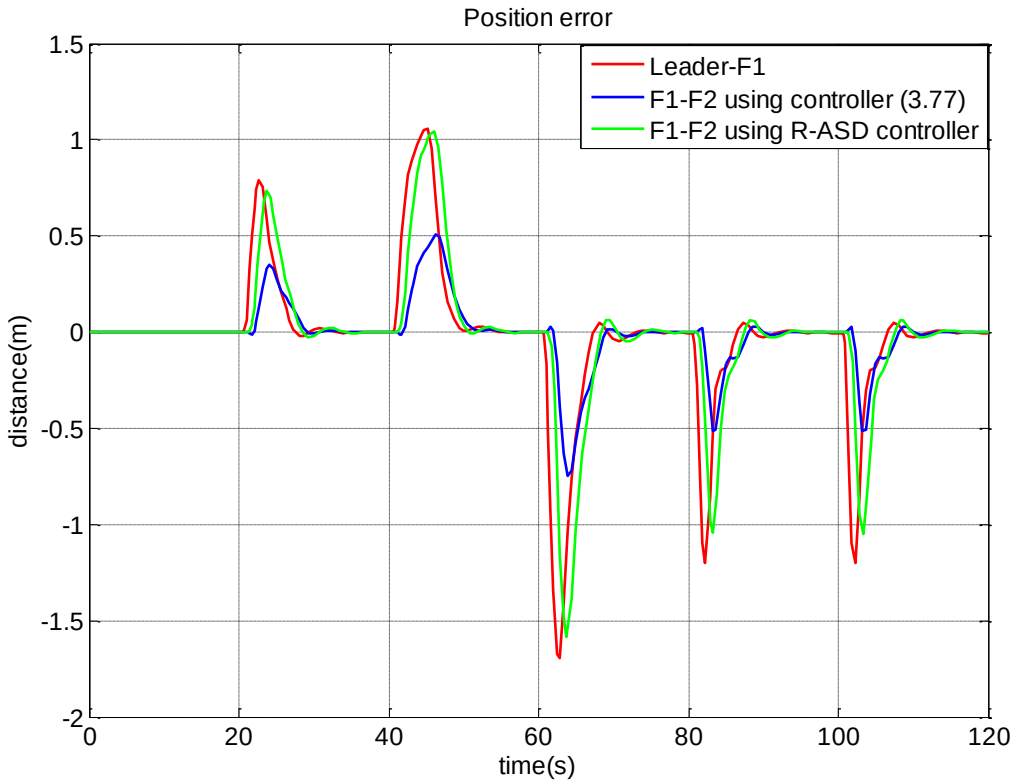

Figure 3-37. Position error with and without using the preceding+1 vehicle's acceleration (F denotes the follower vehicle)

Therefore, for a longer platoon of vehicles, platoon length can be reduced. This helps to alleviate congestion problems. Hence, compared to the R-ASD controller, this controller scheme can help to shorten the platoon's length by allowing the vehicles to travel in a shorter inter-vehicle distance, without deteriorating the string stability condition and the controller performance.

It should be mentioned that the idea of this section was to use extra information about the vehicles in the platoon, other than the preceding vehicle's information, in order to reduce traffic congestion by reducing the platoon's length, while maintaining string stability and satisfying all the objectives mentioned for control design. This information can be provided by any vehicle in front of the ego vehicle and in general it can be about any dynamic information of the vehicles such as speed or position.

In figure 3-38, the position error in the platoon of R-ASD vehicles (vehicles that use the R-ASD controller) is compared with the position error in the platoon of vehicles where all followers except the first follower, are using controller (3.77). As emphasis here is on the platoon's length and inter-vehicle distance, in both platoons all of the vehicles have the same dynamics and use the same headway time. The scenario for this result is based on the speed profile showed in figure 3-14 for the leader vehicle, and only the time span from 40 (s) to 80 (s) is studied.

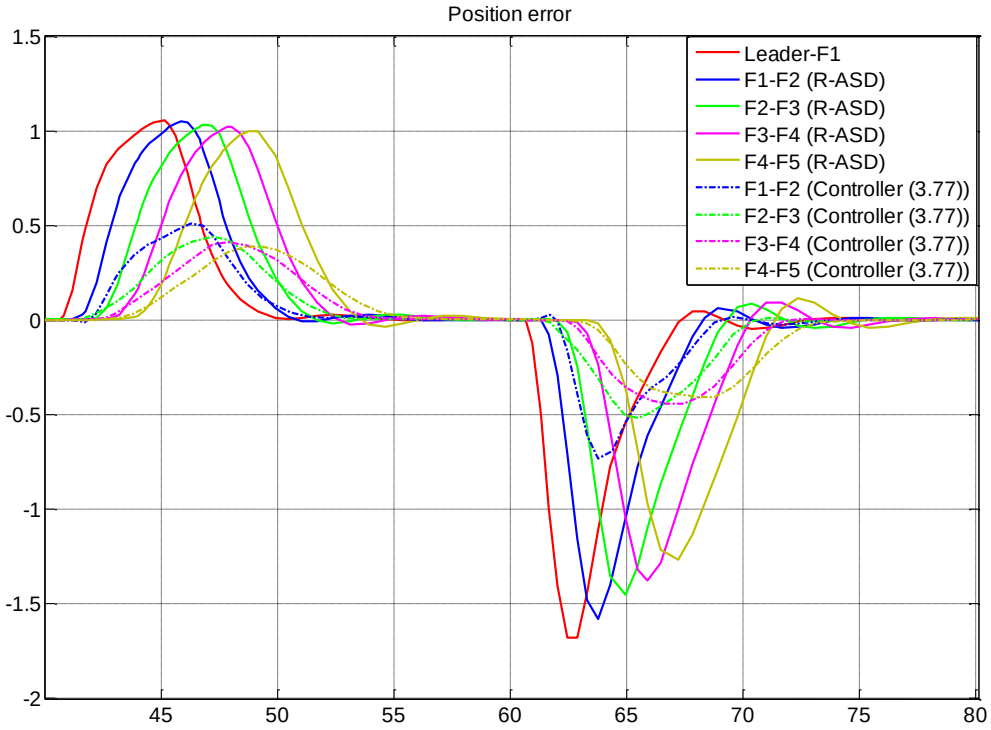

Figure 3-38. Position error in the platoon of the R-ASD vehicles compared to the platoon of vehicles that use controller (3.77) (F denotes the follower vehicle)

Chapter 4: Experimental Validation

In this chapter, experimental results obtained during the testing phase of the project are presented. Besides testing the controller, there were also other components that needed to be tested. One of these components was 'Sensor Fusion' which fuses V2V, V2I and the radar information. Filtering the required signals for the controller using 'Kalman' filter was also a part of this component. So before testing the controller, we must ensure that all of the signals required for the controller are provided correctly and come from a right source.

Different controllers have been tested. In Sections 4.1, the results of the R-ASD controller based on the preceding vehicle are presented. Next, in section 4.2, the results of the controller that uses information from both the preceding and the preceding+1 vehicles (controller (3.77)) are shown.

In appendix A, Model Predictive Controller (MPC) based on only the preceding vehicle is presented, and then the related test results are provided. This controller was developed by R.Kianfar in [13] and was tested during the testing phase. The purpose of introducing this controller is to compare the performance of it with the R-ASD controller based on the preceding vehicle designed in the chapter 3, in handling the constraints of the problem.

4.1 R-ASD Controller Based on the Preceding Vehicle

The aim during the testing phase was to find appropriate values for the controller parameters such that all of the objectives mentioned in section 3.3.2 are satisfied.

As it was discussed in the previous chapter, there are several criteria that the controller should satisfy such as tracking the reference distance, speed, string stability, meeting the constraint on the control input and the constraint on relative distance to the preceding vehicle. Scenarios for testing the controller covered the following **cases:**

1) The steady state case which means that the leader or the preceding vehicle goes from one speed to another. This test is helpful to tune the controller for tracking a reference distance and speed while satisfying string stability.
2) The oscillation test which means that the leader or the preceding vehicle is changing its speed between two different speeds. This test is helpful to excite a certain frequency in the system and examine if the string stability condition is satisfied for that frequency.

When the plots of each test are provided, it is also mentioned which type of test has been performed. The numbering of the tests is based on [14].

Test 197 {headway time= 1(s) and safety distance 10(m)}

In this test, the first case was tested and the following results showing the tracking performance, the control command and the string stability condition were obtained.

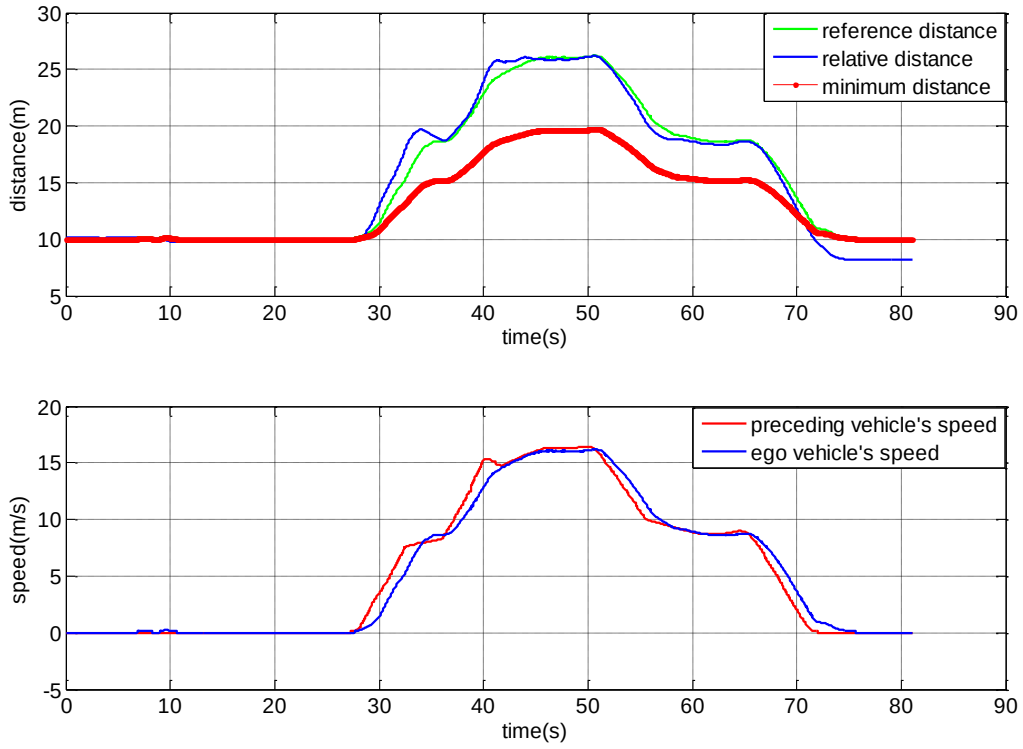

Figure 4-1. Tracking the distance reference and tracking the speed

A typical problem with this type of controller is shown here and that is when the ego vehicle is going to full stop and the minimum distance requirement is violated. One reason is the delay time, because as it is shown in the lower plot of figure 4-1, the speed of ego vehicle has a time delay with respect to the preceding vehicle and therefore in the full stop mode the ego vehicle realizes that the speed of the preceding vehicle is zero with some delay. The other reason was discussed in section 3.3.1.

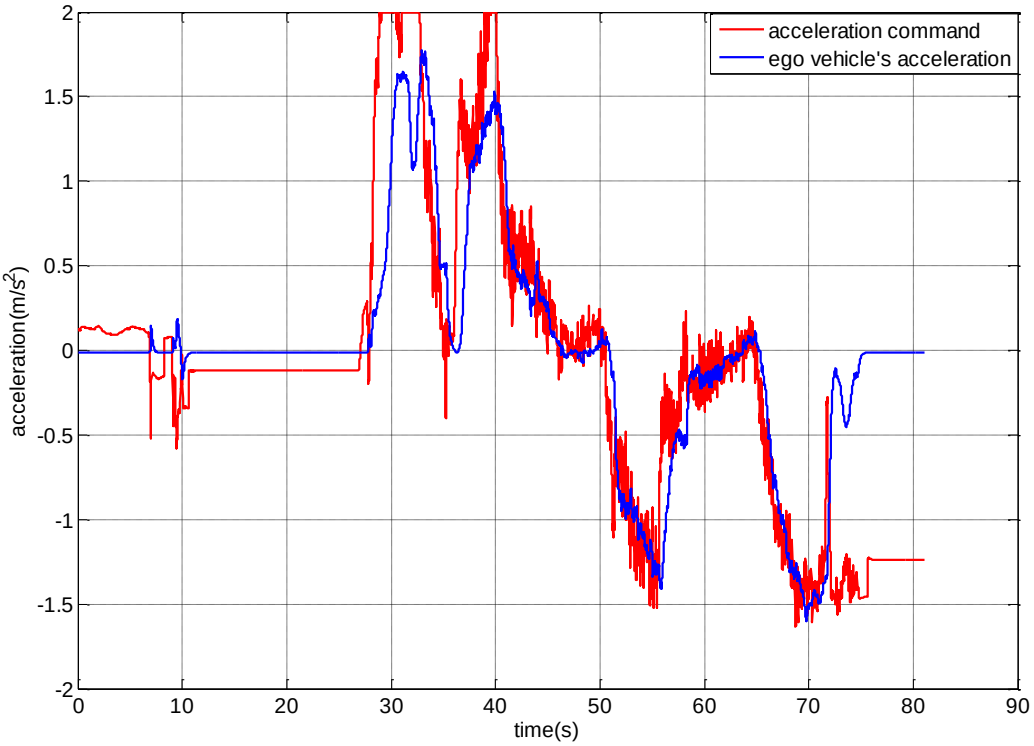

Figure 4-2. Acceleration command and the actual acceleration of the vehicle

The acceleration of the ego vehicle which is read from the CAN bus[1] of the vehicle is noisy. The sensor fusion block should filter out this noise. As the controller uses this acceleration in a feedback loop, the remaining noise on this acceleration is fed to the controller which appears in the control command. In the controller design procedure in the previous chapter; there was no filtering on acceleration signal. The main reason is that the system has a low pass character and therefore this noise on the acceleration command is filtered. Thus, the acceleration of the ego vehicle is almost noise-free as shown in figure 4-2.

In the next figures, the acceleration profiles of the vehicles and the bode plot of string stability condition (5) are shown.

1- CAN bus (Controller Area Network) is a vehicle bus standard designed to allow microcontrollers and devices to communicate with each other within a vehicle without a host computer (http://en.wikipedia.org/wiki/CAN_bus)

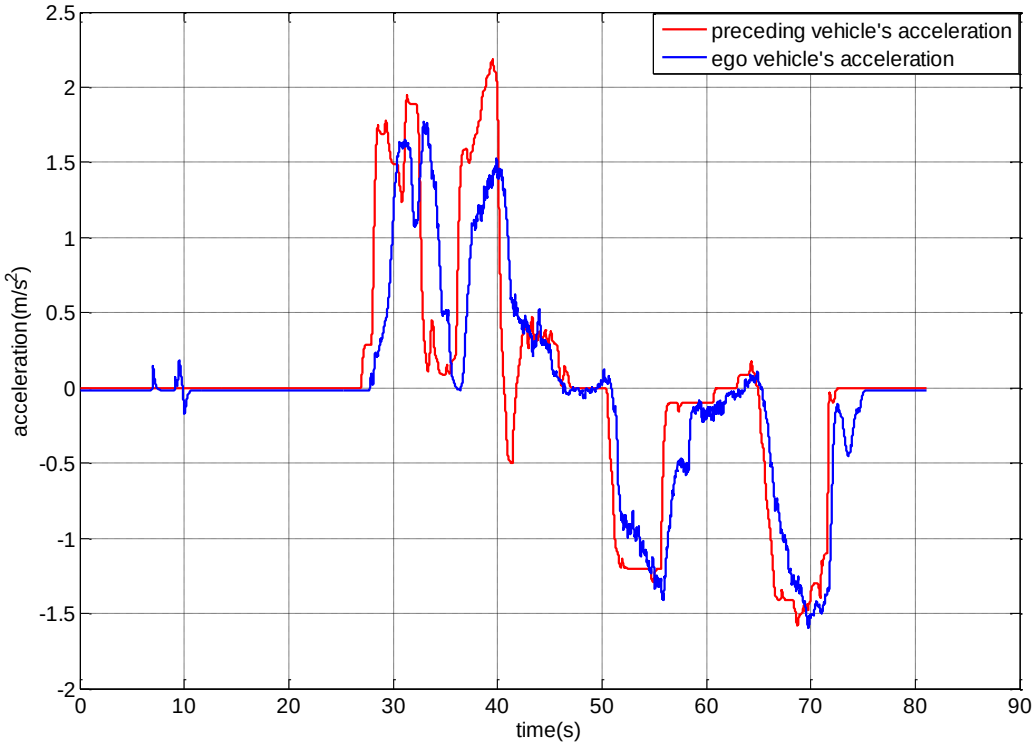

Figure 4-3. Acceleration of the preceding and the ego vehicles (to investigate string stability)

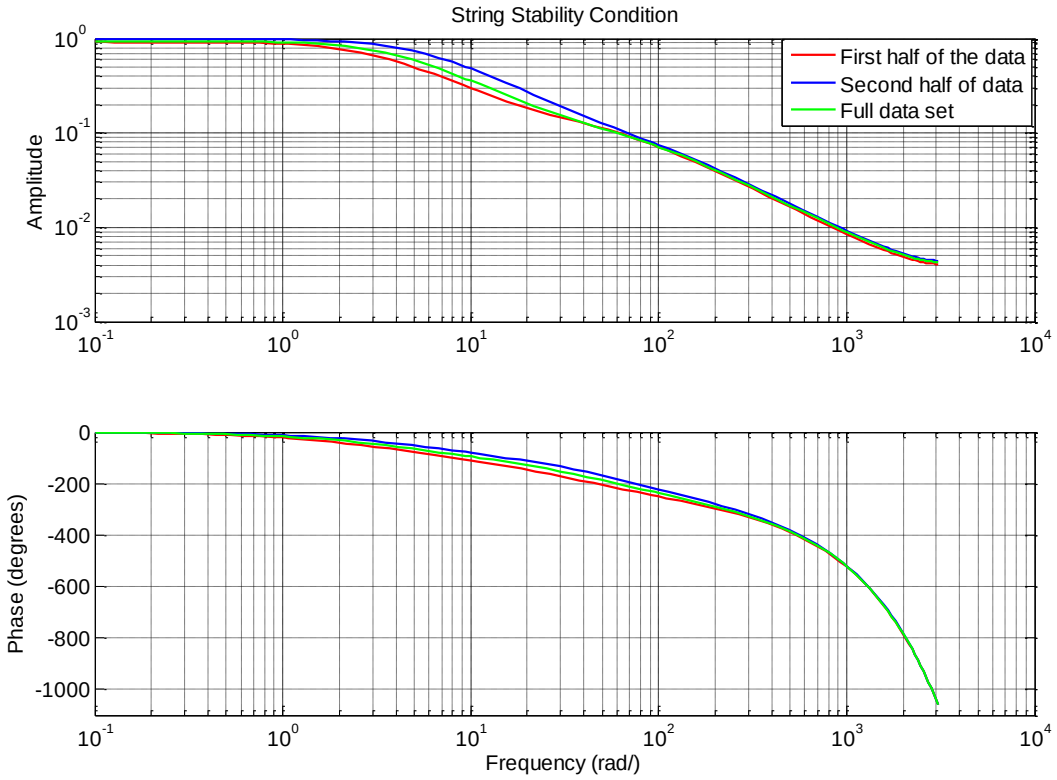

Figure 4-4. Bode plot for string stability investigation (transfer function 3.61)

Figure 4-3 shows that the ego vehicle's acceleration is damping the preceding vehicle's acceleration.

In figure 4-4, a frequency response based on the experimental data is shown. For deriving this, the input data was assumed to be the acceleration of the preceding vehicle and the output data was assumed to be the acceleration of the ego vehicle. Then, based on the system identification technique a simple 'ARX model' [15] was fitted to the data. (This model should be causal which means that the number of zeros should be less than the number of poles. At the same time it should have at least one zero such that the system can be excited (+20 (db/dec) slope for each zero in magnitude frequency response)).

The full data set is divided into two halves. The reason is that sometimes in the beginning when the controller is switched on; the vehicle is moving forward in order to compensate for the initial position error. Therefore, it doesn't make sense to investigate string stability for this case. The bode plot of the full data set (figure 4-4) shows the attenuation of preceding vehicle's acceleration.

Test 199 {headway time=1(s) and safety distance=11(m)}

In this test, the second case which is the oscillation test was performed.

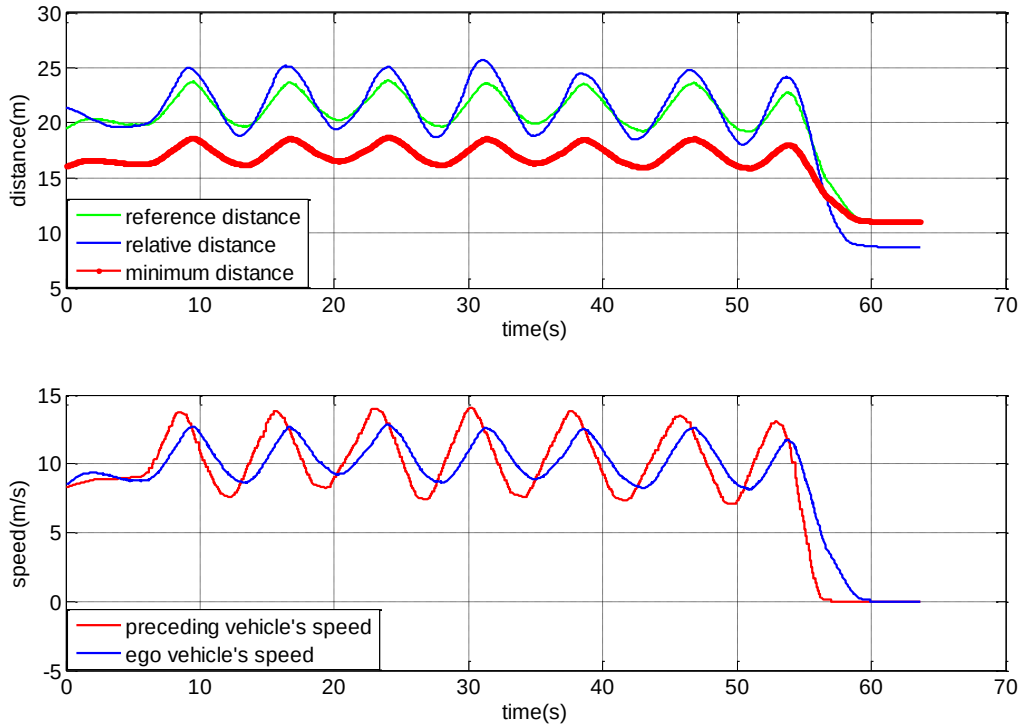

Figure 4-5. Tracking the reference distance and tracking the speed

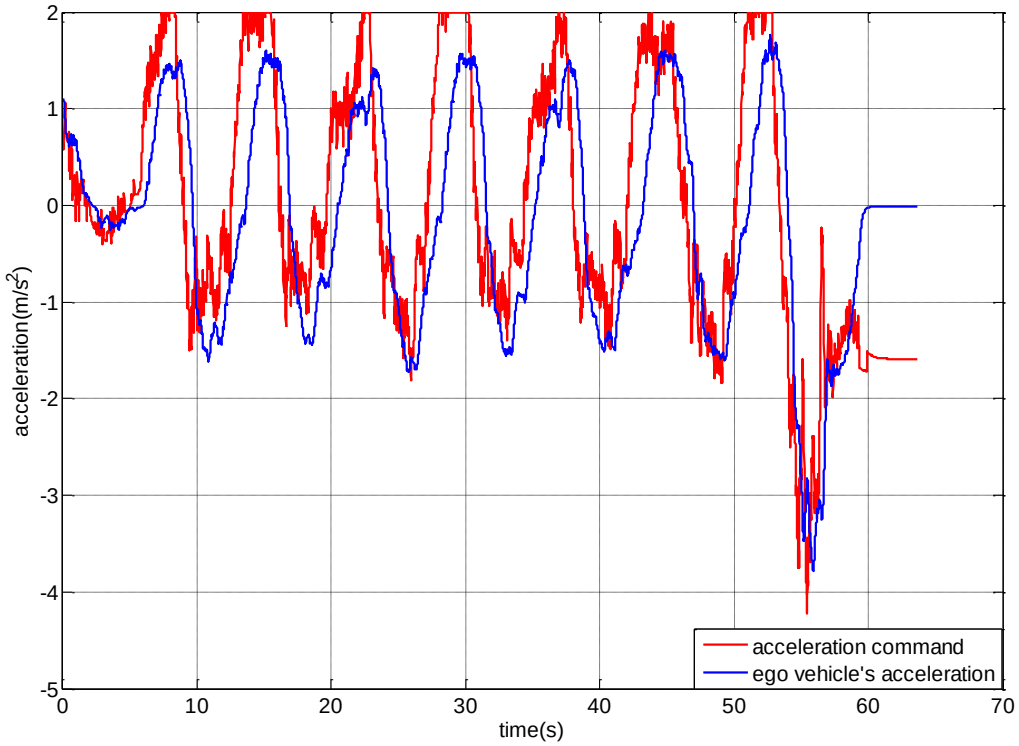

Figure 4-6. Acceleration command and the actual acceleration of the vehicle

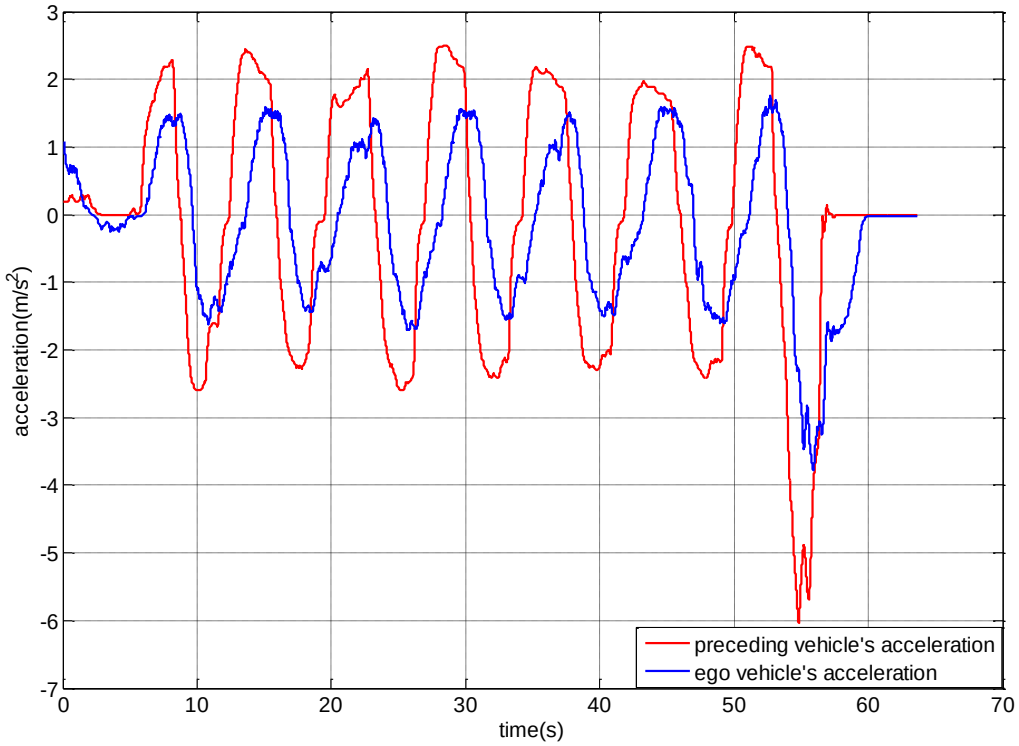

Figure 4-7. Acceleration of the ego and the preceding vehicles (to investigate string stability)

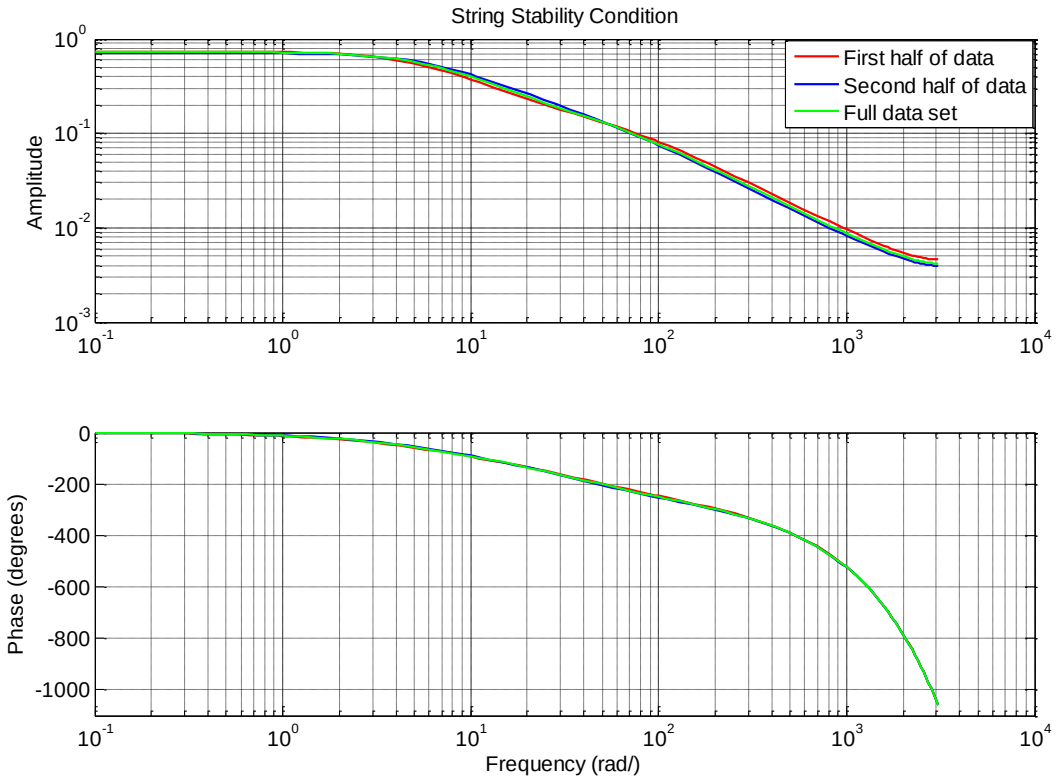

Figure 4-8. Bode plot for string stability investigation (transfer function 3.61)

According to the string stability condition (3.29), by exciting a certain frequency it is possible to see if the string stability condition is satisfied for any frequency of interest.

In the next two pages (figures 4-9 to 4-12), the results of using this controller in the GCDC competition are shown.

Test 403 in the GCDC {headway time=0.7(s) and safety distance=10(m)}

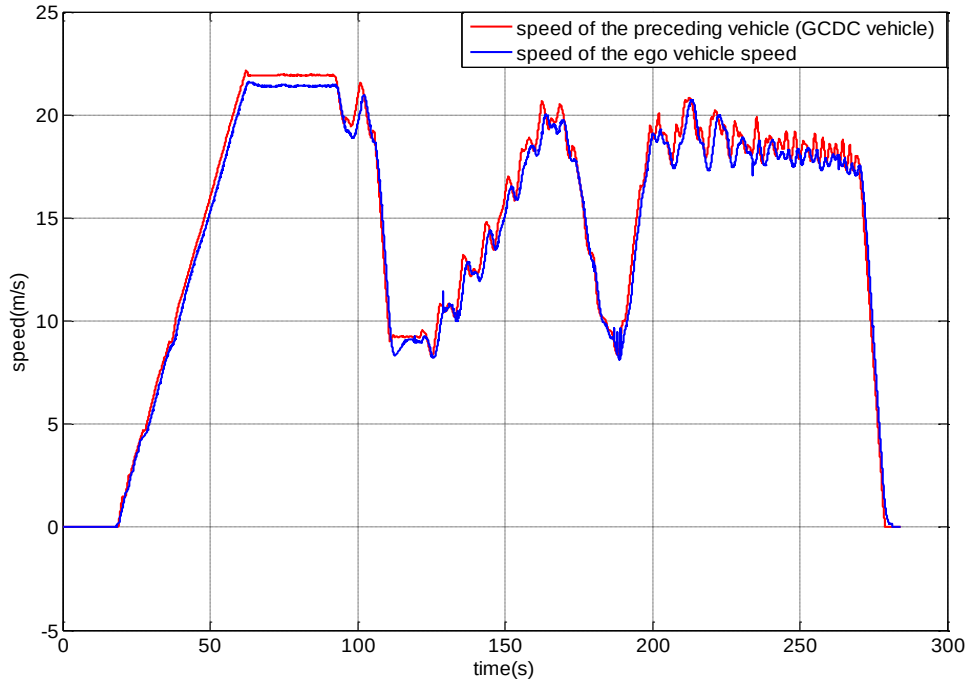

Figure 4-9. Tracking the speed of the preceding vehicle

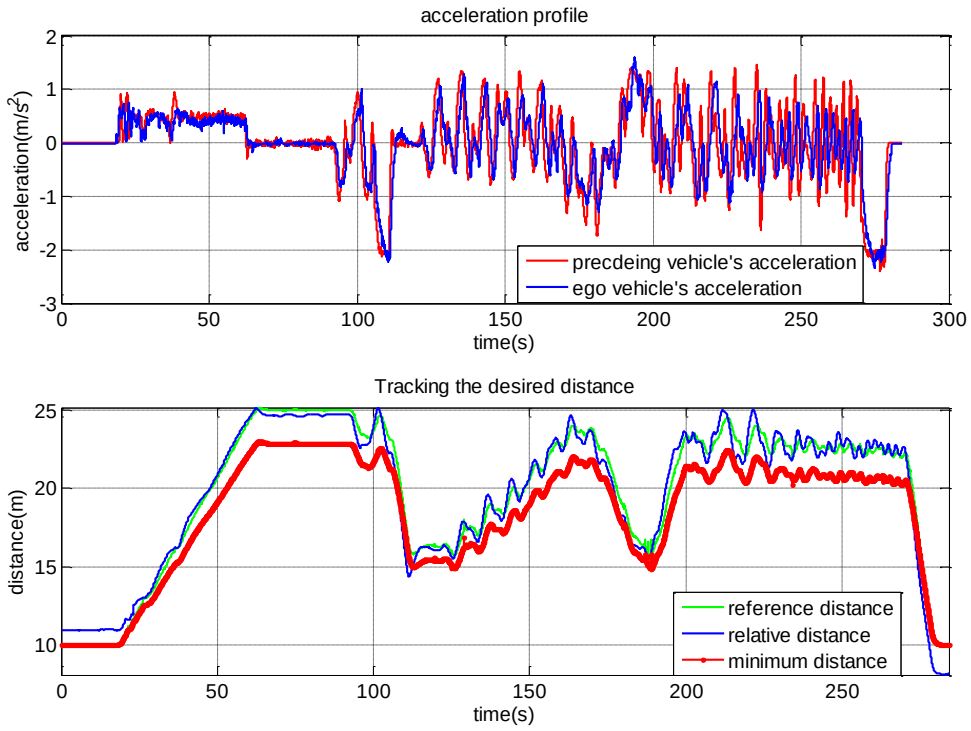

Figure 4-10. Acceleration profiles and tracking the reference distance

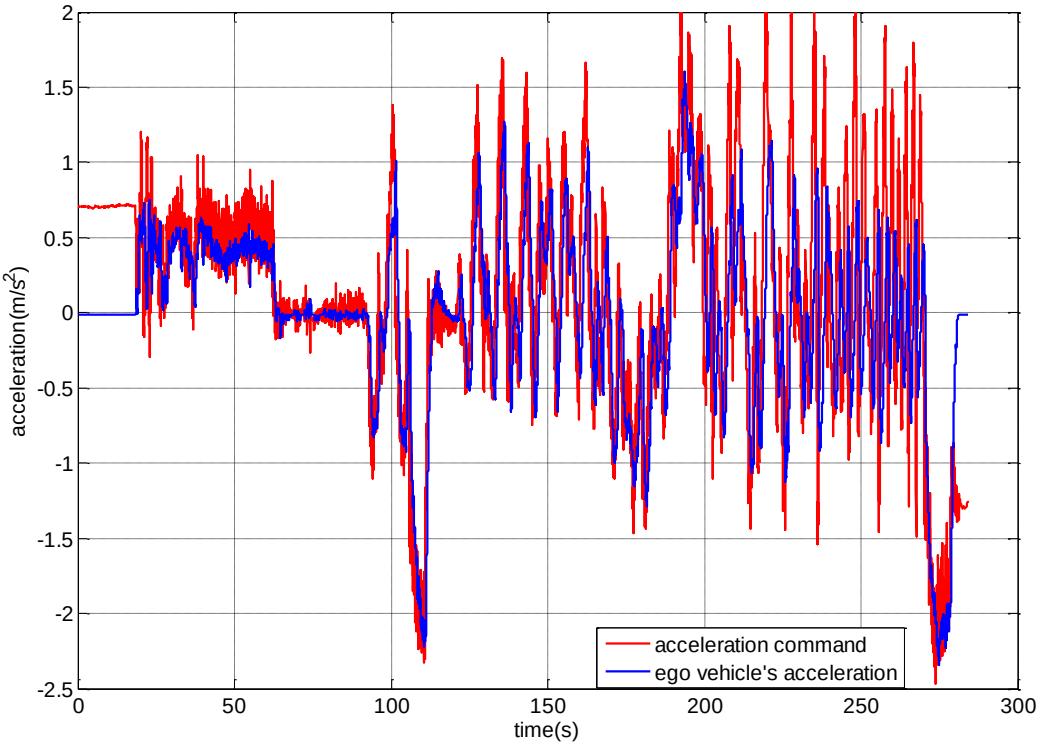

Figure 4-11. Commanded acceleration and actual acceleration

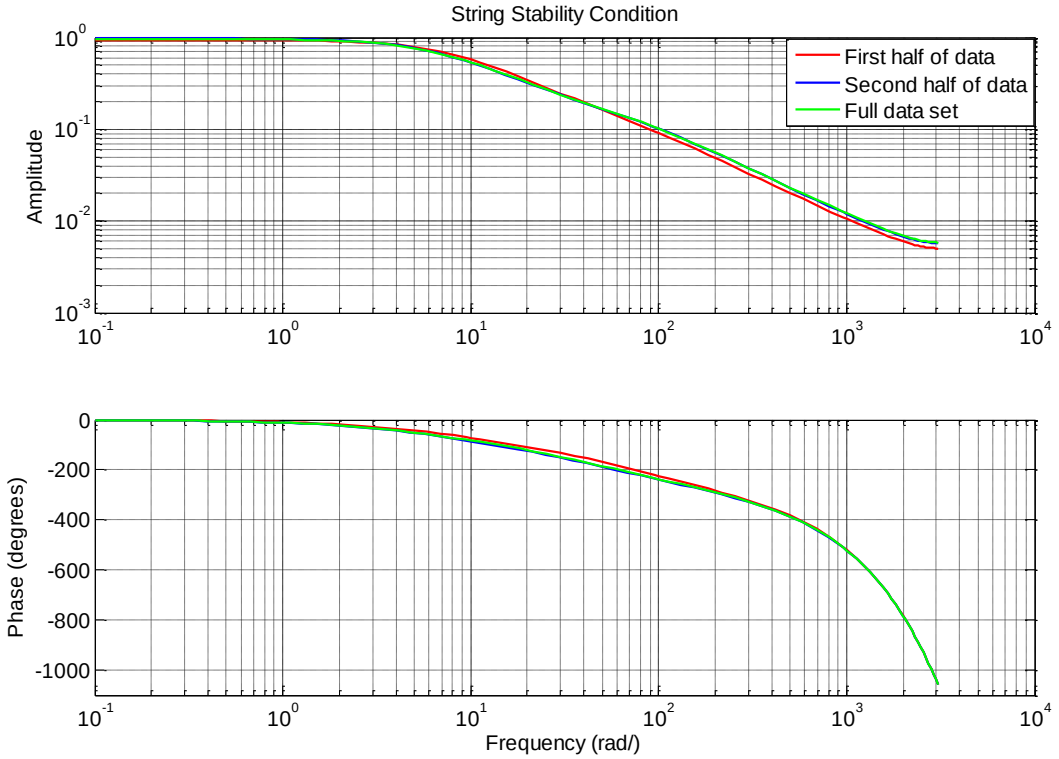

Figure 4-12. Bode plot for string stability investigation (transfer function 3.61)

4.2 Controller Based on Preceding and Preceding+1Vehicles

The controller designed in section 3.3.4 is used for the tests of this part. To be able to test this controller, at least three vehicles are needed: the leader, the preceding and the ego vehicles. All these vehicles should be equipped with V2V communication such that they can communicate the information about their position, speed and acceleration. This was one of the limitations (having access to 3 vehicles with ready setup) for testing this controller.

The result of this part is chosen from the GCDC competition where there were enough vehicles to test this controller.

In this scenario which is chosen from the GCDC competition, the ego vehicle was the first vehicle of the platoon number 1 (figure 1-4), and therefore in the beginning of this scenario, the speed controller was used in order to catch the front platoon. The leader vehicle was the first vehicle of the platoon number 2 and the preceding vehicle is the vehicle behind the leader vehicle.

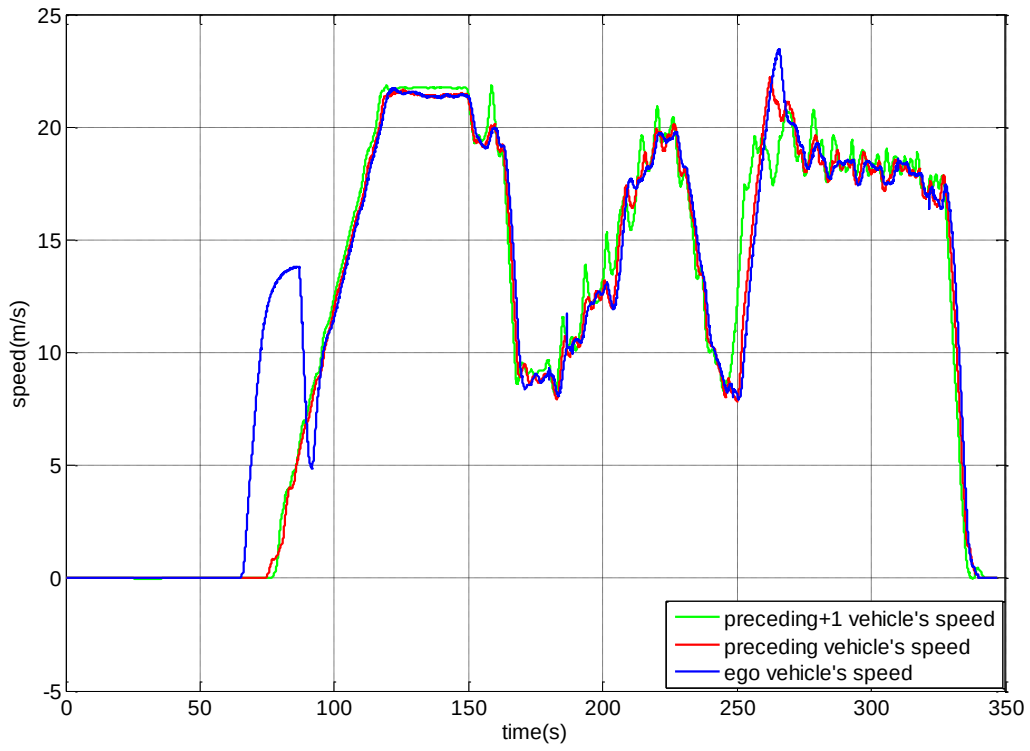

Figure 4-13. Speed tracking

This explains why the speed increased rapidly in the beginning and when the preceding vehicle was detected, it switched to the spacing controller and tried to track the reference distance instead.

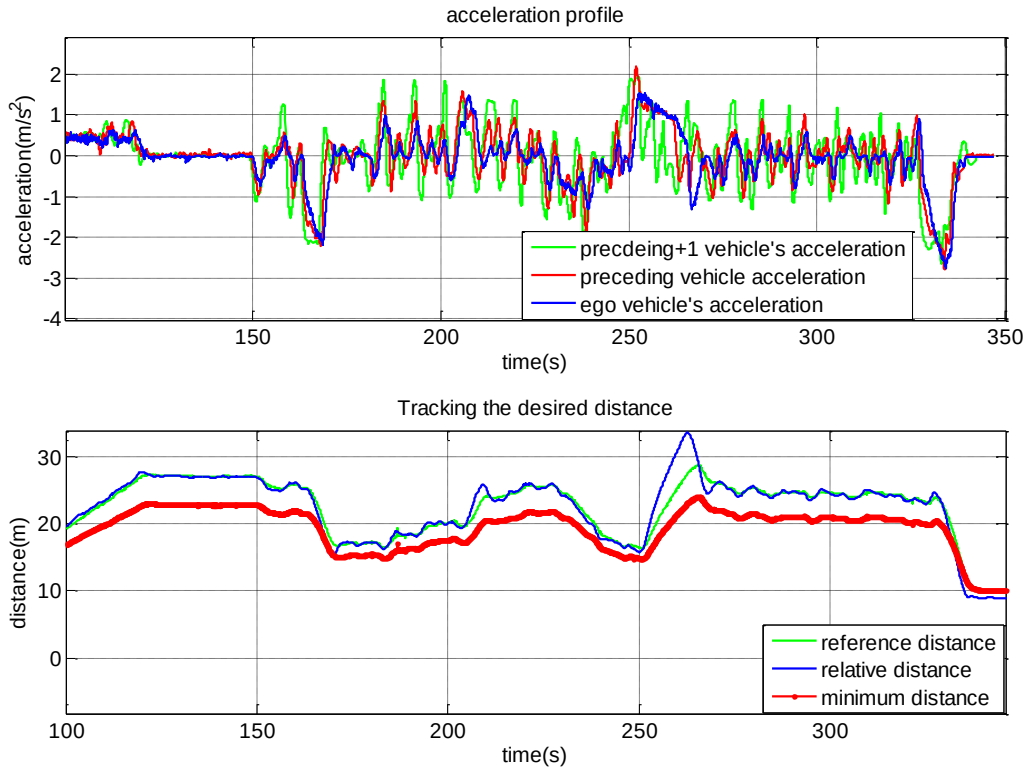

Figure 4-14. Acceleration profiles of the vehicles and tracking the reference distance

In figure 4-14, the acceleration profile of all of the vehicles (upper plot) together with the tracking performance of the controller is shown.

Another limitation with the ego vehicle was the limited acceleration rate. Therefore, when the preceding vehicle accelerated too fast, the ego vehicle wasn't able to track the reference distance fast enough and as a result the difference between the current distance and the reference distance increased. This happened in this test around 250(s) when a large acceleration of the preceding vehicle was observed. The controller tried to attenuate this acceleration but the aforementioned point was affecting the performance.

In figure 4-16, the control input signal and, in figure 4-17, the frequency response of the transfer function (27) in relation to string stability are shown.

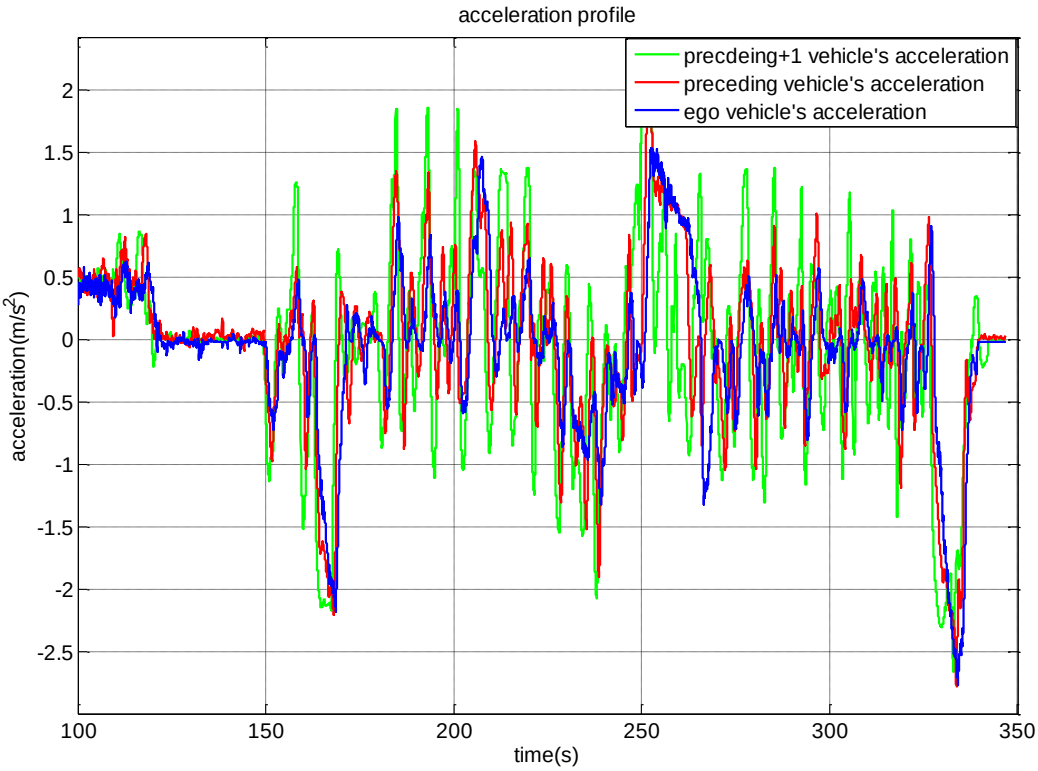

Figure 4-15. Acceleration profiles of the vehicles (to investigate string stability)

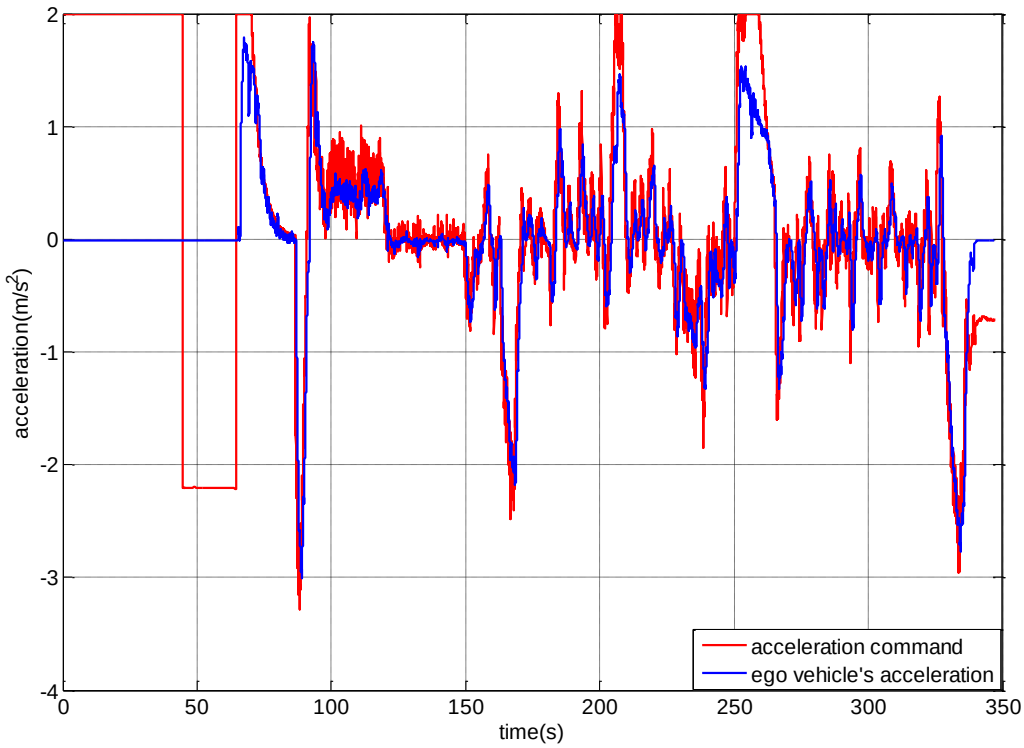

Figure 4-16. Acceleration command and the actual acceleration of the ego vehicle

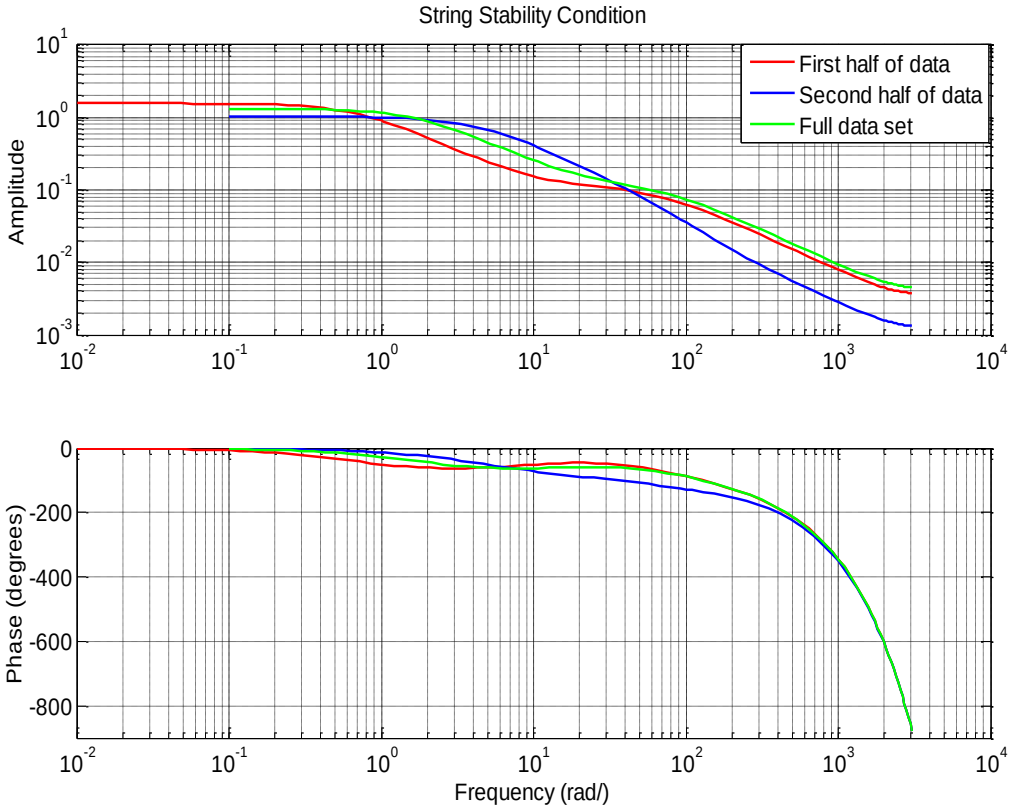

Figure 4-17. Bode plot for string stability investigation (transfer function (3.78))

Conclusions

In this thesis, design and implementation of different controllers for a cooperative driving system were discussed. A brief overview of the ACC systems, cooperative driving and CACC systems, and the platoon of vehicles were presented in the beginning. The proposed model of the vehicle described the relation between the desired longitudinal acceleration to the actual acceleration of the vehicle. Both the speed and the spacing controller design were discussed. Based on different control architectures the spacing controller was designed. In the first strategy, only information from the preceding vehicle was used (the R-D and the R-ASD controllers) while in the second strategy information from both the preceding and the preceding+1vehicles in the platoon were used. The advantage of the R-ASD controller to the R-D controller was that the controller was more robust to the actuation delay as it had higher stability margin for the same system's bandwidth. Adding the information of relative acceleration to preceding+1 vehicle to the R-ASD controller allowed the vehicle to travel in a shorter inter-vehicle distance without deteriorating the performance. In all design strategies, the controller design objectives were zero positioning and speed error, string stability condition and meeting the constraints (such as the constraint on the control input) while having a satisfactory response. Experimental validation was also provided for the aforementioned controllers.

To obtain more safety while driving and to help having less pollution and traffic congestion, more information about the environment is needed which imposes more challenges on the controller design. By overcoming these, it has been shown that cooperative driving is quite beneficial.

.

References

[1] G. J. L. Naus, R. P. A. Vugts, J. Ploeg, M. J .G. van de Molengraft and M. Steinbuch, "String-stable CACC design and experimental validation: A frequency-domain approach, IEEE transactions on vehicular technology, vol. 59, No. 9, November 2010

[2] "GCDC Rules and Technology" (www.gcdc.net)

[3] R. Rajamani, "Vehicle dynamics and control", Mechanical Engineering Series 2006

[4] S. Huang and W. Ren, "Longitudinal control with time delay in platooning" IEEE proc.-Control Theory Appl., vol. 145, No. 2, March 1998

[5] P. Seiler, A. Pant and K. Hedrick, "Disturbance propagation in vehicle strings,", IEEE transaction on Automatic Control, vol. 49, No. 10, October 2004

[6] D. Swaroop and J. K. Hedrick, "String stability of interconnected systems,", IEEE Transaction on Automatic Control, vol. 41, No. 3, March 1996

[7] S. Sheikholeslam and C. Desoer, "A system level study of the longitudinal control of a platoon of vehicles,", Journal of Dynamic Systems, Measurement, and Control – Transaction of the ASME, vol. 114, No. 2, pp. 286-292, June 1992.

[8] ——, "Longitudinal control of a platoon of vehicles," in Proceedings of the 1990 American Control Conference, vol. 1, June 1990, pp. 291-296.

[9] J. Yang, "A simulation study for the control of a platoon of vehicles," in Proceedings of the 1994 American Control Conference, vol. 1, 1994,pp. 423-424

[10] E. Shaw and J. K. Hedrick, "String stability analysis for heterogeneous vehicle string", Proceedings of the 2007 American Control Conference

[11] E. Shaw and J. K. Hedrick, "Controller design for string stable heterogeneous vehicle strings", Proceedings of the 46th IEEE conference on Decision and Control 2007

[12] Katsuhiko Ogata," Modern Control Engineering"

[13] R. Kianfar, P. Falcone and J. Fredriksson, "A receding horizon approach to string stable cooperative adaptive cruise control", IEEE Conference on Automatic Control

[14] GCDC Catalogue, Helmond, the Netherlands, May 2011

[15] L. Jung and T. Glad, "Modeling and Simulation"

[16] J. M. Maciejowski, "Predictive Control with Constraints"

[17] T. Glad and L. Ljung," Control Theory, Multivariable and Nonlinear Methods"

Appendix A
Model Predictive Controller Based on Only Preceding Vehicle

Idea and Formulation of Predictive Control

The idea of the model predictive control is based on choosing an appropriate model for the system under study. According to this model, future values of the output are calculated that depend on future inputs and also on the measurements:

$$\hat{y}(t+k|t), k = 1,2, \dots, M$$

$$u(t+j|t), j = 0,1,2, \dots, j$$

Then a criterion based on these variables is chosen that needs to be minimized with respect to:

$$u(t+j|t), j = 0,1,2, \dots, j$$

This basically turns the problem into an optimization problem that by solving it the control input u can be determined. Later, u is applied to the system and at the next sampling time the prediction of outputs and solving the optimization function is repeated and the control input, u applied to the system. Re-doing the whole procedure explained above for each sampling time is to introduce feedback in the control design. In each sample the optimization problem is solved and the control input is applied to the system. Then new output of the system can be measured which was predicted in the previous step and use it as the starting point and predict the future values of the output again.

The main advantage that made the MPC controller popular in recent years is the ability of it to solve a constrained control problem meaning that it can take into account the constraint on the controlled variables when it calculates the control input.

Formulation of the MPC problem is as follows:

For the model the state-space representation is being used (w (t) and v (t) are noise models):

$$x(t+1) = Ax(t) + Bu(t) + Nw(t) \qquad (1)$$

$$y(t) + Cx(t) + v(t) \qquad (2)$$

The states are estimated using an observer or a Kalman filter. Since w(t) and v(t) are unpredictable, the predicted future states and outputs for k-step prediction are:

$$\hat{x}(t+k+1|t) = A\hat{x}(t+k|t) + Bu(t+k), \quad k = 0,1, \dots \qquad (3)$$

$$\hat{y}(t+k|t) = C\hat{x}(t+k|t) \qquad (4)$$

If we define $\hat{x}(t) = \hat{x}(t|t)$ which denotes the current state based on $(k), k \leq t \; and \; u(k), k < t$, then we can figure out that the predicted output is a linear function of the current state and the predicted control input:

$$\hat{y}(t+k|t) = F\big(\hat{x}(t|t), u(t+j)\big) \quad k = 0,1,\dots,M \quad , \quad j = 0,1,\dots,N$$

$$Y_t = G_u U_t + G_x \hat{x}(t|t) \qquad (5)$$

Where:

$$Y_t = \begin{pmatrix} \hat{y}(t+M|t) \\ \vdots \\ \hat{y}(t+1|t) \end{pmatrix}$$

$$U_t = \begin{pmatrix} u(t+N) \\ \vdots \\ u(t) \end{pmatrix}$$

M and N are called prediction horizon and control horizon respectively. Normally the control horizon is chosen to be less than the prediction horizon (N<M). M usually covers the settling time of the system while N shows the size of the optimization problem.

Usually a quadratic cost function is chosen for the optimization problem:

$$J = Y_t^T Q_y Y_t + U_t^T Q_u U_t$$

This should be minimized considering the following constraints:

$$|u(t)| \leq U_c \quad , \quad |y(t)| \leq Y_c$$

It is a convex quadratic programming problem (QP). Efficient numerical methods exist for solving it. This problem, as it was mentioned has to be solved online at each sample time. It should be noted that the controller is of a nonlinear type! Sometimes instead of penalizing the control input, the change of control input is penalized. In general we can have the following cost function for the optimization problem:

$$\mathrm{J} = \min_{\Delta U_t} \sum_{k=0}^{N-1} \|y(t+k|t)\|^2{}_Q + \|\Delta u(t+k|t)\|^2{}_R + \|u(t+k|t)\|^2{}_S$$

Where Q, R and S are weighting matrices and N is the prediction horizon [16], [17].

Applying MPC Approach to the Problem

The MPC controller, which is used in a test phase, is developed by R.Kianfar [13]. The formulation of this controller is briefly described below.

The system is modeled by 4 states: which are position error, speed error, acceleration of ego vehicle and speed of ego vehicle. The inputs of the system are acceleration command as a manipulated variable and also acceleration of the preceding vehicle as measured disturbance.

The state-space model is then as follows:

$$\begin{bmatrix}\dot{x}_1\\ \dot{x}_2\\ \dot{x}_3\\ \dot{x}_4\end{bmatrix} = \begin{bmatrix}0 & 1 & -h & 0\\ 0 & 0 & -1 & 0\\ 0 & 0 & -\frac{1}{T} & 0\\ 0 & 0 & 1 & 0\end{bmatrix}\begin{bmatrix}x_1\\ x_2\\ x_3\\ x_4\end{bmatrix} + \begin{bmatrix}0 & 0\\ 0 & 1\\ \frac{K}{T} & 0\\ 0 & 0\end{bmatrix}\begin{bmatrix}u_1\\ u_2\end{bmatrix}$$

$$\begin{bmatrix}y_1\\ y_2\\ y_3\\ y_4\end{bmatrix} = \begin{bmatrix}1 & 0 & 0 & 0\\ 0 & 1 & 0 & 0\\ 0 & 0 & 1 & 0\\ 0 & 0 & 0 & 1\end{bmatrix}\begin{bmatrix}x_1\\ x_2\\ x_3\\ x_4\end{bmatrix}$$

$x_1 = x_p - x_e - hV_e - L_{safe}$: Position error

$x_2 = V_p - V_e$: Speed error

$x_3 = a_e$: Ego vehicle acceleration

$x_4 = V_e$: Ego vehicle speed

u_1 : Control command (Acceleration command) u_2 : Preceding vehicle acceleration

There are also constraints on the control input and the states as follows:

$$a \leq u_1 \leq b\text{: Constraint on control signal}$$

$$c \leq \frac{du_1}{dt} \leq d \text{ : Constraint on the rate of control signal}$$

$$d_{min} \leq x_1 \leq d_{max}$$

$$dv_{min} \leq x_2 \leq dv_{max}$$

$$a_{min} \leq x_3 \leq a_{max}$$

$$v_{min} \leq x_4 \leq v_{max}$$

Constraints on the states basically limit how much for example, the distance between the vehicles can deviate from the reference distance. Considering that we have a minimum distance requirement, it makes sense to define a constraint on the position error. Defining constraints is part of the controller design, and it might not be necessary to define

constraint on all the states and the control input and the rate of change of the control input.

More information and a complete design procedure (including the cost function) of this controller is provided in [13]. The simulation results that follow show the performance of the tuned MPC controller.

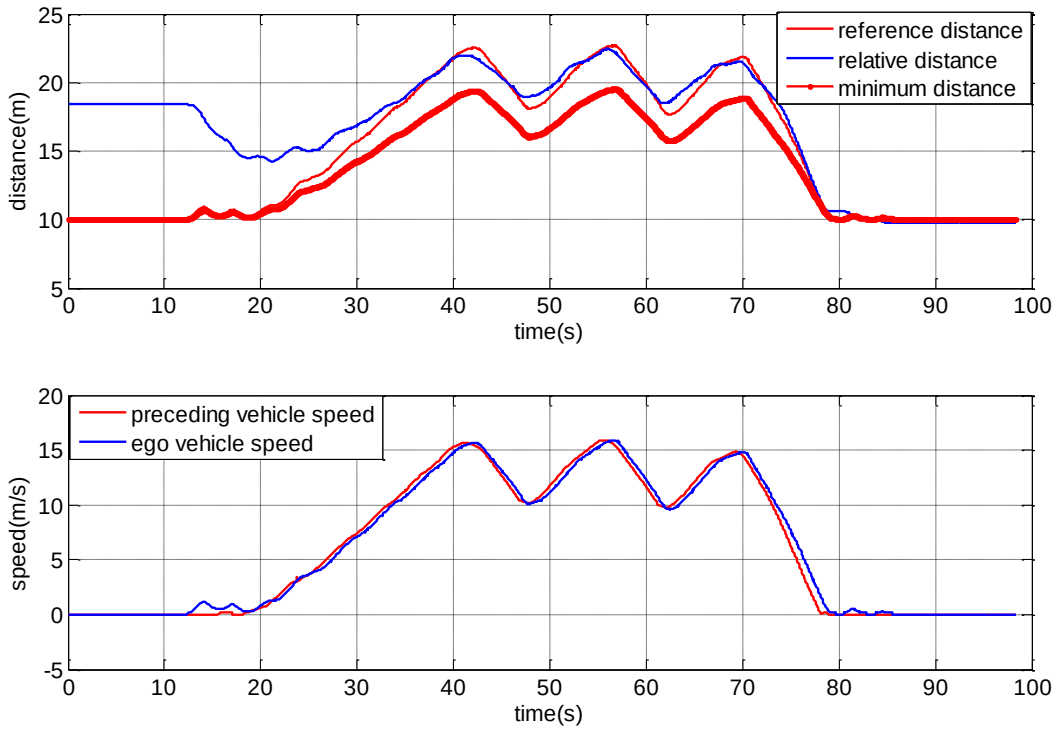

Figure A-1. Tracking the reference distance and tracking the speed by the MPC controller

Figure A-1 shows the tracking performance of the controller. In the beginning there was a large distance between the vehicles and for approximately almost first 20 (s) of data logging, both vehicles were standing still.

In figure A-2, acceleration command and actual acceleration of the vehicle together with the constraints on the acceleration command are shown. Also the string stability condition and position error are plotted to show the promising performance of the controller in to handling these requirements.

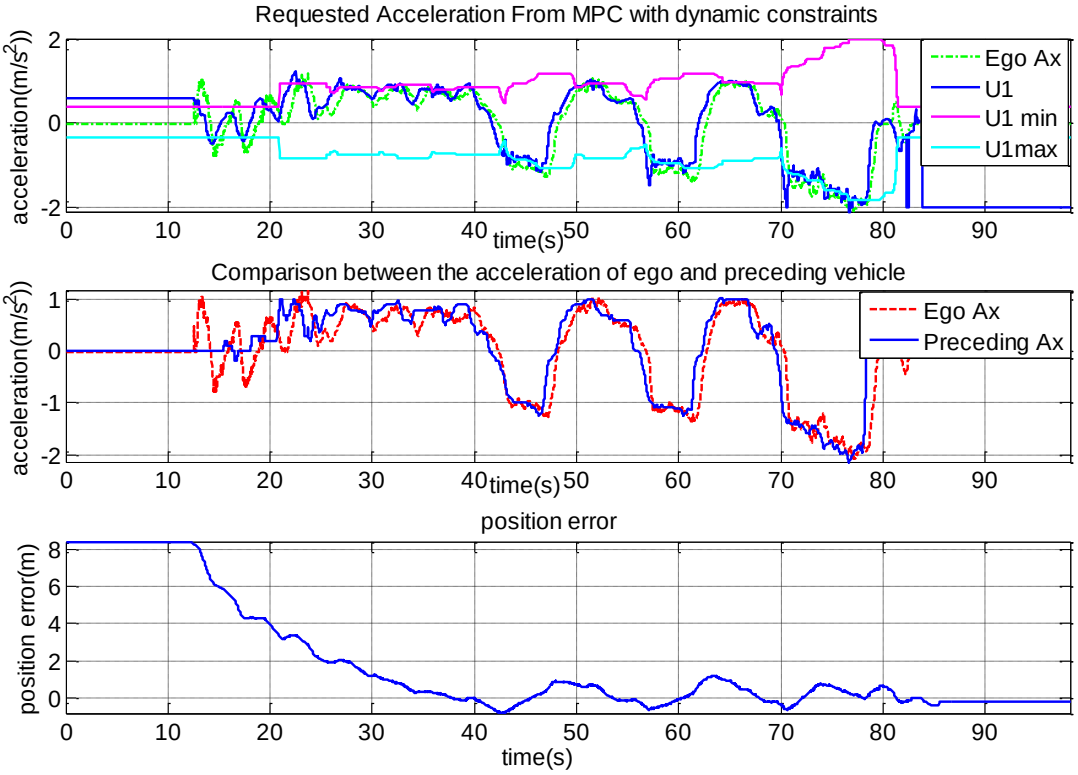

Figure A-2. Acceleration command (U1) and the actual acceleration with dynamic constraints (upper plot), the preceding vehicle's acceleration with ego vehicle's acceleration (middle plot) and the position error (lower plot)

Comparison between the Performances of the MPC Controller and the R-ASD Controller

Performance of two different types of controllers was shown so far. In this section, the aim is to compare the performance of these two controllers from different aspects.

The R-ASD controller (the classical type controller) was designed based on frequency domains analysis. Having a satisfactory performance in tracking the reference distance and speed and string stability condition were the main criteria to determine proper values for the controller parameters.

In the model predictive control design, first a prediction model was obtained in the state space form and then the constraints on control signal and the states that imposed by the problem were defined. Then the weights on control signal and the states are chosen such that all the requirements such as tracking the reference distance and the speed or the string stability condition are met.

The major difference between these two controllers is the ability of the MPC controller to meet the constraints, for example, in tracking the reference distance:

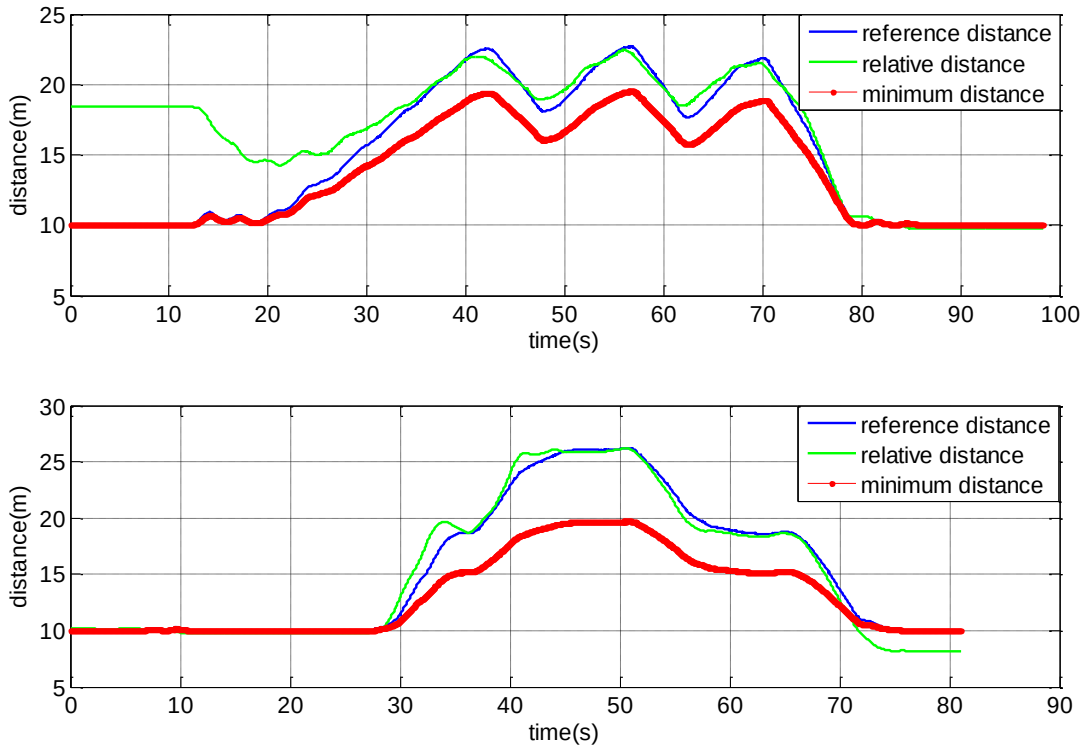

Figure A-3. Comparison between R-ASD and MPC controllers in meeting the constraint on relative distance

Figure A-3 shows that the MPC controller could stop the vehicle at the required distance without passing the minimum allowed distance while the classical controller is passing the minimum distance in the full stop mode. In the formulation of the R-ASD controller

there was no special consideration for meeting the constraints, while in the MPC formulation this was part of the design and tuning of the controller. It is important to mention that by tuning the classical controller it is possible to obtain better result in the full stop case but it won't be possible to guarantee this. Putting too much effort to fix the full stop problem was avoided because other criteria were of the main importance and trying to fix the full stop problem affected the performance of the controller in other modes.

One other noticeable difference between these two controllers was the tuning effort. It means that it took much longer time to tune the MPC controller while the classical controller (the R-ASD controller) was tuned much faster.

To summarize, using an advanced type controller such as the MPC is valuable as it can handle constraint controlled problems which exist in many applications today. But the price for it is that more tuning effort is needed for obtaining a good performance in terms of both requirements and constraints.

The classical controller, on the other hand, was easier to design, analyze and tune, while the main deficiency of it was the weakness to handle the constraints especially when there were different constraints in the problem. For example, by using saturation block, constraints on the control input were satisfied, but it wasn't possible to do the same for the minimum distance requirement, and therefore it led to violation of the constraints in the full stop mode.